FEDERAL AVIATION AGENCY AND NATIONAL AERONAUTICS AND SPACE ADMINISTRATION

JOINT TECHNICAL CONFERENCE ON SLUSH DRAG AND BRAKING PROBLEMS

A COMPILATION OF THE PAPERS PRESENTED

Departmental Auditorium
Washington, D. C.

December 19-20, 1961

FEDERAL AVIATION AGENCY

AND

NATIONAL AERONAUTICS AND SPACE ADMINISTRATION

JOINT TECHNICAL CONFERENCE

ON SLUSH DRAG AND BRAKING PROBLEMS

A Compilation of the Papers Presented

Departmental Auditorium
Washington, D.C.

December 19-20, 1961

Page Intentionally Left Blank

TABLE OF CONTENTS

TECHNICAL PAPERS PRESENTED

December 19, 1961

Conference Opening: Joseph D. Blatt
Director, Aviation Research and Development Service, FAA

SLUSH DRAG

Session Chairman: Harold D. Hoekstra, FAA

TECHNICAL PAPERS PRESENTED

December 20, 1961

BRAKING PROBLEMS

Session Chairman: Philip Donely, NASA

INTRODUCTION

This document contains reproductions of technical papers prepared by staff members of the Federal Aviation Agency and the National Aeronautics and Space Administration for presentation at a Joint Technical Conference on Slush Drag and Braking Problems held at Washington, D.C., on December 19 and 20, 1961. The primary purpose of the conference was to make available as rapidly as possible the results of a recently completed slush drag and braking test program conducted at the FAA's National Aviation Facilities Experimental Center. The NASA's research, past and current, in this field has been reviewed, and the results of related studies have been included in the conference and in this compilation.

A list of conferees is included.

Page Intentionally Left Blank

LIST OF CONFEREES

The following were registered at the FAA-NASA Joint Technical Conference on Slush Drag and Braking Problems, Departmental Auditorium, Washington, D.C., December 19-20, 1961.

AIKEN, William S., Jr.	NASA Headquarters
ANTVIK, G.	SAS and Technical Dept. of Swedish CAB
BALLENGER, Vern W.	Trans World Airlines
BARNES, William B.	FAA
BEACOM, Robert K.	U.S. Air Force
BENDER, John R.	Bendix Corp.
BINCKLEY, Earl T.	U.S. Air Force
BIRDSONG, Charles H.	FAA
BLATT, Joseph D.	FAA
BOLLENBACHER, Comdr. Robert M.	U.S. Navy
BOURNE, Harry K.	United Kingdom Scientific Mission
BUCHANAN, James L.	U.S. Air Force
BUEL, R. L.	Frank G. Schenuit Rubber Co.
BUSH, Charles F.	Goodyear Tire and Rubber Co.
CAHILL, Jones F.	Lockheed Georgia Co.
CARR, Maj. Roger A.	U.S. Air Force
CHAMBERLAIN, George A.	FAA NAFEC
CHAMBERLAIN, Richard K.	General Tire and Rubber Co.
CHANDLER, Harrison C., Jr.	Firestone Tire and Rubber Co.
COLLINAN, William E., Jr.	FAA
COLLINS, H. Graham	Royal Canadian Air Force
CONLEY, D. W.	FAA NAFEC
COOK, Woodrow L.	NASA Ames Research Center
CULBERTSON, James A.	Goodyear Aircraft Corp.
DALLAS, Allen W.	Air Transport Assoc.
DAVIS, James E.	American Airlines
DePAUL, Elder I.	General Tire and Rubber Co.
DICKERSON, William N.	B. F. Goodrich Co.
DIGGS, George C.	Eastern Airlines
DOBI, Nicholas	FAA
DONELY, Philip	NASA Langley Research Center
DOOLEY, Maj. Robert J.	U.S. Air Force
DOWE, Edward J.	Northeast Airlines
DOWNEY, Harry L., Jr.	Firestone Tire and Rubber Co.
DRAKE, Alfred E.	McDonnell Aircraft
EDWARDS, Bruce O.	Business Commercial Aviation Magazine
FEDZIUK, Henry A.	NASA Langley Research Center
FLANIGAN, Gerald P.	Frank G. Schenuit Rubber Co.

FOX, Frederick M.	Washington International Airport
FUENTES, Roland W.	Delta Airlines
GAFFNEY, William C.	The Boeing Company
GALLAGHER, John J.	FAA
GARRARD, G. S.	Aerospace Industries Assoc. of America, Inc.
GARRICK, I. E.	NASA Langley Research Center
GATES, Maj. William T.	U.S. Air Force
GEOFFRION, Donald R.	FAA
GERBER, Ray C.	Air Line Pilots Assoc.
GIESECKE, Hans	FAA NAFEC
GRIMES-GRAEME, A.	BOAC
GRUNDY, Capt. George G.	U.S. Air Force
HAINES, S. C.	Goodyear Tire and Rubber Co.
HALL, Laurence J. W.	Air Registration Board (London)
HANING, Lt. Col. William F., Jr.	U.S. Air Force
HANLEY, William J.	FAA NAFEC
HARDING, James H.	Pan American World Airways
HARN, Edwin W.	FAA
HART, H. A.	FAA
HAUETER, O. R.	Continental Air Lines, Inc.
HEINE, C. J.	Canadair Services Limited
HENDERSON, Comdr. Henry H.	U.S. Navy
HOEFS, Kenneth W.	The Boeing Company
HOEKSTRA, Harold D.	FAA
HOEKSTRA, Thomas B.	Univ. of Michigan
HOFFMAN, M. C.	Goodyear Aircraft Corp.
HOOVER, Isaac H.	FAA
HORNE, Walter B.	NASA Langley Research Center
HOWELL, Wayne D.	FAA NAFEC
HOYT, F. Russell	American Assoc. of Airport Executives
HUMPHREY, Ernest W.	U.S. Navy
HUNTER, W. H.	NASA Headquarters
IORI, Luigi	FAA
JEFFREY, Col. A. F.	U.S. Air Force
JONES, Robert F.	B. F. Goodrich Co.
JOYNER, Upshur T.	NASA Langley Research Center
KAMINSKI, Eugene J.	FAA NAFEC
KEEL, James S.	U.S. Air Force
KIBARDIN, Victor M.	FAA
KLUEG, Eugene P.	FAA NAFEC
KNIGHT, Ross A.	Airport Operators Council
KOLLHOFF, Charles W.	Braniff Airways
KOLNICK, Joseph J.	NASA Langley Research Center

KONECZNY, W. E.	FAA
KREBS, Lt. Comdr. Paul E.	U.S. Navy
LAECHELIN, C. E.	General Dynamics Corp.
LAW, Hervey F.	Port of New York Authority
LAWTON, William K.	National Business Aircraft Assoc., Inc.
LEAK, John S.	Civil Aeronautics Board
LeBLANC, A. F.	FAA
LELAND, T. J. W.	NASA Langley Research Center
MARCY, John	FAA NAFEC
McGUIRE, R. C.	Eastern Air Lines
McKEE, W. H.	Lockheed Georgia Co.
McKELVEY, R. E.	Fairchild Aircraft
McKENZIE, Gordon W.	Trans World Airlines
McLEAN, George D.	American Airlines
MEISSNER, V. S.	FAA
MENARD, E. M.	U.S. Rubber Co.
MESSIER, R. F.	U.S. Rubber Co.
MIDDLESWORTH, Charles M.	FAA NAFEC
MILLER, Lt. Col. D. E.	U.S. Air Force
MILLER, W. B.	FAA
MISNER, Milton	FAA
MOLNER, E. L.	Frank G. Schenuit Rubber Co.
NEWHAM, Douglas F.	BOAC
ORTMAN, Comdr. Oliver	U.S. Navy
OSTERMAN, J. A.	Lockheed Georgia Co.
OWEN, Edward M.	Cleveland Pneumatic Industries
PACE, George D.	Univ. of Michigan
PETTERSSON, Joel	Transaero Inc.
PIERCE, R. N.	Frank G. Schenuit Rubber Co.
PITNER, Robert N.	Hydro-Aire Co.
RADLEY, Barry	International Air Transport Assoc.
RAGSDALE, Lt. Comdr. Homer C., Jr.	U.S. Navy
RAITHBY, K.D.	Defence Research Staff (British)
REEDE, Cornelis H.	KLM Airlines
REEDER, John P.	NASA Langley Research Center
REKAS, Joseph	BUWEPS, U.S. Navy
REYNOLDS, Glenn W.	BUWEPS, U.S. Navy
RIDDLE, B. C., Jr.	NASA Langley Research Center
ROONEY, Eugene P.	Northeast Airlines
SAWYER, Richard H.	NASA Langley Research Center
SCHUMACHER, Paul W. J.	Wright-Patterson Air Force Base

SHEARD, Lt. Col. Alvin J.	U.S. Air Force
SHRAGER, Jack J.	FAA NAFEC
SIMPSON, William A.	Aerospace Industries Assoc.
SOMMERS, Daniel E.	FAA NAFEC
SPAULDING, Morril B., Jr.	Attorney
SPENCER, C. C.	Airline Pilots Assoc.
STEKETEE, Frank	Convair
STOPHLET, Richard B.	FAA
SUGDEN, Geoffrey C.	BOAC
SUGG, Robert W.	Ministry of Aviation (London)
SULLIVAN, Leo J.	Lockheed Aircraft Corp.
THARP, Thomas A.	General Tire and Rubber Co.
THOMAS, Edwin L.	Air Transport Assoc.
THOMPSON, Harvey M.	Allegheny Airlines
THOMPSON, James K.	FAA NAFEC
THORNTON, Eual	FAA
TITUS, Frederic E.	United Air Lines, Inc.
TOOMEY, James, Jr.	U.S. Air Force
VARNER, Stuart L.	Cleveland Pneumatic Industries, Inc.
VARY, Veryl V.	U.S. Air Force
VIERLING, B. J.	Aircraft Supply Co.
WALKER, Norman W.	British Embassy
WALLEY, William R.	Douglas Aircraft Co.
WARD, K. E.	General Dynamics Convair
WEST, David H.	FAA
WETMORE, Joseph W.	NASA Langley Research Center
WHETSTONE, Jabez C.	Lockheed Georgia Co.
WHITTEN, James B.	NASA Langley Research Center
WILKINSON, Frank Y.	FAA
WILLS, Robert W.	BUWEPS, U.S. Navy
WOHLRAB, Floyd J., Jr.	Trans World Airlines
WOODHAM, R. M.	Cornell-Guggenheim Aviation Safety Center
WYGLE, Brien S.	The Boeing Company
ZAHRINGER, James F.	FAA
ZALOVCIK, John A.	NASA Langley Research Center

1. INTRODUCTION TO THE SLUSH PROBLEM

By Isaac H. Hoover

FAA

Runway slush is one of the many operational problems that all aircraft operating in cold climates have to overcome. In tropical climates slush is frequently replaced by standing water, which has many of the same undesirable effects on aircraft operation.

Slush has a slippery texture which makes braking extremely poor, particularly at high speeds. Being a fluid, it is displaced by tires rolling through it, causing a significant retarding force. In the process, it is sprayed around in fairly well-defined patterns which cause additional drag on an aircraft, sometimes referred to as impingement drag or mudguard effect. Experience has shown that a good deal more slush is sprayed around than is actually displaced by the tires. This slush impacts on the lower side of the fuselage, the wing roots, the landing gear, and the inboard flaps with sufficient force to cause several types of damage to the airframe structure and systems. In addition, the spray can cause serious ingestion problems with engines located at the wing roots or with pod-mounted engines located near the tail, and sometimes acts as a carrier for assorted runway debris to intensify the ingestion problem further.

Pilots and air-carrier representatives do not have to be reminded of the aborted flights and incidents which occur when slush which sticks to the airplane freezes prior to cleanup of the aircraft, or at altitude. Inability to get a gear-up indication because of ice in the uplock mechanism or around the doors and door linkage, and an assortment of frozen mechanical units, primarily in flight-control systems, are frequent winter obstacles to schedule reliability and safe operations.

Slush can cause several types of control problems during runway operations. Varying depths and densities cause differential drag on the main gears. Hydroplaning and extreme wetness make the nose-wheel lateral traction close to zero so that nose-gear steering is of little use at high steering speeds. On take-off, by the time comfortable aerodynamic control is attained on aerodynamically boosted rudders, the main gears are suffering the same fate as the nose gear, and nearly all wheel braking is gone. At this point the aircraft is like a sailboat without a keel and in an unfortunate spot to experience an engine failure. In addition to these problems, slush drag and spray cause a nose-down pitching moment which must be overcome during rotation on take-off.

Control problems during landing are similar: the possibility of asymmetrical drag and poor braking; and poor nose-wheel lateral traction to combat these conditions plus cross wind and the possibility of asymmetrical reverse thrust. Keeping the tires firmly in contact with the runway during the complete take-off and landing roll is one of the most important problems facing aircraft landing-gear designers today.

Finding detailed answers to all slush problems will most likely take a few years; however, the solutions to the fundamental questions Can aircraft be operated safely in slush? If so, in how much, and what precautions must be taken? are being vigorously pursued.

Slush, as a substance, is a difficult thing to define. It could probably be best described as a heterogeneous mixture of small ice crystals and water which behaves more like a fluid than a solid - more simply, as watery snow.

When rain turns to snow, that portion which falls on streets, sidewalks, and runways makes a rather dense but shallow slush, while that falling on grass remains as wet snow. Deeper slush results from the opposite situation when rain falls on and saturates snow, and when snow melts and saturates itself. Slush produced in this manner tends to be distributed somewhat unevenly, with very dense and deep concentrations at the same locations where standing water is found on runways.

Water has a specific gravity of 1. Dense or heavy slush has a specific gravity near 1, and slush specific gravities can range down to approximately 0.5. In this range, the color also varies from clear to hazy to gray shades, lightening as the density decreases. At a specific gravity of 0.5 it is very white. One of our learned colleagues has chosen to draw the line between slush and wet snow with a very practical but sometimes messy "stomp test." You "stomp" in it with your feet, and if it packs down it is wet snow. If it doesn't pack, you should have been able to tell that it wouldn't by looking at it. Aside from getting a shoe full of ice water, this method is a fairly reasonable way of separating the two. Since by definition slush is required to behave like a fluid, a generalization may be made to the effect that the effects of slush and water on an airplane are identical after a linear density correction is made. This is not strictly true, but viscosity and other factors appear to be second-order effects and can be ignored when working to the accuracies that are practical with slush. The significance of distinguishing slush from wet or dry snow by the fluidity is stronger than it might appear at first glance. A fluid being displaced from the path of a tire must be accelerated from zero to at least the velocity of the wheel. The force required to do this has an equal and opposite reaction which acts on the tire as drag. This slush-displacing force is considerably larger than the force required just to compact snow in the path of the tire.

At high airplane ground speeds the displacement drag, acting as hydraulic pressure on and perpendicular to the tire, causes the tire to lift up off the runway surface in a condition known as hydroplaning. This occurs when the vertical component of the hydraulic force on the tire is equal to the portion of the airplane weight carried by that wheel. Because this exact speed is difficult to detect, "hydroplaning speed" will be used loosely to mean the speed at which the effects of hydroplaning are noted. Unbraked wheel spin down, which occurs when the wheel just begins to lose contact with the runway, occurs at a lower hydroplaning speed than the slush-drag reduction which occurs when the wheel is riding high in the water or slush.

Runway slush is not a new problem to aviation. Occasionally, propeller-driven aircraft have experienced difficulties with standing water on poorly drained runways or have encountered slush of assorted depths and possibly have suffered minor damage; but serious accidents caused by slush have been very few. Only under very unusual circumstances, such as one case of an imprudent attempted take-off in what was reported to have been 5 inches of slush, have aircraft been unable to rotate to a lift-off attitude and become airborne. With the jet airplane the story is somewhat less optimistic.

The big jet airplane does not have the thrust-weight ratio, the surplus of runway, or the low take-off speed that usually characterizes the propeller-driven aircraft. Neither can it assume a take-off attitude early, lift off considerably below normal take-off speed if necessary, and be well off the ground when the needle goes by 120 knots. The big jet takes off fast and lands fast, and this procedure greatly magnifies the importance of any runway contaminant problem, whether it be ice, snow, water, or slush.

Strong interest in the slush problem developed with the introduction of the jets, which tended to be critical for take-off runway length. An accident in Germany with a propeller-driven airplane at about the same time heightened this interest when slush drag was finally listed as a probable cause; however, the incident which started official concern and regulatory action within the FAA was a domestic one.

That incident, which occurred in April 1959, involved a heavily loaded jet departing from New York International Airport on a transcontinental flight with what was reported to have been approximately $1\frac{1}{2}$ inches of slush on the runway. Acceleration was normal, and time to 100 knots was 1 second less than that allowed under the given conditions. Shortly thereafter the airplane ran out of the used portion of the runway and into virgin slush, where the crew noticed an appreciable loss of acceleration. After using nearly all the available runway, the airplane was reported to have cleared the fence by approximately 5 feet. Inspection after the flight revealed considerable slush damage to the aircraft.

That incident resulted in the issuance of an FAA Circular Memorandum which prohibited take-offs with more than a surface covering (any measurable amount) of slush on the runway.

Research by the NASA at Langley Research Center, which was corroborated by a Boeing take-off in six-tenths of an inch of slush at Seattle, indicated that the "no slush" rule was unnecessarily restrictive. A relaxation of the rule was made in March 1960 with the issuance of Operations Division Circular Memorandum 60-7, which prohibited take-offs when there was more than 1/2 inch of slush or standing water on the runway and required correction factors to be applied to take-off runway lengths in slush depths from 0 to 1/2 inch.

All segments of the aviation community have been reasonably satisfied with the 1/2-inch rule, even though it is arbitrary and founded on only a moderately scientific basis. Probably the least satisfied segment was the FAA itself. FAA's desire for an objective slush accountability regulation led ultimately to the test program that is described in subsequent papers of this volume.

In 1960, slush-drag tests conducted by the NASA at the Langley Research Center on single wheels and single tandem wheels established that slush drag closely resembled a velocity-squared function. The hypothesis was advanced that the drag could be predicted by using a fundamental momentum formula which accounted for slush depth and density, and tire frontal area. This method assumed impingement drag and rear-wheel drag on tandem gears to be zero, and was based on tests at speeds below 104 knots.

At approximately the same time, theoretical work was proceeding along somewhat similar lines in the United Kingdom, the Netherlands, and other European countries, as well as in the United States. Some methods took account of wing lift. Spray-impingement drag on the airplane and spray interference on truck-type gears were not taken into account. No test work had been done on transport-size wheels or dual wheels, or on dual-tandem truck bogies, either scale or full size, to account for spray interference. No test work had been done with an airplane configuration in conjunction with the test wheels to assess spray impingement or try to measure its drag.

The real proof was absent in all approaches, since statistical data on slush operations were not available and no full-scale airplane tests had been made under controlled conditions to validate the scale tests and theoretical approaches.

In the spring of 1961, the FAA, with technical assistance from the NASA, planned full-scale tests to measure the drag on a jet transport operating on a runway covered with slush and/or standing water. Much

of the following program is based on those tests, which were conducted between September 25 and October 9, 1961, at FAA's National Aviation Facilities Experimental Center (NAFEC) near Atlantic City, N. J.

The overall objective of FAA activity in the field of slush research is the same as that of the rest of the aviation community: to permit safe and profitable operation on slush-covered runways. The intent is not to dispense with the snowplows and other runway-clearing equipment, but to reach the optimum compromise between the operational capabilities of aircraft and the practical limits of snow and slush-clearing equipment. If aircraft cannot be operated in more than some finite depth of slush without unduly compromising their economic usefulness or their operational safety, then runways and runway-clearing equipment must be designed so that slush depths can always be maintained below that depth.

FAA felt that the first step in reaching the overall objective was to define the capabilities of present-day aircraft, so that an objective slush accountability regulation could be issued to replace the present arbitrary one-half inch rule. The accomplishment of this end implies that another large part of the overall objective be undertaken; that of developing a sound method of day-in, day-out decision making on the big question: Can operations proceed with the runway "as is," or must operations be suspended until the runway has been cleared? This objective requires that the problem of slush measurement be solved.

Snow committees composed of pilots, airport operators, and airline representatives have done a good job, especially from consideration of the unknowns they have to deal with, and individual judgment will never be completely replaced by any type of mechanical device. What is needed, however, is a device or system to assist these people in quickly and accurately assessing the runway condition in a uniform manner. After confidence is gained in the device or system, then measurement could be turned over to someone else for daily use.

The test program which was completed recently at NAFEC took a broad first cut at the overall objective. It was planned basically to validate the method of calculating slush drag and take-off roll proposed in NASA Technical Note D-552 (ref. 1) by full-scale airplane tests under controlled conditions, and if the correlation was not achieved, to collect sufficient data under a variety of conditions to help develop a usable theory.

The specific goals of the slush-drag measurement program were to determine slush-drag forces at speeds from 100 to 160 knots in slush depths up to 2 inches and to determine the incipient damage boundary, slush spray patterns, and hydroplaning characteristics, all in terms of

velocity and slush depth. It was recognized that this program could not do everything that would be desirable in the field of slush research, but is was planned to obtain useful data for this winter's operation. No attempt was made to evaluate the particular test airplane as such, since information collected was to be used to try to generalize for all aircraft, including to a limited extent, the supersonic transport.

Early investigation in the program included testing in both slush and in water until the extensive development program at NAFEC demonstrated the feasibility of manufacturing a consistently reproduceable and representative slush in a controlled depth over a sufficiently large test area. At that point, the effort toward using water as a test medium was stopped. The location for the tests was settled by this same demonstration, since NAFEC was the ideal place to support the aircraft and back up the production of suitable test beds with the many types of supporting services required. Further, NAFEC was chosen in preference to a far north location where snow supply and distribution is free, because there was a requirement for controlled conditions, both in depth and density; and safety was a matter of great concern. In this respect, a minimum of 4,000 feet of dry runway was provided behind the test strip in which to effect a safe stop.

Originally, the intent was to complete the program in July, 1961, so that the data would be reduced, analyzed, and distributed prior to the beginning of this winter's slush season. However, a decision to use a test vehicle with reverse thrust as a backup for brakes eliminated the available KC-135 and a revised schedule was prepared which coincided with delivery of the FAA's new Convair 880M.

One slight additional delay occurred when Hurricane Esther passed along the coast near Atlantic City in mid-September, but winds had subsided and the necessary airborne instrumentation was reinstalled by September 25, when dry calibration and instrumentation checkout runs commenced.

The papers presented at this conference explain the test program that was conducted at NAFEC, present the significant data, explain what was learned about slush-spray patterns and hydroplaning characteristics, cover some recent related NASA research, compare the results of the program with previous work and with theory, attempt to analyze slush depth, density, and velocity effects, consider operational effects from the pilot's viewpoint, and relate the experience in slush measurement in various forms.

REFERENCE

1. Horne, Walter B., Joyner, Upshur T., and Leland, Trafford, J. W.: Studies of the Retardation Force Developed on an Aircraft Tire Rolling in Slush or Water. NASA TN D-552, 1960.

Page Intentionally Left Blank

2. EXPERIMENTAL TECHNIQUES

By Charles M. Middlesworth, John F. Marcy,
Daniel E. Sommers, and Don W. Conley

FAA

I. INSTRUMENTATION AND PROCEDURES

TEST PROGRAM

The test program was conducted from September 15 to October 8, 1961. A series of braking tests was included at the end of the test program. This phase of the work was later enlarged into a separate program of braking tests on the Convair 880-M, the results of which are covered in the second half of this volume. Due to the large scope and unusual nature of the slush task, it was necessary to obtain and evaluate new materials, equipment, and techniques to provide a suitable slush environment.

The test program was established to provide information on the following:

1. Damage to the aircraft from slush or water impingement

2. The relation of drag or retardation forces on the aircraft to ground velocity and extent of runway slush

3. Substantiation of slush drag or retardation forces calculated from deceleration values by actual or attempted take-off in slush

4. Relation of possible "hydroplaning" or aquaplaning characteristics of the aircraft to velocity and extent of slush encountered on the runway

5. Comparison of slush-drag data obtained in this investigation with previous published data, notably NASA Technical Note D-552

The slush test program was divided into two parts: (1) deceleration and (2) take-off. The major emphasis was on the first part of the program, which consisted of a total of 19 unbraked test runs, of which 13 runs were in the slush test strip and six runs on the dry test strip. Two additional runs comprised the second part, consisting of an attempted take-off and an actual take-off in slush. The aircraft at take-off after

a test run is shown in figure 1. In the deceleration tests, the engines of the aircraft were used only to provide the desired test velocity. The energy of the aircraft as it traversed the test strip at idle power was essentially all kinetic, neglecting idle thrust. Loss in kinetic energy due to retardation forces opposing the motion of the aircraft was evidenced by a decrease in velocity. Position and velocity were measured by tracking the aircraft on the ground with phototheodolites, tapeswitches, and AN/SPN-12. These parameters were also measured on the aircraft by use of an airspeed recorder. Actual deceleration was measured directly by an accelerometer placed inside the aircraft. Normal take-off configuration, weight, tire pressure, and idle power (5 percent or less of maximum power) were held relatively constant in all the tests to simplify calculations. Test conditions and safety considerations limited the aircraft to a weight of only 150,000 pounds, compared with the rated maximum take-off weight of 193,000 pounds. The lower weight made it possible to achieve the higher deceleration-test speeds of 140 and 160 knots. In addition, lower weight reduced the problem of aircraft braking and take-off within the 4,000 feet of runway distance remaining after the test run. The idle power setting of the engines, rather than complete shutdown, was used to provide more rapid means for increasing engine power to maximum in an emergency, either for take-off, or for additional braking from reverse thrust.

Drag forces due to slush alone were determined by subtracting from the total force the component due to the dry test strip. The drag or retardation forces were calculated simply by multiplying the mass of the aircraft by its deceleration in accordance with Newton's basic law of motion ($F = Ma$). In order to separate out the slush-drag component due to the main landing gear from the total aircraft slush drag, a test run was made with the nose gear running dry through a slot down the center of a specially prepared slush bed. Data were reduced to standard day conditions by calculation from meteorological data and the manufacturer's performance data. Performance data derived in the tests were substantiated by actual and attempted take-off of the aircraft in slush.

TEST OPERATION AND PROCEDURES

All operations were coordinated from a centrally located instrumentation and test-control van at the side of runway 31-13 near the test area. From this position, liaison between personnel responsible for each operation was maintained prior to and during each test by means of an intercom system, radio, public address system, and telephone. Location of various operations at the test site is shown in figure 2.

Test runs were planned in relation to a stationary 1,000-foot-long test area on runway 31-13 located between 5,000 and 6,000 feet from the

threshold of 31. Tests to obtain drag forces on a dry runway and through slush were planned as deceleration runs with test-area entry speeds of 100, 120, 140, and 160 knots at a minimum engine thrust output. To obtain these conditions, the starting position for the aircraft in each test was calculated from Convair flight-test data, taking into consideration the acceleration distance to a throttle chop position, distance for engines to spin down to idle thrust before entrance into the test area, and sufficient distance for stopping after exit from the test area if brakes only were available. All 100-, 120-, and 140-knot runs were conducted on a heading 310°. The 160-knot test runs were conducted during a landing on a heading of 130° to obtain the necessary test-area entry speed. In stopping the aircraft after exit from the test bed, the pilot used a combination of reverse thrust and brakes and encountered no difficulty in stopping throughout the tests. Two take-off runs were conducted, one through a 3,000-foot slush bed with an entrance velocity of 100 knots and the other through a 1,500-foot slush bed with an entrance velocity of V_R (124 knots IAS). Control of the aircraft heading through the slush bed was maintained by use of the rudder only. The distances required for each run are shown in figure 3.

Gross weight of the aircraft was controlled within the limits of 148,200 and 152,400 pounds by refueling to a maximum capacity prior to each test run. Refueling was done at the same spot each time to obtain a consistent fuel load. The length of time that each power setting was utilized during each run was recorded. The aircraft configuration established for all tests was that required for normal take-off; that is, inboard leading-edge Krueger flaps in the down position, trailing-edge flaps at the 22° position, and outboard leading-edge slats open. The center of gravity was maintained at a constant 27.7 percent of the mean aerodynamic chord. Tire pressures were measured before and after each run and were maintained between 150 and 160 lb/sq in. for main-wheel tires and 125 to 130 lb/sq in. for nose-wheel tires. Actual test conditions are presented in table I.

All test operations were geared to a brake-release time for the test aircraft. The time of brake release as well as the type of runs to be conducted each day were established at a briefing/debriefing meeting held with test-operation personnel the day before each test. The general procedure for the test operation was as follows:

1. Three hours prior to brake release, preparation of the test area commenced.

2. One hour 15 minutes before brake release, all instrumentation and cameras were set up and checked for operation. The aircraft was fueled and towed to a starting position. Communications were established with the various personnel responsible for different phases of operation.

3. Fifteen minutes before brake release, the aircraft engines were started, primarily to allow warmup time for airborne instrumentation. The test area was cleared of nonessential personnel and equipment. Slush density and depths were measured. The pilot was given information in regard to wind direction and velocity as well as temperature so that he could adjust engine power for the run. Clearance to commence run was obtained from the appropriate authority.

4. Thirty seconds before brake release, aircraft engine power was increased to maximum thrust.

5. Five seconds prior to brake release the pilot counted down so that all personnel were alerted, and then the run was commenced.

6. Twenty seconds after the aircraft came to a stop, engines were shut down and the aircraft was inspected for damage, after which it was either towed or taxied back to the refueling spot at the threshold of runway 31.

7. A debriefing meeting was held 1 hour after each slush run.

TEST VEHICLE

The test vehicle was a Federal Aviation Agency (FAA) Convair 880-M which was powered by four pod-mounted General Electric turbojet engines, rated at 46,600 pounds' total maximum thrust. The aircraft was provided from the FAA Aeronautical Center, Oklahoma City, Okla., and was maintained by Center personnel. An FAA test pilot, along with the designated first pilot and flight engineer, operated the aircraft during these tests. A number of modifications to the aircraft were necessary to install the instrumentation. Changes included removal of the nosewheel doors and outboard landing lights to permit camera installation, removal of access doors and attachment of a camera carriage in that location in the lower fuselage, installation of electrical wiring from the antiskid sensing unit in all wheel wells to a recorder within the main cabin, mounting of cameras within the pilot and passenger compartments, mounting of NASA instrumentation and recorders within the passenger compartments, and installation of various electrical connections to the aircraft power supply to operate the equipment.

Engineering specifications of the Convair 880-M and its powerplant as obtained from the manufacturer are given below:

1. Powerplant: General Electric CJ-805-3B
   (a) Maximum thrust (take-off): 11,650 lb/engine
   (b) Maximum thrust (idle): 300 lb to 450 lb/engine

2. Weight, gross:
   (a) Test: 150,000 lb (average)
   (b) Maximum take-off: 193,000 lb
   (c) Distribution (static): 12,950/170,500 lb (7.6 percent of aircraft weight on nose gear)

3. Wing area, aerodynamic:
   (a) 2,000 sq ft

4. Tire size:
   (a) Main (8): 39 × 13 type, 22-ply, type VII; pressure 130 to 150 lb/sq in.
   (b) Nose (2): 29 × 7.7 type, 12-ply, type VII; pressure 110 lb/sq in.

5. Tire friction coefficient:
   (a) 0.015 maximum unbraked

6. Lift and drag coefficients, landing:
   (a) C_D = 0.194 (spoilers out)
   (b) C_L = 0.190 (flaps down)

7. Lift and drag coefficients, take-off:
   (a) Obtained from manufacturer's curves

8. Angle of attack, take-off:
   (a) 3° before rotation
   (b) 13.8° after rotation

9. Flaps, take-off:
   (a) Main, 22° deflection
   (b) Krueger extended
   (c) Spoilers retracted
   (d) Leading-edge slats open

10. Take-off velocity, normal configuration:
   (a) V_R = 145 knots IAS (193,000 lb)
   (b) V_R = 124 knots IAS (150,000 lb)

INSTRUMENTATION

Ground

The major effort in the instrumentation of the task was concerned with the measurement of aircraft position, velocity, and acceleration

or deceleration with reference to time and position along the runway test strip. Accuracy of this instrumentation is important since the degree of accuracy of the calculated drag forces is thereby determined. Velocity and deceleration data used in these calculations were obtained mainly by phototheodolites and the airborne accelerometer, respectively. The equipment was extensive since backup systems were needed in case of failure and for cross-checks. Other equipment was used to record weather conditions, which included wind direction and velocity, temperature, and barometric pressure, to permit reduction of test data to standard day conditions.

Phototheodolites.- These items are part of the permanently established NAFEC test facilities designed for visually tracking aircraft both in azimuth and elevation. A photograph of a phototheodolite tower (P 13) in use is shown in figure 4. This is one of three towers 66 feet in height. The fourth tower is 44 feet in height. This facility provided aircraft position-time data in increments of 0.050 second. The phototheodolites are mounted atop towers located nearly opposite one another at both ends of runway 13-31 as shown in figure 2. A well-defined target point on the aircraft was used by the operators to sight against the crosshairs in the center of the field of view. In the earlier tests two black squares painted on top of the fuselage above the aircraft's center of gravity were used as a target area. In later tests the vertical edge of the tail of the aircraft was used as the target, since the first target was too difficult to track. The field of view was photographed by a camera attachment with a 60-inch telephoto lens which operated at 20 frames of 35-mm film per second. A reproduction of one of the frames is shown in figure 5. The tail of the aircraft is photographed against the background of the crosshairs. The horizontal lines along the left margin of the figure are coded time signals. At the bottom of the figure, reading from left to right, are given the azimuth angle, elevation angle, and frame number. The angles were corrected for displacement of the target point from the crosshairs. From data consisting of bearing angles supplied by phototheodolites keyed to a common time base, and from accurately surveyed distances between phototheodolite stations, the position of the aircraft was calculated by triangulation. Four phototheodolites were used in the tests to provide greater accuracy. Optical tracking limited the test runs to daylight and clear visibility. Basic accuracy of the device was $\pm 0.001^{\circ}$, which is the smallest scale division to which bearing angles are read.

Tapeswitches.- Tapeswitches were bonded with epoxy cement to the runway as a temporary measuring facility. Typical installation of one tapeswitch across the entire 50-foot width of the test strip is shown in figure 6. A total of 57 tapeswitches were used to provide aircraft position-time data in increments of 20 feet. This covered a distance of 1,120 feet, including 80 feet ahead of the 1,000-foot test bed and 40 feet beyond the end of the test strip. Other tapeswitches were attached to the runway at four separate locations to provide audio beep signals radioed to the aircraft. These gave the pilot a signal at each

of three points shown in figure 2: where to cut engines, when he was entering the slush-bed area, and when he had departed the slush area. The tapeswitches were about $1\frac{1}{2}$ inches in width and $\frac{3}{8}$ inch in height, tapered from the edges to provide less obstruction. Detailed views of the construction are shown in figure 7. In the two upper views the metal contacts and insulators are pried open for easier identification. Two flexible strips of metal about 1/2 inch wide and 0.005 inch thick, separated by a distance of 0.010 to 0.015 inch, constituted the active contact surfaces. The strips were insulated from each other at the edges by a nylon spacer strip about 1/8 inch wide and about 0.010 inch thick running the entire length of the tapeswitch. The metal strips were embedded in a vinyl material for support and insulation. Pressure of 25 lb/sq in., or finger pressure, applied at any point on the tapeswitch produced sufficient deformation to bring the two metal strips into contact with each other, completing a closed circuit to produce a signal. The material used was designated by the manufacturer as Road Switches, Type RB-W. This particular type of heavy-duty switch was supplied by the Tapeswitch Corporation of America and was designed for road traffic.

In the earlier tests, the 57 tapeswitches were connected end-to-end for a single continuous circuit. A 12-volt battery and a 200-ohm dropping resistor were placed in series with a 3,000-cps galvonometer. Passage of a vehicle over the tapeswitches caused a succession of short circuits which closed the battery circuit, thereby deflecting the galvanometer and producing a series of square wave pulses. Coded time pulses of 0.01 second from the central real-time system were recorded simultaneously by a second galvanometer to provide accurate time-interval measurements between tapeswitches. A section of an oscillogram record is shown in figure 8. It shows the passage of the nose wheel across the first three tapeswitches, followed by the front and rear bogie wheels. Distance between the nose gear and main gear may be calculated from the time pulses and the known surveyed distances of 20.00 (±0.02) feet between tapeswitches. Likewise, the average velocity of the aircraft may be calculated from the time interval between two corresponding points on the oscillogram, as shown in the figure. Only one galvanometer channel was used to record all 57 tapeswitches. A separate channel, as shown in figure 8, was used to record aircraft velocity furnished by the AN/SP-12 simultaneously with tapeswitch position-time data.

In later tests (after test 14), for easier maintenance and greater reliability, the tapeswitches were rewired. Ten galvanometers were used to record the 57 tapeswitches divided into separate groups of normally 6 tapeswitches per channel. Maximum recording speed also was increased from 25 inches per second to 100 inches per second for greater resolution of the test data. Coded time pulses only 1/10 as long, or 0.001 second, were provided for the same purpose. A section of the oscillogram record for these later tests is shown in figure 9. It

shows enlarged views of the tire footprints as the wheels pass over several tapeswitches. Consistency of contact make-and-break between two adjoining tapeswitches as the main gear crosses the tapeswitches at 105 knots is shown to be excellent. This indicates the high degree of accuracy in velocity measurements possible with tapeswitches.

AN/SPN-12.- The AN/SPN-12 equipment was provided by the Department of the Navy for the duration of the tests. The equipment is designed for use as a Doppler radar system to monitor the speed of aircraft during landing aboard an aircraft carrier. Velocity-time data on a continuous basis were recorded simultaneously with tapeswitch data in order that the velocity measurements might be keyed to 20-foot increment positions, as shown in figure 8. A separate recorder at the AN/SPN-12 location was used near the end of the program to reduce the excessive hash in the transmitted signals found in the earlier test recordings. AN/SPN-12 measurements also were intended as a backup system and to provide immediate readout of velocity in knots directly from a dial. The location of this instrumentation relative to the test vehicle and other equipment within the test site is shown in figure 2.

Airborne

Test equipment on the aircraft was supplied and operated by personnel of the NASA Langley Research Center. This included the following items: accelerometer, airspeed indicator, and attitude indicator. These instruments, designed by NASA, were packaged as one complete unit and are shown in figure 10. Indications of the three instruments were recorded on separate film drums attached to each instrument (not shown in the figure). The airspeed recorder was intended as a backup device. Each oscillogram trace was made by rotation of the light beam, normal to the direction of film travel, from galvanometer mirrors attached to the sensing elements of the instrument. The film record speed was 1.0 inch per second. In addition, NASA provided a recorder for measurement of aircraft wheel rotation.

Accelerometer.- The sensing element of the accelerometer consisted of a pendulum mass mounted on a pivot shaft supported by jewel bearings, to which was attached a reflecting mirror. Movement of the sensing element in response to acceleration was limited by spring tension which determined the sensitivity and frequency response of the instrument. Specifications for this instrument were:

Range, g units	±0.5
Sensitivity, g/in.	0.54
Frequency response, cps	9.5 (flat to 6.0)
Damping, percent of critical	67

Overall accuracy (for temperature range of 0° to 120° F):	
Static, percent of full scale	±1
Dynamic, percent of full scale	±2
Recording accuracy, g units	±0.005

A typical record of the accelerometer for a 1,000-foot slush-test run is shown in figure 11. A rapid increase in deceleration of the aircraft is shown (about 1/2-inch deflection of the trace downward) when the nose wheels suddenly encounter the slush upon entering the test strip. Maximum deceleration is delayed about 0.25 second until both the nose and main wheels have entered the slush. Decelerations are measured from the zero line to the line faired through the oscillations which are characteristic of the instrument response and not of any particular significance. Variations in deceleration values show that drag forces are not constant through the test strip, which could indicate the degree of unevenness in the slush cover. Recorded deceleration values shown vary from 0.228g (minimum) to 0.311g (maximum) in slush and average 0.043g on the dry runway.

Attitude recorder.- The sensing element of the attitude recorder consisted of a gyro unit to indicate angular movement in pitch. The spin axis of the gyro was maintained perpendicular to the surface of the earth as a reference position. Rotation of the gimbal with reference to the horizontal was indicated by an optical system of 18 reflecting mirrors mounted on the sensing element. Specifications for the instrument were:

Range, deg	0 to 360
Sensitivity, deg/inch for ±5° pitch	10.893
Gyro drift (bench), deg/10 min	0.04
Recording accuracy, deg	±0.052

A typical record of the attitude gyro for a 1,000-foot slush-test run is shown in figure 11. Very little change in attitude of the aircraft is noticeable, and corrections for this effect were only 1 to 2 percent.

Airspeed recorder.- The sensing element of the airspeed recorder consisted of a corrugated nesting-type diaphragm surrounded by an airtight capsule. The unsupported end of the diaphragm moved almost linearly with the change in differential pressure. Motion of the diaphragm was recorded optically, as with the accelerometer. A typical record of the airspeed recorder for a 1,000-foot slush-test run is shown in figure 11. The instrument was corrected for temperature by a bimetal arm connected to the diaphragm. Specifications for this instrument were:

Range:	
Knots	0 to 170
In. H_2O	0 to 20
Sensitivity:	
In. H_2O per in. trace deflection	2 to 2.5
Knots per in. trace deflection at 170 knots	17
Natural frequency, cps	200
Accuracy:	
From hysteresis and friction, percent	0.25
From temperature, percent	±0.25
From acceleration, percent	0.10
From reading, percent	±0.125

Aircraft wheel rotation (rpm).- Indication of wheel rotation to detect aquaplaning was greatly facilitated by tying into the existing Hydro-Aire Mark 1 antiskid system which is standard equipment on the Convair 880-M aircraft. In this sytem, each of the eight main landing wheels and the pair of nose wheels is provided with an rpm-counter pick-off. Rotation of each wheel produces four electrical pulses per revolution to operate the system and detect wheel slippage for antiskid braking. NASA tapped a small part of the signal from each wheel, and these parts were recorded on nine separate channels of an oscillograph. Film record speed was 1.0 inch per second. The recording equipment, together with other airborne equipment, was mounted on a board approximately 3 feet by 3 feet secured to metal mounting brackets inside the passenger compartment at about the center of gravity of the aircraft. The instrumentation is shown in figure 10. A record of the rotation of the aircraft wheels is shown in figure 12. This is one of two records which showed a complete stoppage in slush of one of the rear main wheels (solid trace). This is unusual since the record shows very little slippage for the other three wheels. By comparing the frequency or spacing between cycles (shown as dots) inside and outside the slush area, the degree of wheel slippage was determined. All four front main wheels show considerable slippage, while the nose wheels, surprisingly, show only a slight slippage. However, in other slush tests the slippage is about the same in both cases, which shows the inconsistency in this type of data. Complete wheel rotation and slippage data for all tests are given in paper no. 3 by Eugene P. Klueg. These data are of particular interest as regards the aquaplaning characteristics of the aircraft.

DATA REDUCTION

Phototheodolite

The processing of these data was extensive and was facilitated by the use of specialized equipment. Phototheodolite data were converted to a time history of aircraft position by use of an IBM 7090 computer. An average location was computed for each time by using all four station readings. Station readings which differed markedly from this average were discarded and a new average was computed. Position-time points at 0.05-second intervals were corrected by applying a 5-point least-squares smoothing process. This provided a smoother curve by averaging position data over a period of 0.25 second, which is equivalent to a distance of 50 feet at a speed of 200 feet per second. Velocities were determined by computing the slope of the smoothed position-time curve at intervals of 0.05 second. The slope of the curve at a point was considered to be the value which minimized the quantity

$$D = \sum_{n=-10}^{10} \left(y_{nt} - y_n\right)^2$$

where

D deviation

y_n ordinate of the position-time curve at point n

y_{nt} ordinate at point n of a straight line drawn tangent to the curve at point $n = 0$

n a reading point (zero at the point of tangency)

Accelerations were determined by computing the slope of the velocity curve by a similar method, except that the summation was carried out over 41 points instead of 21 (± 20 instead of ± 10). Extensive smoothing and fitting of the curves is required by the limited accuracy of the position-time data. Accuracy of these data is estimated to be in the range of 1/4 to 1 foot.

Tapeswitch

The position of the aircraft at 20-foot intervals was read from the records made by the wheels of the landing gear as these wheels shorted

successive tapeswitches. The tapeswitch data did not distinguish whether the left or right bogie made the first contact. The oscillograms recorded a sharp break in the zero reference trace at the instant closing of the tapeswitch, which was read off the central coded time signals (divided into 0.001-second pulses) appearing on the same oscillograms (fig. 9). Time was read to 0.0001 second, which corresponds to a position error of ±0.02 foot, an error equal to that of the surveyed position of the tapeswitch. To achieve optimum accuracy, recording speed was increased to 100 inches per second. Incomplete tapeswitch-data processing indicated that the position accuracy of the aircraft on a dry runway could be determined to within ±0.10 foot. However, corresponding data in slush showed considerable variation in position accuracy of the aircraft. Examination of the different oscillograms revealed that the tread print of the tire passing over the tapeswitch was not of constant length as measured from the time the tapeswitch closed. Although oscillogram records of adjacent tapeswitches indicated that the aircraft was in position to close the tapeswitch under consideration, this did not always occur. The oscillograms on which this condition was evident were again read, using both the nose wheel and rear bogie wheel for a time measurement of position. Consistency of the data for both nose wheel and rear bogie wheel improved to about that obtained for the dry runway tests. It would seem that slush buildup under the front tires of the main gear obstructed the closing of the tapeswitch. Since most of the slush is pushed out of the path of the rear tires by the front tires, the rear tires would be expected to provide more reliable data, as was the case. While errors of ±0.10 foot in position would appear small, this is equivalent to an error at 200 feet per second of ± 1 foot per second in velocity, and ±20 feet per second squared or ±0.62g in the acceleration or deceleration. Because of the need for extreme accuracy in position measurement, only average values of velocity and acceleration or deceleration may be derived from position-time data. The more accurate the basic data, the smaller the test strip that need be taken for a reliable measurement of average acceleration or deceleration. Accuracy of these measurements increases as the square of the distance increment. The average calculated values of acceleration or deceleration would be 25 times more accurate for 100-foot increments (6 tapeswitches) than for 20-foot increments (2 tapeswitches). Therefore, the smoothing process to be adopted is dependent on the accuracy of the basic data. Excessive smoothing would tend to obliterate rapid changes in acceleration or deceleration of the aircraft, such as may result from uneven slush on the runway. The tapeswitch data have not been completely reduced because of limited time.

AN/SPN-12

Continuous velocity-time data were obtained from the deflection of the oscillograph trace of the AN/SPN-12 (fig. 8). Output voltage

was essentially linear with velocity in the 100-to 160-knot range. Calibration of the device in knots per volt was obtained directly from the radar frequency. Accuracy was affected by hash in the signal which made reading of the recording traces difficult. The data have not been completely reduced because of limited time.

Weather

Wind direction and velocity data at a 20-foot elevation were obtained from a remote-recording weather station located within 1,000 feet of the center of the test strip. Prior to and during the test run, dial readings of wind direction and velocity were recorded. These data, together with atmospheric and temperature data, were tabulated to convert aerodynamic drag of the aircraft to standard conditions.

Airborne Accelerometer

The choice of the accelerometer rather than position-tracking devices for deceleration measurement is of considerable interest. In the actual range of deceleration measurements, 0.04g for a dry run and 0.30g for a slush run, accelerometer accuracy of ±0.005g is equivalent to about 10 percent to 2 percent, respectively, or about ±750 pounds drag. The advantage of the accelerometer in drag force calculations is limited to obtaining data at a point or over a relatively short distance increment. However, for average deceleration data over distance increments greater than 200 feet, the accuracy provided by the tracking devices exceeds that of the accelerometer.

Photographic Coverage

Extensive use of motion-picture photography was made to record the results of the high-speed aircraft encountering the slush. Cameras both on the ground and on the aircraft were situated so as to reveal the dispersal of the slush by the landing gear, buildup of slush ahead of tires, and the impingement of the displaced slush against various parts of the aircraft structure. The effect of slush on the stability of the aircraft was shown by one camera located in a helicopter over the test area for a top view, and by two cameras fitted with telephoto lenses located at the end of the runway for a head-on front view.

The type and location of the cameras on the ground in relation to one another and to the test site are shown in figure 13. Twenty-one cameras are listed. The helicopter provided excellent coverage from above. The cameras at the end of the runway, equipped with long-range

telephoto lenses, provided excellent head-on views of the aircraft. The type and location of each camera on the aircraft and the specific area viewed by each camera are shown in figure 14. The cameras located under the fuselage were obscured to a large extent by slush thrown up by the wheels. Cameras at the wing tips provided better coverage. Movie films taken of the test runs are to be edited and made into a documentary motion picture of the task. The pictorial presentations of slush in relation to the aircraft given in subsequent papers show how the complete photographic coverage provided a more complete understanding of the problem.

II. TEST-AREA PREPARATION

TEST BED

Slush was provided on the test strip by crushing cake ice with ice crusher-slinger machines and spraying the resulting snow-ice directly on the runway between wooden forms of a predetermined depth. Leveling was performed manually by swinging long boards down against the top of the wooden forms and pushing the snow-ice forward. When the snow-ice had melted down to a predetermined depth and the resulting slush had the appearance and consistency of natural slush, the test bed was considered ready for a test run. The overall snow-ice laydown operational plan and a sequence of photographs of a test bed being prepared are shown in figures 15 and 16.

A total of eight ice crusher-slinger machines were used to prepare each test bed. Each machine was attached to a tractor-trailer loaded with 120 cakes of ice, which provided a capability of crushing ice continuously while both tractor-trailer and ice crusher-slinger machine were in motion. The ice machines used were portable, gasoline powered, and capable of crushing 300-pound cakes of ice at a rate of about 50 tons per hour each. The specific weight of the snow-ice produced by the machines was about 37 pounds per cubic foot with the following weight distribution of the particles: 85 percent less than 1/4 inch in diameter, 12 percent between 1/4 inch and 1/2 inch in diameter, and 3 percent greater than 1/2 inch in diameter.

The theoretical initial depth of snow-ice required to obtain a certain depth of slush is shown by the graph in figure 17. The 5,000 feet of temporary wooden forms which were placed on the runway for the purpose of controlling the depth were cut to dimensions which followed this theory. However, in all cases the actual depth laid down was greater than that aimed for (table I). This was due to the leveling technique

and the fact that the wooden forms were not flush with the runway, as can be seen by the illustration of figure 18. The result was a variation in depth and density throughout the test bed. Variation was also caused by the fact that those areas of the test bed that were prepared first experienced longer melting periods than those prepared last. This effect was not appreciable for the first test bed of the day, since preparation began during the colder part of the day (6 a.m.). However, those test beds prepared later in the morning usually had several areas where the slush had melted to water.

Originally, testing in slush depths up to 3 inches was contemplated. Since laboratory experiments showed that a good slush consistency could not be obtained at depths greater than 2 inches under natural water run-off conditions, dikes were utilized. It should be noted that on the second slush-test run (8A), the interior dikes were torn out by the aircraft. However, this fact did not hinder the program, since all tests were conducted in slush 2 inches deep or less. The dike installation and runway elevations are shown in figure 19.

SLUSH MEASUREMENTS

Approximately 15 minutes prior to release of the airplane brakes, slush samples were taken throughout the test bed with special scoops. Each sample was measured for depth and was weighed. Knowing the cross-sectional area of each scoop, the runway loading (lb/sq ft) and specific weight or density were calculated. Photographs of the tools used to obtain slush samples and make measurements are shown in figure 20. The technique used for slush measurements is illustrated in six steps in figure 21. It should be noted that this technique is basically the same as that used by NASA in their slush test with a single wheel. The approximate locations where samples were taken in the test bed are shown in figure 22.

TABLE I.- AIRCRAFT TEST-RUN CONDITIONS

[Average density of slush, 1.585 slugs/cu ft; specific gravity, 0.817; all aircraft velocities are ground velocities]

Test no.	Date (1961)	Time, e.d.t.	Nominal slush depth, in.	Nominal vel., knots	Aircraft heading, deg	Direction of travel (a)	Position of slush bed, ft (a)	Ambient temp., °F	Atm. pressure, in. Hg	Wind		Aircraft gross weight, lb	Aircraft velocity at slush bed				Effective slush depth (av.), in.
										Direction, deg	Vel., knots		Enter		Exit		
													knots	ft/sec	knots	ft/sec	
Deceleration test runs, 100 to 140 knots																	
1	9/25	0813	0	120	310	→	4,960-5,960	73½	29.81	0	13	151,600	111.6	188.5	107.6	181.7	0
2	9/25	1159	0	120	310	→	4,960-5,960	81½	29.77	350	11	151,600	111.9	189.0	108.0	182.4	0
3	9/26	1441	0	140	310	→	4,960-5,960	80	29.92	290	11	151,800	125.8	212.5	121.7	203.9	0
5	9/28	1056	0	140	310	→	4,960-5,960	74	30.06	325	7	152,400	129.4	218.6	124.9	210.9	0
7	10/4	1600	0	120	310	→	4,960-5,960	60	29.91	310	15	151,900	112.4	189.8	108.1	182.5	0
8	9/26	0742	1	120	310	→	4,960-5,960	70	29.84	235	7	151,400	115.8	195.5	102.4	172.9	1.26
8A	9/27	0816	½	120	310	→	4,960-5,960	59	30.14	40	3	151,900	115.4	194.9	102.1	172.5	.74
8B	10/9	0903	½	120	310	→	4,960-5,960	60	30.04	300	8	148,700	115.8	195.6	102.4	173.0	1.22
9	9/29	1146	½	140	310	→	4,960-5,960	60½	30.24	0	12	150,000	130.4	220.3	115.1	194.4	1.11
11	10/9	0815	1	120	310	→	4,960-5,960	60	30.04	315	7	150,700	115.8	195.5	98.9	167.0	1.49
12	10/1	0736	1	140	310	→	4,960-5,960	50½	30.30	5	4	150,800	134.7	227.5	122.6	207.1	1.07
14	9/29	0916	1½	120	310	→	4,960-5,960	58	30.24	25	11	151,100	119.1	201.2	94.6	159.7	1.94
15	10/1	1017	1½	140	310	→	4,960-5,960	70	30.31	135	12	151,800	135.7	229.2	117.2	197.9	1.61
19	10/6	0901	[b]1½	120	310	→	4,960-5,960	62	30.22	300	6	151,700	115.1	194.3	99.1	167.4	[c]1.34 to 1.43
20	10/5	1345	1½	105	310	→	4,960-5,960	66	30.19	265	10	151,500	101.4	171.2	89.9	151.8	1.23
20A	10/6	1110	1½	105	310	→	4,960-5,960	73	30.21	295	9	151,700	97.5	164.7	76.5	129.2	1.96
Deceleration test runs, 160 knots																	
4	9/27	1500	0	160	130	←	4,960-5,960	71½	30.09	140	7	149,600	153.8	259.8	149.3	252.2	0
10	10/5	0817	½	160	130	←	4,960-5,960	44	30.22	295	5	148,200	157.6	266.1	150.3	253.8	.91
13	10/5	1119	1	160	310	→	4,960-5,960	61	30.24	295	3	148,800	156.6	264.5	147.0	248.2	1.14
Acceleration and take-off test runs																	
17	10/7	0915	1	100	310	→	3,000-5,960	62	30.17	345	6	150,900	100.0	168.9	130.9	[d]221.1	[e]0.90
18	10/8	0803	1	124	310	→	3,500-5,960	58	30.10	0	0	150,400	127.7	215.6		[f] V_R	1.32

[a] From 31 end of runway 13-31.

[b] Slush-bed depth variable, 1 to 1½ in.

[c] First 500 ft of slush bed slotted for nose gear; slush bed normal for last 500 ft of 1,000 ft.

[d] Rotation and take-off outside of test bed.

[e] Slush depth for only first 1,500 ft of test bed.

[f] Rotation and take-off inside of test bed.

Figure 1 L-61-6971

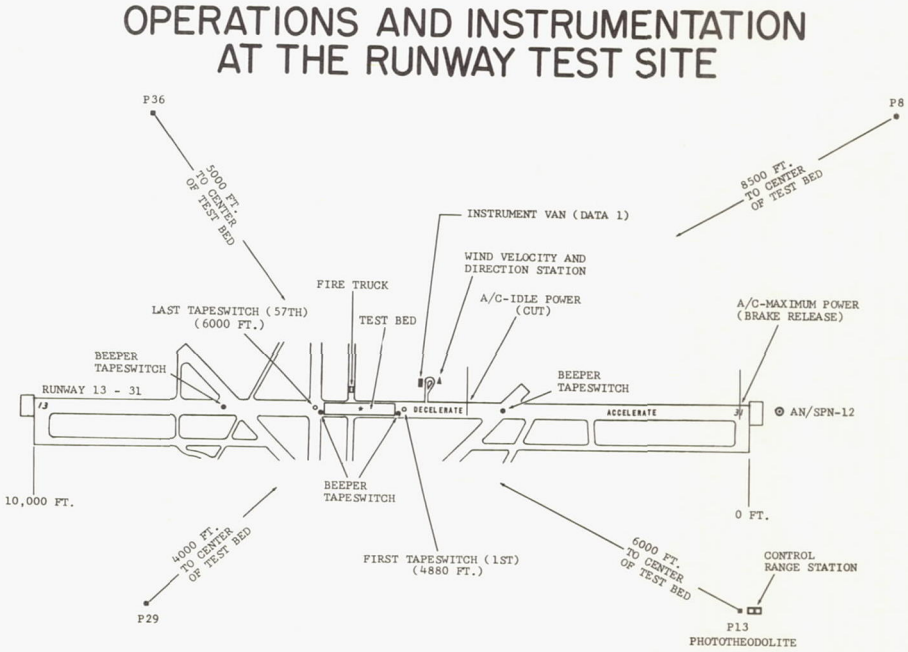

Figure 2

AIRCRAFT TEST-RUN OPERATIONS

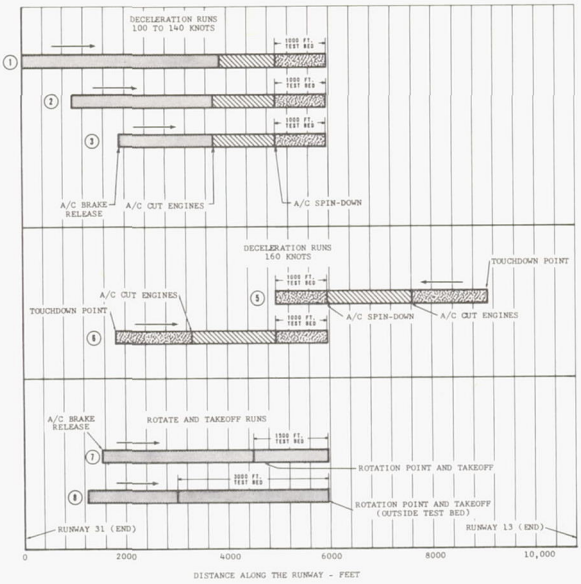

ACCELERATION DISTANCE

THRUST DECAY DISTANCE

DECELERATION DISTANCE

	TEST NUMBER	NOMINAL VELOCITY TO SPIN DOWN (KNOTS)
1	3, 5, 9, 12, 15	140
2	8B, 11, 19, 1, 2, 8, 8A, 14, 7	120
3	20 AND 20A	105
5	4, 10	160
6	13	160
7	18	124 (V_R) IAS
8	17	100

Figure 3

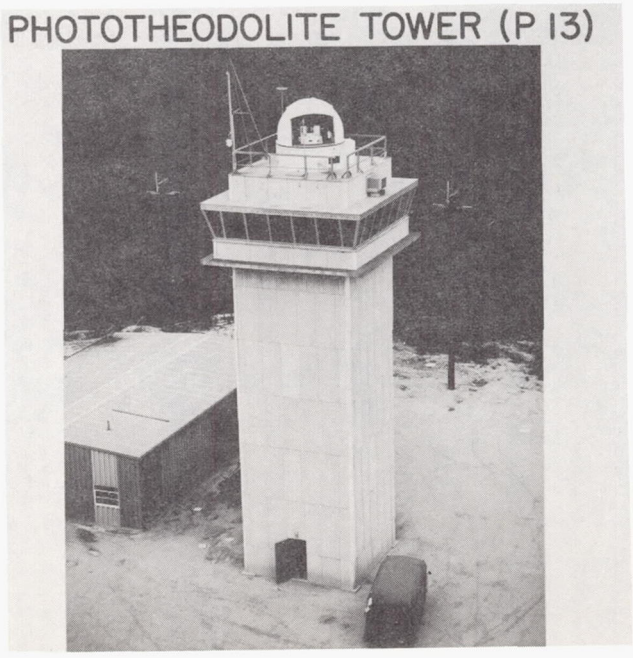

Figure 4 L-61-6969

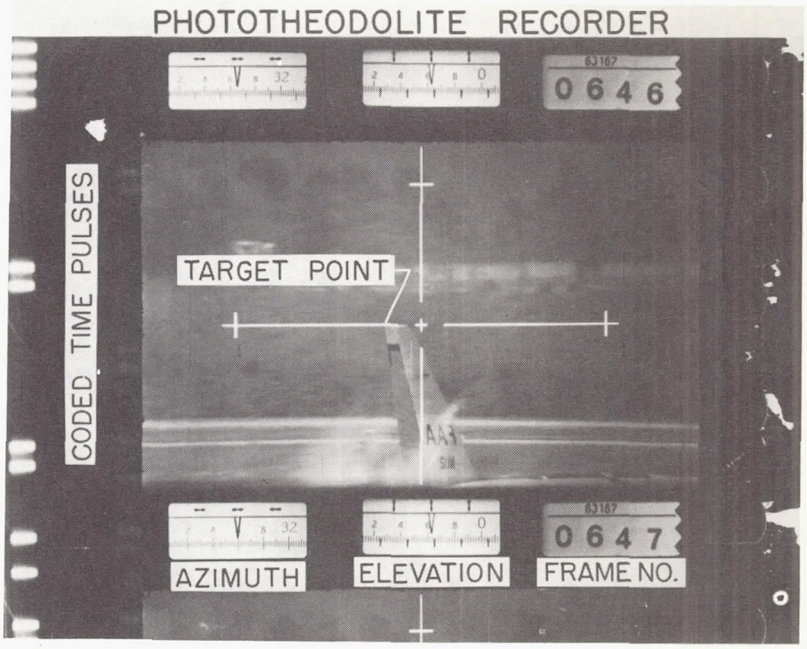

Figure 5 L-61-6972

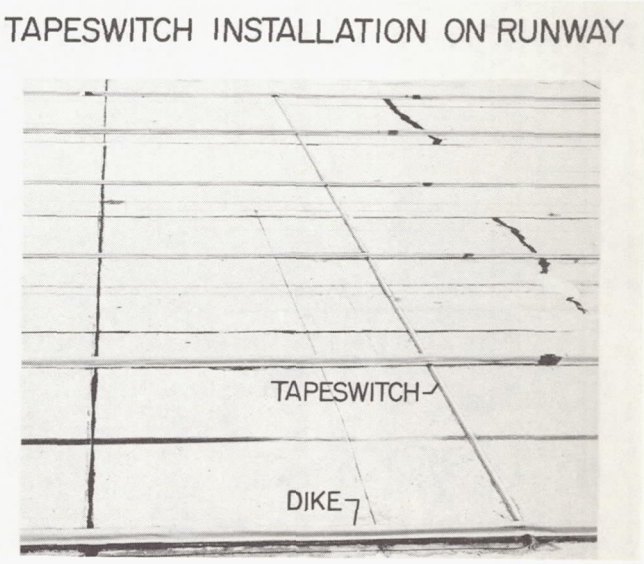

Figure 6 L-61-6970

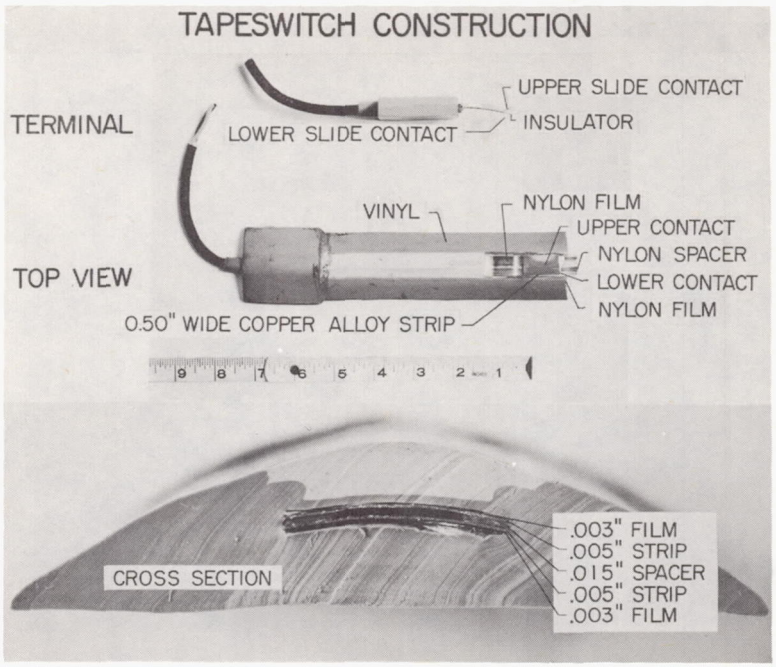

Figure 7 L-61-6973

TAPESWITCH AND AN/SP-12 RECORD

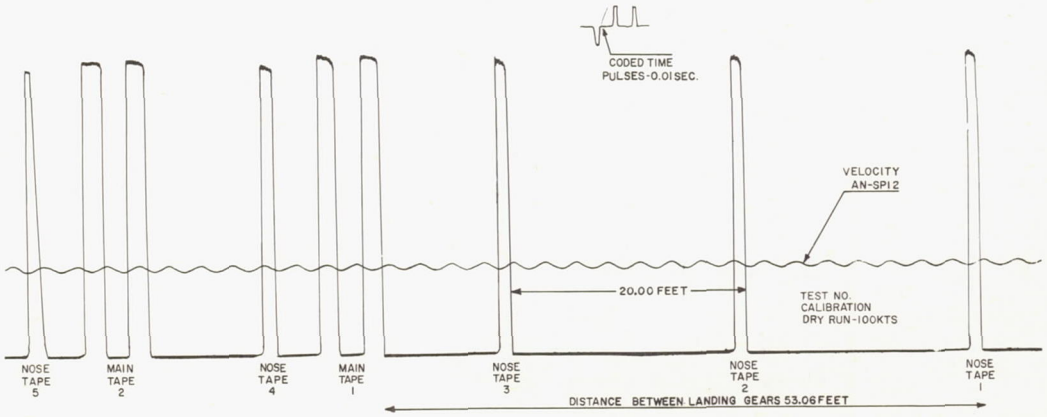

Figure 8

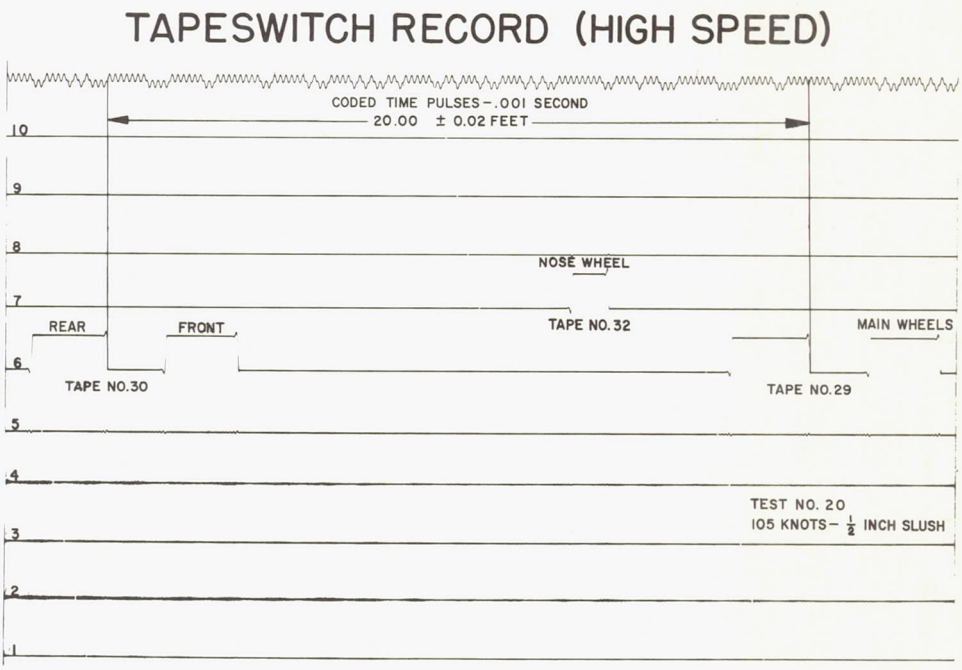

Figure 9

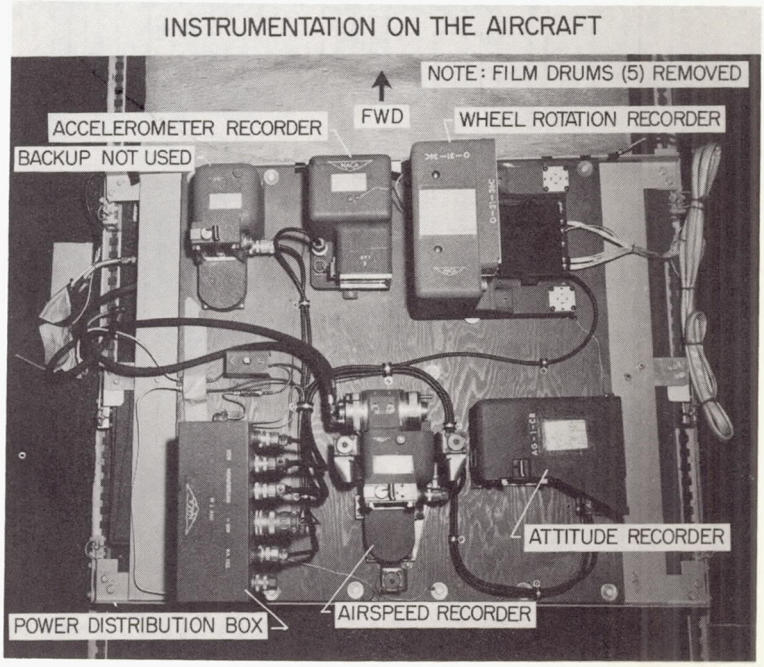

Figure 10

L-61-6974

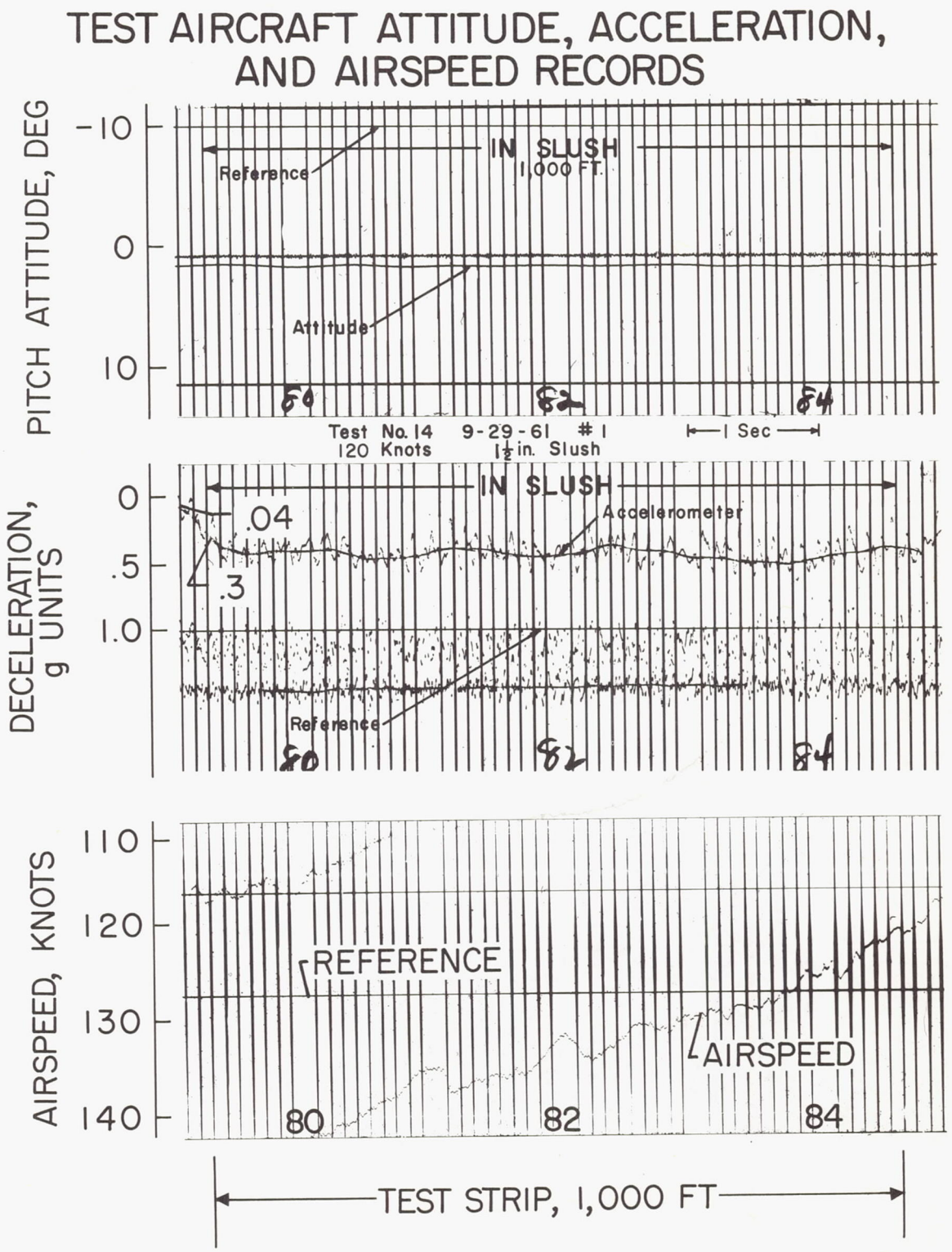
TEST AIRCRAFT ATTITUDE, ACCELERATION, AND AIRSPEED RECORDS
PITCH ATTITUDE, DEG
-10
0
10
Reference
IN SLUSH
1,000 FT.
Attitude
80
82
84
Test No. 14 9-29-61 #1
120 Knots 1½ in. Slush
1 Sec
DECELERATION, g UNITS
0
.5
1.0
IN SLUSH
.04
.3
Accelerometer
Reference
80
82
84
AIRSPEED, KNOTS
110
120
130
140
REFERENCE
AIRSPEED
80
82
84
TEST STRIP, 1,000 FT

Figure 11

AIRCRAFT WHEEL ROTATION RECORD

TEST NO. 14; 9-29-61 NO. 1; 120 KNOTS; 1 1/2 IN. SLUSH

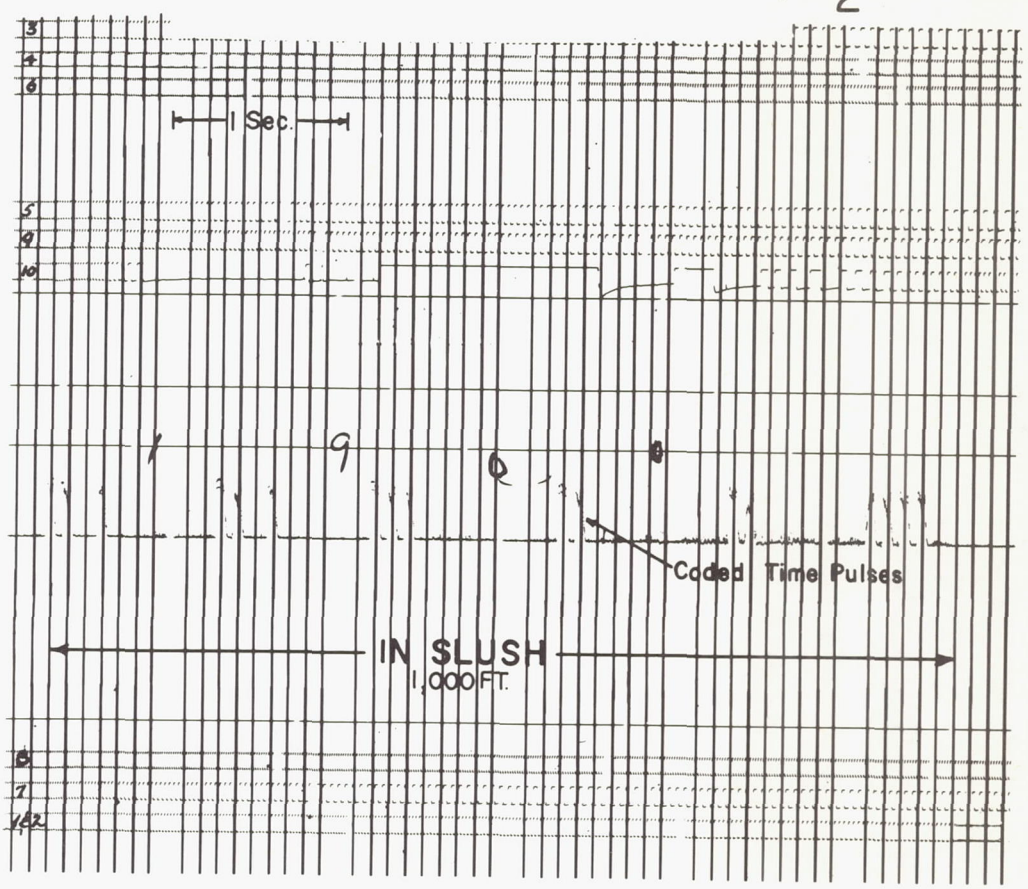

AIRCRAFT WHEEL LEGEND

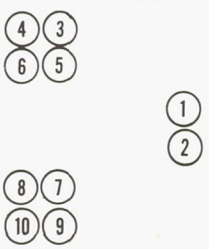

Figure 12

CAMERA LOCATION AT THE RUNWAY TEST SITE

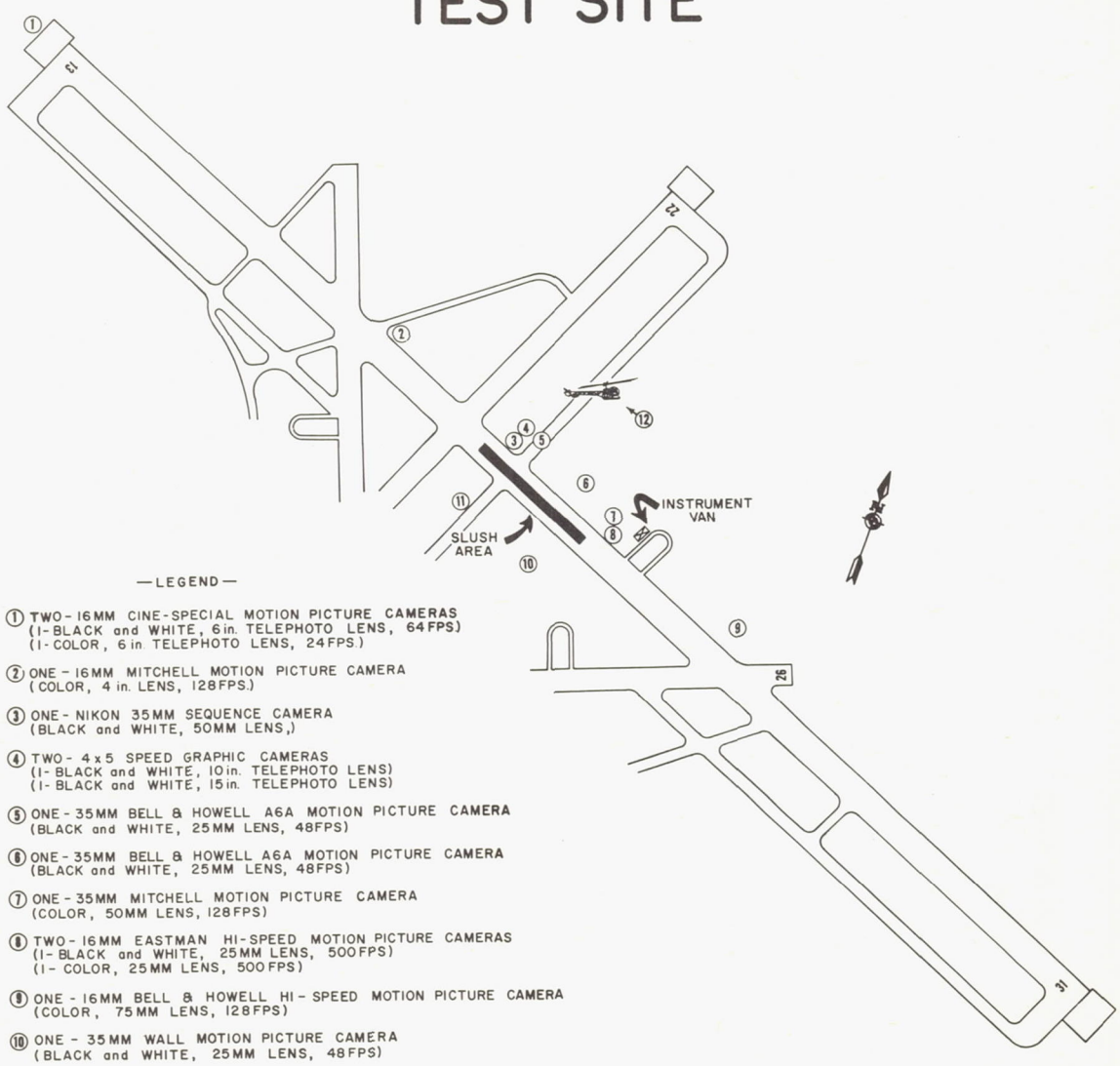

—LEGEND—

① TWO - 16MM CINE-SPECIAL MOTION PICTURE CAMERAS
(1- BLACK and WHITE, 6in. TELEPHOTO LENS, 64FPS)
(1- COLOR, 6 in. TELEPHOTO LENS, 24FPS.)

② ONE - 16MM MITCHELL MOTION PICTURE CAMERA
(COLOR, 4 in. LENS, 128FPS.)

③ ONE - NIKON 35MM SEQUENCE CAMERA
(BLACK and WHITE, 50MM LENS,)

④ TWO - 4 x 5 SPEED GRAPHIC CAMERAS
(1- BLACK and WHITE, 10in. TELEPHOTO LENS)
(1- BLACK and WHITE, 15in. TELEPHOTO LENS)

⑤ ONE - 35MM BELL & HOWELL A6A MOTION PICTURE CAMERA
(BLACK and WHITE, 25MM LENS, 48FPS)

⑥ ONE - 35MM BELL & HOWELL A6A MOTION PICTURE CAMERA
(BLACK and WHITE, 25MM LENS, 48FPS)

⑦ ONE - 35MM MITCHELL MOTION PICTURE CAMERA
(COLOR, 50MM LENS, 128FPS)

⑧ TWO - 16MM EASTMAN HI-SPEED MOTION PICTURE CAMERAS
(1- BLACK and WHITE, 25MM LENS, 500FPS)
(1- COLOR, 25MM LENS, 500FPS)

⑨ ONE - 16MM BELL & HOWELL HI - SPEED MOTION PICTURE CAMERA
(COLOR, 75MM LENS, 128FPS)

⑩ ONE - 35MM WALL MOTION PICTURE CAMERA
(BLACK and WHITE, 25MM LENS, 48FPS)

⑪ ONE - 35MM WALL MOTION PICTURE CAMERA
(BLACK and WHITE, 25MM LENS, 48FPS)

⑫ HELICOPTER OVER SLUSH BED
ONE - 35MM BELL & HOWELL EYEMO MOTION PICTURE CAMERA
(COLOR, 50MM LENS, 48FPS)

NOTE: THE FOLLOWING CAMERAS HAD NO SPECIFIC LOCATIONS:

ONE - 16MM ARRIFLEX MOTION PICTURE CAMERA
(COLOR, 25MM LENS, 24 & 50FPS)

TWO - 16MM BOLEX MOTION PICTURE CAMERAS
(COLOR, 25 & 75MM LENSES, 24FPS)

THREE - 4 x 5 SPEED GRAPHIC CAMERAS
(BLACK and WHITE, 135MM LENS)

Figure 13

CAMERA LOCATION AND COVERAGE ON THE AIRCRAFT

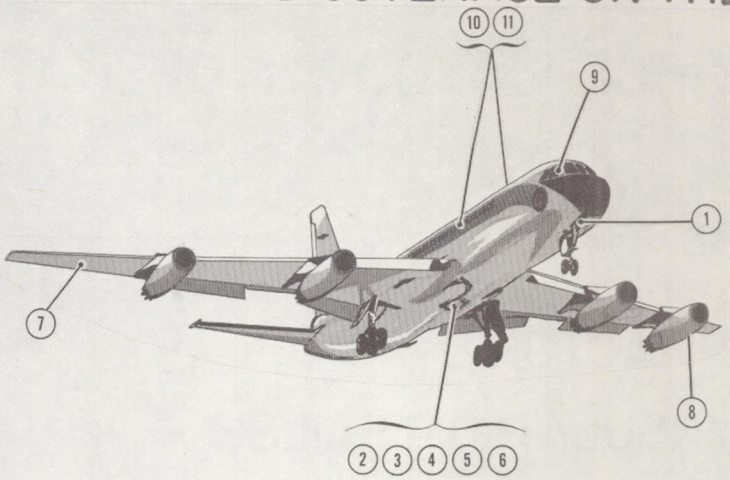

1 — LOCATED ON THE NOSE WHEEL WELL HATCH DOOR.
ONE – 70MM MAURER KB-10A RAPID SEQUENCE CAMERA.
(75MM LENS – 5FPS)

2 — LOCATED IN POD UNDER AIR CONDITIONING COMPARTMENT.
ONE – 16MM BELL & HOWELL GSAP CAMERA.
(25MM LENS – 64FPS)

3 — LOCATED IN POD UNDER AIR CONDITIONING COMPARTMENT.
ONE – 16MM FAIRCHILD GSAP CAMERA.
(35MM LENS – 64FPS)

4 — LOCATED IN POD UNDER AIR CONDITIONING COMPARTMENT.
ONE – 16MM BELL & HOWELL GSAP CAMERA.
(10MM LENS – 64FPS)

5 — LOCATED IN POD UNDER AIR CONDITIONING COMPARTMENT.
ONE – 16MM BELL & HOWELL GSAP CAMERA.
(10MM LENS – 64FPS)

6 — LOCATED IN POD UNDER AIR CONDITIONING COMPARTMENT.
ONE – 16MM FAIRCHILD GSAP CAMERA.
(35MM LENS – 64FPS)

7 — LOCATED UNDER RIGHT WING.
ONE – 16MM FAIRCHILD GSAP CAMERA.
(17MM LENS – 64FPS)

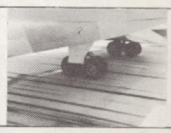

8 — LOCATED UNDER LEFT WING.
ONE – 16MM FAIRCHILD GSAP CAMERA.
(17MM LENS – 64FPS)

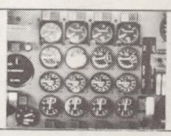

9 — LOCATED ON OVERHEAD STRUCTURE IN COCKPIT.
ONE – 35MM FLIGHT RESEARCH MULTI-DATA MOD. 4C CAMERA.
(101MM LENS – 10FPS)

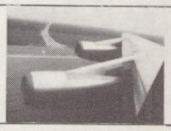

10 — LOCATED AT NINTH RIGHT CABIN WINDOW IN FUSELAGE.
ONE – 16MM BELL & HOWELL KRM CAMERA.
(10MM LENS – 64FPS)

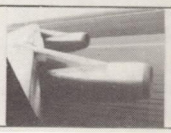

11 — LOCATED AT NINTH LEFT CABIN WINDOW IN FUSELAGE.
ONE – 16MM BELL & HOWELL KRM CAMERA.
(10MM LENS – 64FPS)

Figure 14

L-61-6975

SNOW-ICE LAYDOWN OPERATION

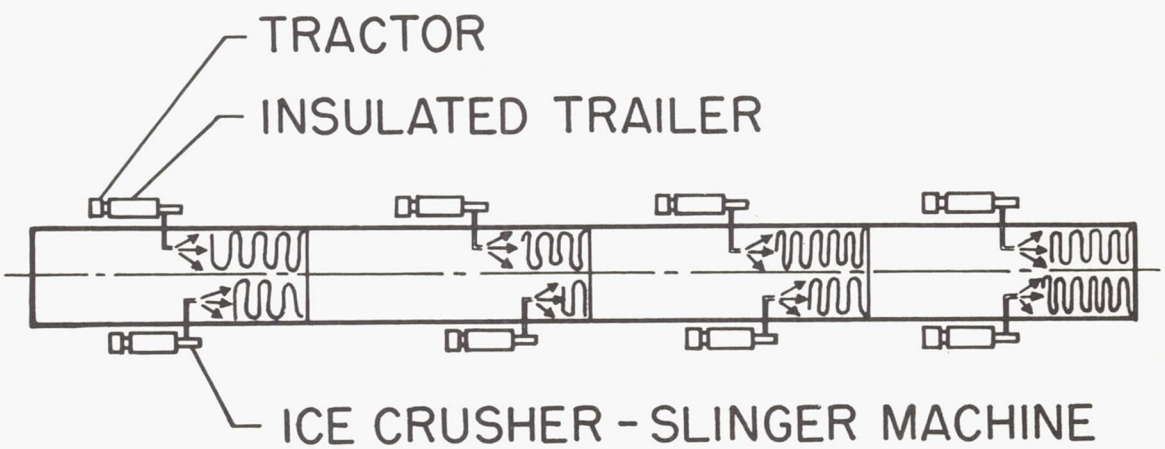

TEST BED	NO. OF RUNS
50' BY 1,000'	13
50' BY 1,500'	1
50' BY 3,000'	1

Figure 15

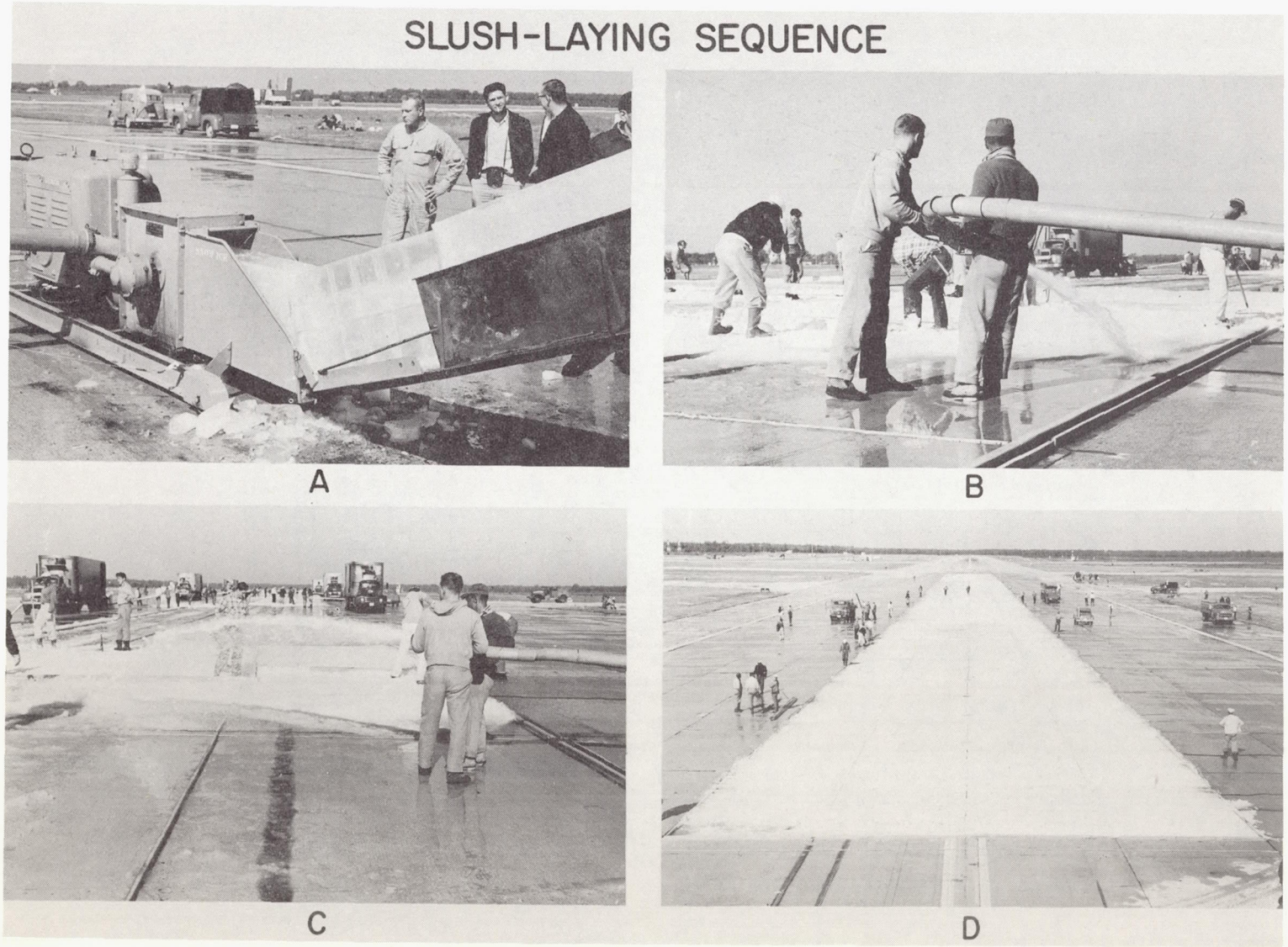

Figure 16

L-61-6977

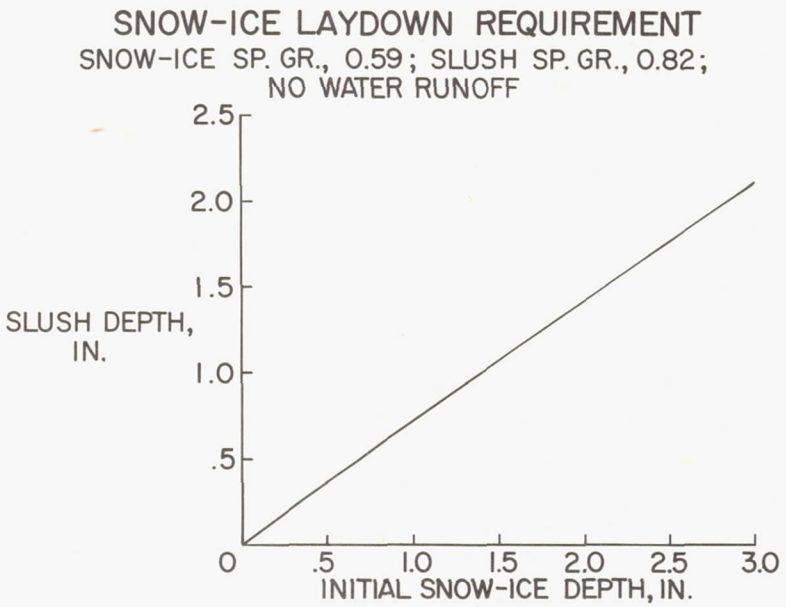

Figure 17

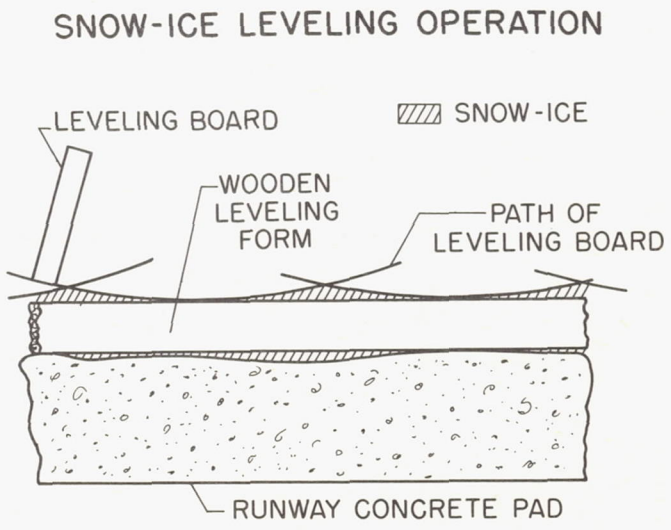

Figure 18

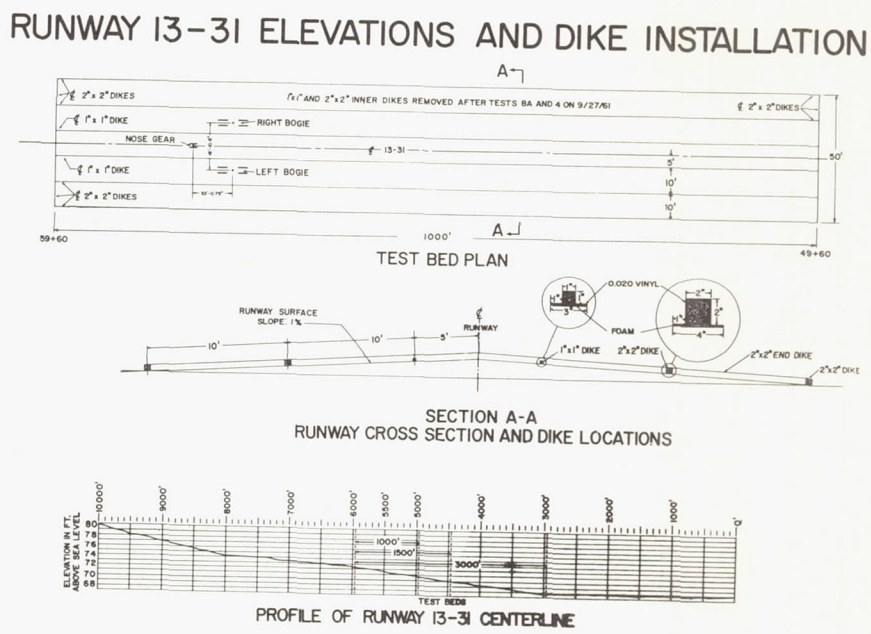

Figure 19

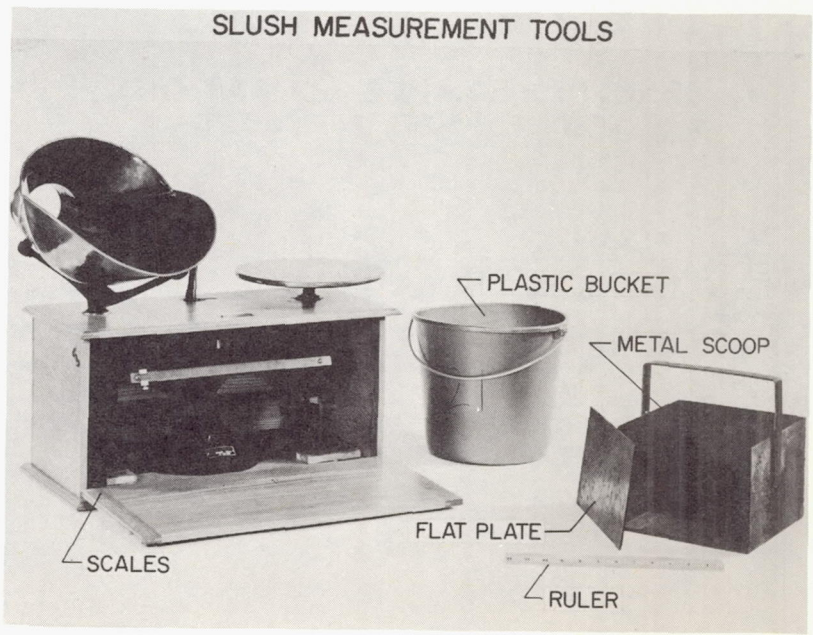

Figure 20 L-61-6976

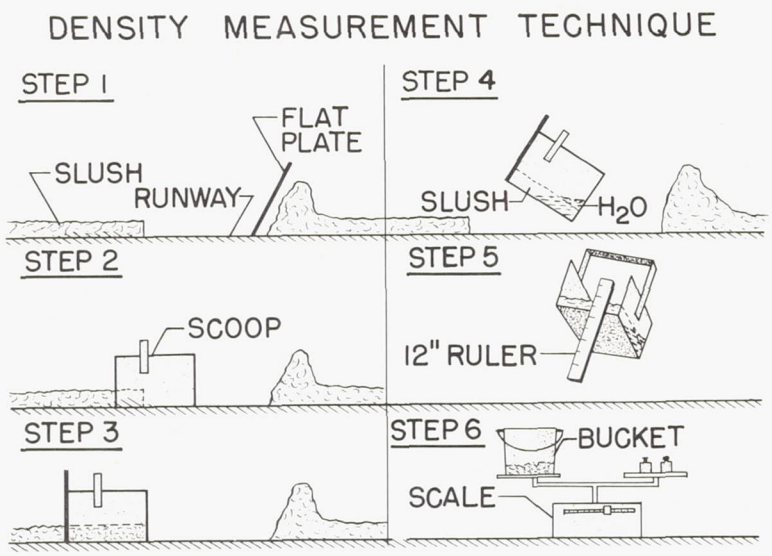

Figure 21

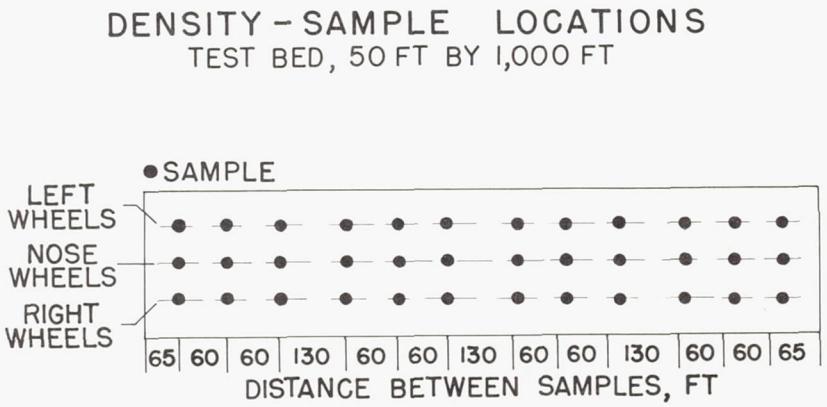

Figure 22

3. EFFECT OF SLUSH ON AIRCRAFT DRAG AND WHEEL ROTATION

By Eugene P. Klueg

FAA

INTRODUCTION

It is the purpose of this paper to present the results obtained from the full-scale tests at the National Aviation Facilities Experimental Center and to discuss the retardation and other effects of slush on the runway performance of the test aircraft.

In order to determine the effect of slush on the runway performance of the aircraft, the relation of the added drag resulting from the tires rolling in slush and from spray impingement and interference to the ground speed of the aircraft and the amount of slush on the runway must be determined. Therefore, factors of primary concern are the accelerating and decelerating forces acting on the aircraft, the ground speed and runway slush conditions.

METHODS OF ANALYSIS

As discussed in paper number 2 by Middlesworth, Marcy, Sommers, and Conley, the runway slush conditions were determined by measuring the slush depths and runway loadings at various locations throughout the test bed. The results of these measurements for a typical test (test 14) are shown in figure 1. The variations for the main-wheel tires are shown by the solid line. The effective depth presented in this figure (broken line) represents the depth which would occur for the runway loading measurements taken if the density of the slush throughout the test bed were constant. The effective depth was determined by dividing the measured slush loadings by the specific weight of slush determined to be the average value for all tests. For the purpose of comparing various tests, all depth data presented will be for an effective depth corresponding to the average specific weight of 51 lb/cu ft. The effective slush depths for each test are tabulated in table I. Sample calculations are given in the appendix.

A comparison of the acceleration and deceleration data resulting from accelerometer measurements with the values determined from the phototheodolite position-time data indicates that the accelerometer responded to depth variations and the resulting changes in the decelerating forces much more rapidly than did the phototheodolite data.

Therefore, the accelerometer was used as the primary instrumentation in determining the forces acting on the aircraft for each test in slush. However, because of the magnitude of the forces and since there were no rapid changes in the decelerating forces, the phototheodolite measurements were used to determine the forces acting on the aircraft during the dry runway tests.

A comparison of the ground-speed data obtained from tapeswitch and phototheodolite measurements indicates that the two systems correlate to within approximately 1/4 knot. However, the phototheodolites were much more reliable than the tapeswitches and were therefore used as the primary source of ground-speed data. Likewise, because of the reliability and accuracy, the phototheodolites were used as the primary position-time instrumentation.

Correlation of position, ground speed, and deceleration was accomplished by use of the central time system. An example of the relation of the aircraft deceleration and ground speed to its position in the slush bed for a typical test (test 12) is shown in figure 2. This distance represents the relative position of the main gear trucks to the start of the test bed.

EFFECT OF SLUSH ON WHEEL ROTATION

An example of the effect of slush on the rotation of the wheels is shown in figure 3 for a typical deceleration test in slush. As the aircraft enters the slush, the wheels start to spin down and after overcoming the wheel inertia resulting from the high rotational velocity prior to entering the slush, the wheel rotations stabilize. The four forward main wheels and the nose wheels are noted to spin down to a greater degree than do the aft main wheels. The rotation of the four forward main wheels 3.6 seconds after the nose wheel tires enter the slush ranges between 5 and 8 rps compared with 16.5 rps for the same ground speed on a dry runway surface. Likewise, the nose wheels are rotating at 13 rps compared with 25 rps on a dry runway. However, the aft main wheel rotations are seen to decrease very little as compared with the nose and forward main wheels. This pattern occurred in all tests with the exception of tests 14 and 15 when an outboard aft main wheel completely stopped.

The combined results of wheel rotations for each deceleration test in slush are shown in figures 4 and 5 and in table II. Figures 4 and 5 present the ratios of wheel rotations in slush to the wheel rotations on the dry runway in the speed range from 80 to 155 knots. The data points shown result from values occurring during each test after the wheels have stabilized.

EFFECT OF SLUSH ON AIRCRAFT DRAG

For each test in slush, average values of resultant retardation forces, ground speed, and effective slush depths for each of the four equally divided (250-foot) segments of the 1,000-foot-long test bed are tabulated in table III.

The resultant retarding forces given in this table were corrected to no-wind standard atmospheric conditions at sea level. The average depth for each 250-foot segment is determined from the three samples taken along each of the three paths traversed by the nose and main wheel tires. The data tabulated in this table are graphically presented in figure 6. The resulting retarding forces shown are a result of the following forces acting on the aircraft:

(1) Drag on the tires rolling in slush (including rolling friction)

(2) Aerodynamic drag

(3) Slush spray impingement and interference drag

(4) Accelerating force of four engines operating at idle thrust

The boundaries in which the tests were conducted and the data obtained are shown to be within the speed range from 80 to 155 knots and with effective slush depths from 0.75 to 2.25 inches, which are

From 0.75 inch to 1.25 inches

From 1.25 to 1.75 inches

From 1.75 to 2.25 inches

Also shown in this figure and tabulated in table IV are the resultant retardation forces determined from the dry runway deceleration tests. The dry runway curve shown was determined from the data points in the following manner:

(1) It was assumed that the relation of the resultant retardation force to ground speed is defined by the following equation of the force:

$$F = CV^2 + \mu W - T$$

where

F resultant retardation force

C constant

μ rolling friction coefficient

W aircraft gross weight

T total engine thrust

V aircraft ground speed

(2) This relation was used to fit a curve to the data points by the method of least squares.

The retarding effect of slush alone is then determined from the difference between the retardation forces acting on the aircraft when operating in slush and the forces occurring on a dry runway at the same velocity. This difference is shown in figure 7 for normalized slush depth data of 1, 1.5, and 2 inches. These data were normalized by assuming a linear relation between the slush drag force and the effective depth for any one speed. Effective slush depth data between 0.75 inch and 1.25 inches are presented normalized to 1 inch. Likewise, data in the range from 1.25 to 1.75 and from 1.75 to 2.25 inches are presented normalized to 1.5 and 2 inches, respectively. The curves shown in this figure for slush depths of 0.5, 1, 1.5, and 2 inches were determined from the data points in the following manner:

(1) It was assumed that the relation of slush drag to ground speed and the amount of slush is defined by the following equation:

$$D_S \approx \rho d V^2, \quad V < 110 \text{ knots}$$

where

D_S slush drag

ρ slush density

d slush depth

V aircraft ground speed

(2) From this relation a curve was fitted to the data points by the method of least squares.

(3) It was further assumed that the linear relation between slush drag and depth holds true above 110 knots, and the data points were normalized to a depth of 1 inch.

(4) After normalizing the data in the speed range from 110 to 155 knots, a curve was fitted to the data points. The data points normalized to 1-inch depth and the resulting 1-inch-depth curve are shown in figure 8.

It should be noted that the slush drag forces (fig. 8) reach a maximum at approximately 120 knots, after which an increase in ground speed results in a decrease in slush drag. Two factors are believed to cause this - mainly planing of the tires in slush and a decrease in the drag attributable to spray impingement on the aircraft.

EFFECT OF SLUSH ON TAKE-OFF

Figure 9 illustrates the effect of slush on the take-off performance of the test aircraft operating on a runway covered with slush to depths of 0.5, 1, 1.5, and 2 inches. The ratio of the aircraft acceleration in slush a_S to the acceleration on a dry runway a_D for the various depths of slush is the result of the following accelerating and drag forces acting on the aircraft:

(1) Accelerating force of four engines operation at maximum

(2) Aerodynamic drag

(3) Rolling friction drag

(4) Slush drag resulting from the curves established in figure 7

Conditions used in the calculation of these curves are as follows:

(1) Sea-level altitude

(2) Temperature of 60° F

(3) Zero wind

(4) Zero runway slope

(5) Gross weight of 150,000 pounds

(6) Flaps down 22°

Figure 9 shows that the available acceleration at 120 knots for 1 inch of slush is less than 50 percent of that available on a dry runway. It is also noted that the aircraft operating on a runway covered by 2 inches of slush would not be able to accelerate beyond 110 knots since at this speed the retarding forces are equal to the total available thrust. This speed is approximately 17 knots below the rotational velocity of the

aircraft. A lower thrust-to-weight ratio could be expected to make this condition become even more serious since the acceleration on a dry runway would decrease.

EFFECT OF NOSE WHEEL ON SLUSH DRAG

A test was conducted in which a path traversed by the nose-wheel tires was cleared of slush in the first half of the test bed. The basic results of this test are shown in figure 10. At the time of entry of the main-wheel tires into the slush bed, the ground speed was 115 knots. With the nose wheels on a dry runway surface, the aircraft traveled approximately 450 feet down the test bed before the nose-wheel tires entered the slush. In the next 500 feet of travel, all wheels were in slush. The aircraft ground speed at the time the nose-wheel tires came out of the slush was approximately 99 knots. The average deceleration for the first half of the test bed with main-wheel tires in slush was 0.137g while the average deceleration for the last half of the bed with all tires in slush was 0.182g. In comparison, an average deceleration on a dry runway surface in this speed range is 0.035g. Taking into account the differences between the average velocities and depths in the two portions of the test bed, these results indicate that approximately 38 percent of the total slush drag developed in this test is a result of spray impingement from the nose-wheel tires as well as the drag developed on these tires rolling in slush. The remaining 62 percent is then caused by the spray impingement from the main tires and the drag developed on these tires.

CONCLUSIONS

1. During the deceleration tests in slush, the forward main and nose wheels were noted to spin down considerably while the aft main wheels rotated with only a small amount of slippage noted.

2. The test results show that for the test aircraft at a gross weight of 150,000 pounds, the maximum slush drag occurs at approximately 120 knots after which the drag decreases with an increase in speed.

3. Results from the test in which a path was cleared for the nose-wheel tires indicate that a large percentage of the total slush drag results from the drag on nose-wheel tires and the spray developed by these tires.

4. The test results also indicate that the additional drag force resulting from slush covering the runway is a substantial force which for the greater depths affects the take-off performance of the aircraft considerably.

APPENDIX

SAMPLE CALCULATIONS

The following calculations were made to determine the data presented for test 12 in tables I and III.

Effective Slush Depths

Tabulated in table V are the measured slush depths and slush loadings taken at various locations along the path of the nose and main wheel tires. Also tabulated are the effective depths determined by dividing the measured slush loading by a specific weight of 51 lb/cu ft (specific gravity, 0.817).

$$d_{eff} = \frac{(W_S/A)}{w}$$

where

W_S weight of slush

A area from which the sample was taken

d_{eff} effective slush depth

w specific weight of the slush

The specific weight of 51 lb/cu ft was determined to be the average value of all tests with a standard deviation of 5 lb/cu ft.

Average slush depths were then determined for each 250-foot segment by averaging the nine effective depths resulting from slush samples taken along each of the three paths traversed by the nose and main wheel tires. Figure 11 shows the relation between the effective depths at various locations and the average value for each 250-foot segment.

Average Ground Speeds and Average Resultant Retardation Forces

The position, ground speed, and deceleration histories of test 12 are shown in figure 12.

The average ground speed of the aircraft was determined for each 250-foot segment by graphical integration of the following equation:

$$\overline{V} = \frac{\int_{t_1}^{t_2} V \, dt}{t_2 - t_1}$$

where

V	aircraft ground speed
t	time

The resultant retardation forces acting on the aircraft were determined by multiplying the measured deceleration by the mass of the aircraft. (See fig. 13.) These forces were corrected to no-wind, standard atmospheric conditions at sea level by use of the following equations:

$$D_0 - D = D_0 \left[1 - \frac{\rho}{\rho_0} \left(1 + \frac{V_w}{V} \right)^2 \right]$$

$$F_{cor} = F_{uncor} + (D_0 - D)$$

where

D	aerodynamic drag
ρ	density of air
V_w	head wind velocity
V	aircraft ground speed
D_0	aerodynamic drag for standard conditions
ρ_0	standard density of 0.002378 slug/cu ft
F	resultant retardation force

The aerodynamic drag correction $(D_0 - D)$ for test 12 is shown in figure 14.

The average resultant retardation forces were then determined for each 250-foot segment by graphical integration of the following equation:

$$\bar{F} = \frac{\int_{t_1}^{t_2} F \, dt}{t_2 - t_1}$$

where F is the resultant retardation force and t is the time. The corrected resultant retardation forces and the average value for each 250-foot segment are shown in figure 15.

TABLE I.- EFFECTIVE-SLUSH-DEPTH DATA FOR DECELERATION TEST RUNS

[Specific gravity, 0.817]

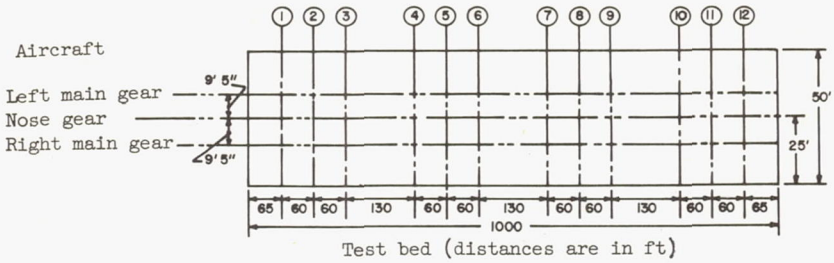

Test bed (distances are in ft)

Test	Slush depth, in. at station number -											
	1	2	3	4	5	6	7	8	9	10	11	12
Left main gear												
8	----	1.10	----	----	0.97	----	----	----	----	----	----	----
8A	----	.69	0.38	----	.88	0.51	0.76	0.77	----	0.72	----	0.89
8B	1.44	1.21	2.46	1.67	1.52	1.60	----	.79	----	1.07	1.19	1.22
9	1.05	.86	.88	----	----	.79	1.49	----	----	----	----	1.27
10	1.08	.93	1.04	.70	.60	.10	1.02	1.09	1.17	.72	----	.92
11	1.02	1.32	1.20	1.56	1.28	1.62	1.12	1.28	2.14	.91	1.73	1.94
12	1.32	1.33	1.18	1.15	.96	1.17	.91	.91	.91	1.48	1.69	----
13	1.10	1.76	1.34	1.04	.88	.90	.73	----	.08	----	1.86	----
14	----	1.68	2.23	2.17	1.34	1.72	2.33	1.42	2.09	2.76	2.10	2.18
15	1.56	1.78	----	1.57	1.04	1.29	1.21	2.27	1.17	2.25	2.95	2.11
19	1.78	1.55	1.28	1.37	.85	.89	----	1.63	1.16	1.66	1.25	----
20	----	1.22	1.40	----	.95	1.39	.93	----	1.42	.46	1.20	----
20A	2.00	1.56	1.86	1.70	1.20	1.65	1.84	1.97	1.14	2.90	3.54	2.31
Nose gear												
8	----	1.11	----	----	1.28	----	----	0.92	----	----	----	----
8A	----	----	0.53	0.70	----	0.88	0.81	----	----	----	----	----
8B	0.88	.79	.92	1.18	1.16	1.35	.86	.88	0.92	1.57	0.99	----
9	1.06	1.70	.91	1.83	1.37	1.31	1.30	1.46	.64	1.35	1.07	----
10	.84	----	1.04	.58	.68	.87	1.02	----	.78	.69	.73	0.89
11	1.22	1.26	1.60	2.02	1.48	1.97	1.30	1.44	1.48	1.32	1.38	----
12	.78	.85	.72	1.16	.73	1.36	1.12	1.29	.35	1.27	1.12	1.36
13	1.02	----	1.24	1.11	1.04	1.39	1.68	1.17	1.22	----	1.12	----
14	1.97	1.33	1.82	2.48	1.75	1.76	1.66	1.32	2.36	2.23	2.23	1.82
15	1.37	1.66	1.25	1.60	1.34	1.38	1.67	1.53	1.60	1.83	2.08	1.77
19	0	0	0	0	0	0	1.58	1.35	1.03	1.08	1.37	1.64
20	----	1.10	1.23	.84	.15	1.43	.46	1.84	1.14	----	1.83	1.48
20A	1.96	2.01	1.89	----	1.63	1.61	2.06	2.23	1.73	2.92	1.89	2.76
Right main gear												
8	----	1.97	----	----	1.46	----	----	----	----	----	----	----
8A	----	----	0.79	1.21	----	0.57	0.82	----	----	----	----	----
8B	1.22	1.02	----	.95	1.68	1.49	.89	1.53	----	----	0.94	----
9	1.23	.93	----	----	----	1.25	.84	----	0.61	1.24	.31	1.01
10	.33	1.08	----	.57	.75	1.35	1.13	.70	----	1.73	1.05	1.51
11	1.28	1.60	1.12	1.69	1.26	2.05	1.48	1.78	1.44	----	1.52	1.80
12	1.30	.97	.53	.66	.73	1.28	1.15	1.15	1.15	----	1.15	1.15
13	1.06	1.65	1.25	----	.72	.78	1.79	----	1.21	.60	1.10	.97
14	----	1.84	1.80	1.84	1.61	2.48	1.81	2.12	2.36	2.48	2.09	----
15	1.88	1.34	1.63	----	1.72	1.76	1.53	1.45	2.03	1.03	.76	1.35
19	1.45	1.44	1.11	1.25	1.71	1.37	----	1.63	1.51	1.56	1.63	1.63
20	----	1.43	1.95	----	.96	1.91	1.04	1.82	1.32	.59	1.32	1.56
20A	2.00	1.26	1.78	1.62	1.67	2.18	1.69	1.97	2.05	----	1.99	2.26

TABLE II.- WHEEL-ROTATION DATA FOR DECELERATION TEST RUNS

Test (a)	Ground speed, knots (b)	Wheel rotation, rps, for wheel[c] number -								
		1 and 2	3	4	5	6	7	8	9	10
8	105	16.7	9.5	16.2	7.2	16.5	7.0	16.5	5.8	17.0
8A	110	15.2	10.0	16.2	7.2	17.0	7.2	16.7	9.5	15.9
8B	110	13.3	7.3	16.0	5.5	16.4	8.0	17.7	9.4	17.1
9	115	15.7	8.4	16.8	6.8	18.7	16.8	19.1	14.2	17.8
10	153	34.0	20.7	23.4	18.3	23.3	19.0	24.2	19.5	22.9
11	105	12.8	7.5	15.7	5.9	15.5	6.5	14.0	7.7	15.3
12	125	20.5	10.7	20.5	8.7	19.1	9.2	19.0	10.5	11.0
13	150	23.1	19.4	28.7	14.3	21.9	12.5	23.1	12.3	23.1
14	100	9.1	5.4	15.7	5.3	16.5	5.2	14.6	15.8	4.0
15	120	12.0	5.3	0	5.0	17.0	4.5	19.0	5.4	18.0
19	105	16.3	9.3	17.7	6.5	17.5	5.8	17.2	6.7	10.2
20A	80	14.9	13.8	12.8	9.0	13.8	9.8	12.8	10.0	13.5
20A	90	14.3	10.7	13.3	6.7	14.8	5.6	14.6	6.8	14.9
4	151	37.9	24.1	23.7	23.7	23.9	23.9	24.1	23.8	23.6
5	125	28.6	19.4	19.3	18.8	19.1	18.6	18.8	18.9	18.6
7	111	26.9	18.1	17.8	17.8	18.9	17.9	17.6	17.6	17.8

[a]All tests are in slush except tests 4, 5, and 7, which are on dry surface.

[b]Velocity at which the minimum wheel rotation occurs.

[c]Wheel nomenclature:

Wheels 1 and 2 - Nose, left and right
Wheel 3 - Main, left front outboard
Wheel 4 - Main, left rear outboard
Wheel 5 - Main, left front inboard
Wheel 6 - Main, left rear inboard
Wheel 7 - Main, right front inboard
Wheel 8 - Main, right rear inboard
Wheel 9 - Main right front outboard
Wheel 10 - Main, right rear outboard

TABLE III.- TEST RESULTS

Test	Date (1961)	Time e.d.t.	Slush depth, in.	Average ground speed, knots	Resultant retardation force, lb (a)	Slush depth, in.	Average ground speed, knots	Resultant retardation force, lb (a)	Slush depth, in.	Average ground speed, knots	Resultant retardation force, lb (a)	Slush depth, in.	Average ground speed, knots	Resultant retardation force, lb (a)
1,000-ft test area (b)			0 to 250 ft			250 to 500 ft			500 to 750 ft			750 to 1,000 ft		
8	Sept. 26	0742	0.71	114.0	23,024	0.83	110.5	23,155	1.17	106.8	24,992	----	103.3	17,731
8A	Sept. 27	0816	.80	114.5	18,500	.75	110.6	25,100	.99	106.8	19,700	0.86	103.3	20,200
14	Sept. 29	0916	----	116.8	34,200	1.91	111.4	39,300	1.94	104.9	39,000	2.24	97.2	41,700
9	Sept. 29	1146	1.08	128.7	25,700	1.31	124.9	27,300	1.06	120.7	28,990	----	116.1	33,630
12	Oct. 1	0736	.99	133.3	21,988	1.02	130.3	23,600	.99	126.9	25,600	1.32	123.5	28,600
15	Oct. 1	1017	1.56	133.8	36,000	1.46	129.2	33,600	1.62	124.5	38,200	1.79	119.1	39,800
10	Oct. 5	0817	.90	156.7	19,854	.76	154.7	17,942	.99	152.8	18,354	1.03	150.8	18,878
13	Oct. 5	1119	1.30	155.1	21,958	.98	152.6	17,495	1.13	150.2	22,992	1.13	147.6	22,632
20	Oct. 5	1345	1.39	99.9	24,800	1.14	97.4	13,500	----	94.4	19,650	1.21	90.7	18,100
c19	Oct. 6	0901	1.44	113.2	21,600	1.24	109.7	19,500	1.41	105.5	27,900	1.45	100.1	26,900
20A	Oct. 6	1110	1.81	94.9	28,602	1.66	89.6	25,978	1.85	83.9	27,496	2.57	78.2	25,746
11	Oct. 9	0815	1.29	114.1	26,146	1.66	110.0	31,200	1.50	104.9	26,663	----	100.1	23,500
8B	Oct. 9	0903	1.24	114.3	24,610	1.40	110.0	28,600	.98	107.2	21,300	----	103.8	18,216
3,000-ft test area (d)			0 to 500 ft			500 to 1,000 ft			1,000 to 1,500 ft			1,500 to 2,000 ft		
17	Oct. 7	0915	1.21	103.0	16,088	1.07	109.0	16,717	1.13	115.6	19,976	----	121.1	17,610
1,500-ft test area (e)			0 to 200 ft											
18	Oct. 8	0803	1.38	128.1	12,138	----	-----	------	----	-----	------	----	-----	------

[a]All forces are resultant retardation forces except those for tests 17 and 18, which are acceleration forces.

[b]Test area divided into four segments of 250 feet each.

[c]In the first 500 feet of test area, the main wheel tires only are in slush. In the remaining 500 feet, main and nose wheel tires are in slush.

[d]Test area is 3,000 feet long and is divided into six segments of 500 feet each. Test 17 is an acceleration and aborted rotation run. Slush measurements were taken for the first 1,500 feet.

[e]Test area is 1,500 feet long and is divided into six segments of 200 feet each. The aircraft rotated in the first segment.

TABLE IV.- DRY RUNWAY DECELERATION TEST RESULTS

Test	Date (1961)	Time, e.d.t.	Ground speed, knots	Average resultant retardation force, lb
1	Sept. 25	0813	109.9	5,580
2	Sept. 25	1159	110.0	5,640
3	Sept. 26	1441	123.3	7,840
4	Sept. 27	1500	152.6	9,130
5	Sept. 28	1056	126.9	7,050
7	Oct. 4	1600	110.5	5,620

TABLE V.- SLUSH MEASUREMENTS FOR TEST 12

[Specific gravity, 0.817]

Sample locations at -	Measured depths, in.			Effective depths, in.			Runway loading, lb/sq ft		
	Left main gear	Nose gear	Right main gear	Left main gear	Nose gear	Right main gear	Left main gear	Nose gear	Right main gear
65 ft	1.19	1.00	1.50	1.32	0.78	1.30	5.60	3.33	5.54
125 ft	1.38	1.00	.88	1.33	.85	.97	5.65	3.63	4.13
185 ft	1.00	.88	.69	1.18	.72	.53	4.75	3.08	2.26
315 ft	1.13	1.00	.63	1.15	1.16	.66	4.88	4.98	2.79
375 ft	1.00	.88	.75	.96	.73	.73	4.06	3.11	3.10
435 ft	1.25	1.56	1.31	1.17	1.36	1.28	4.98	5.76	5.44
565 ft	1.00	1.44	1.38	.91	1.12	1.15	3.87	4.74	4.90
625 ft	1.00	1.50	1.13	.91	1.29	1.15	3.85	5.47	4.88
685 ft	1.00	.38	1.25	.91	.35	1.15	3.87	1.47	4.88
815 ft	1.50	1.25	----	1.48	1.27	----	6.28	5.38	----
875 ft	1.50	1.50	1.00	1.69	1.12	1.15	7.17	4.78	4.87
935 ft	----	1.25	1.00	----	1.36	1.15	----	5.76	4.90

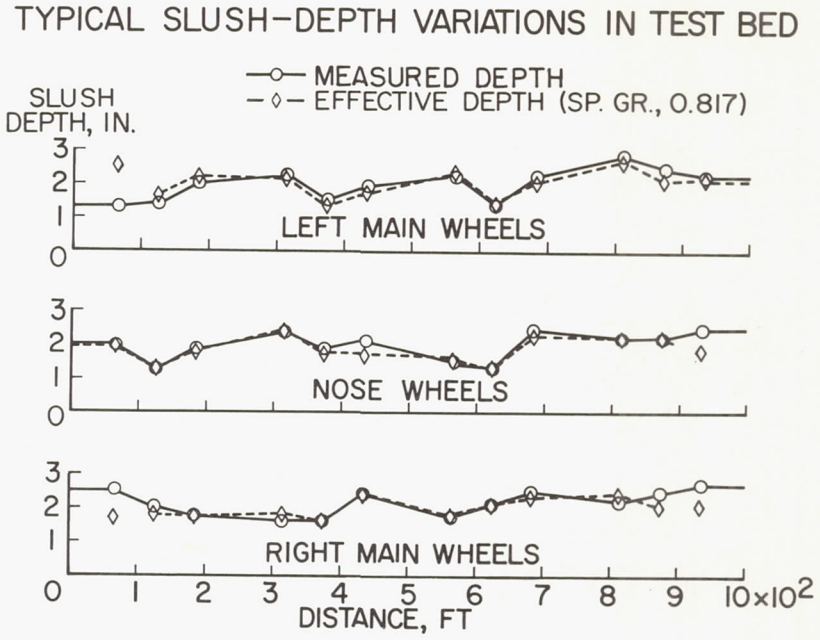

Figure 1

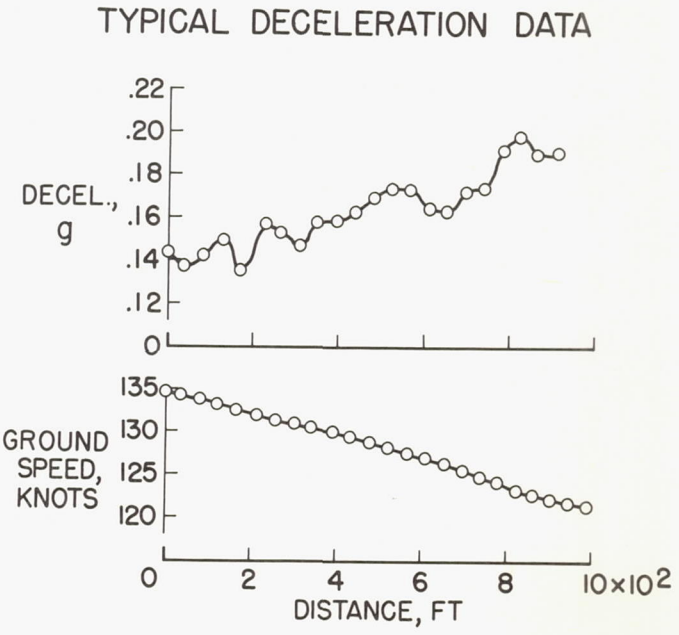

Figure 2

TYPICAL SLUSH EFFECT ON WHEEL ROTATION

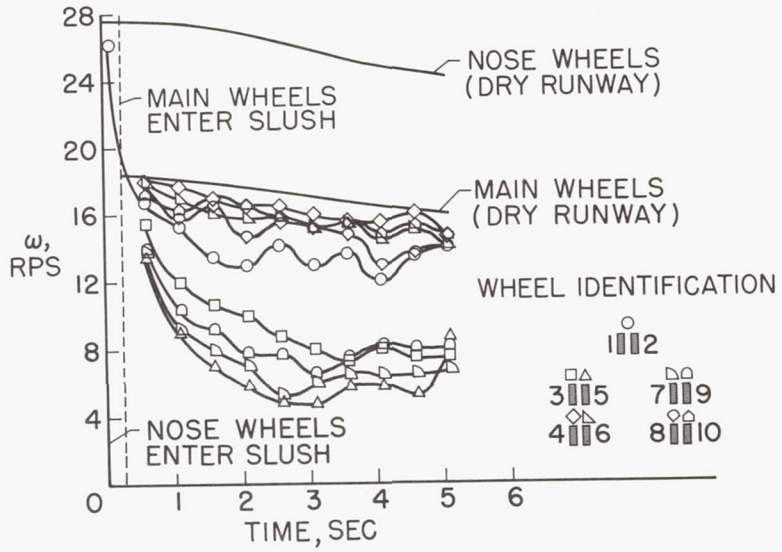

Figure 3

SLUSH EFFECT ON MAIN WHEEL ROTATION

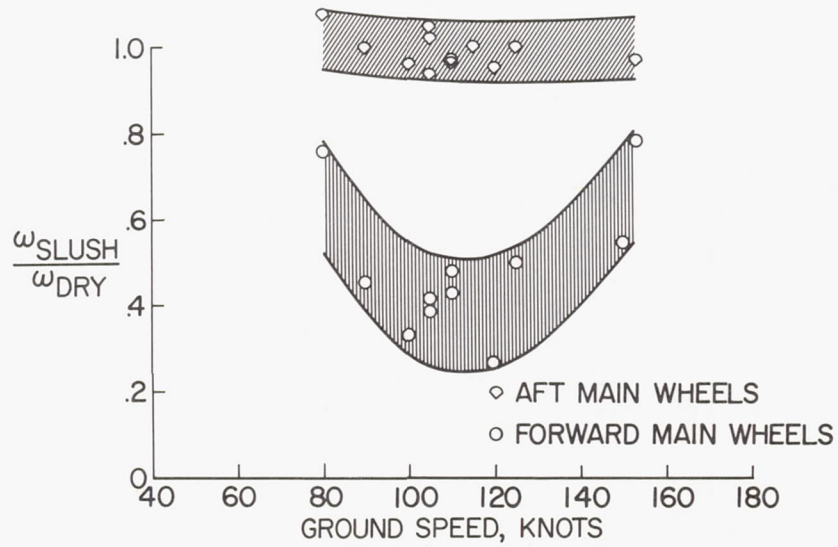

Figure 4

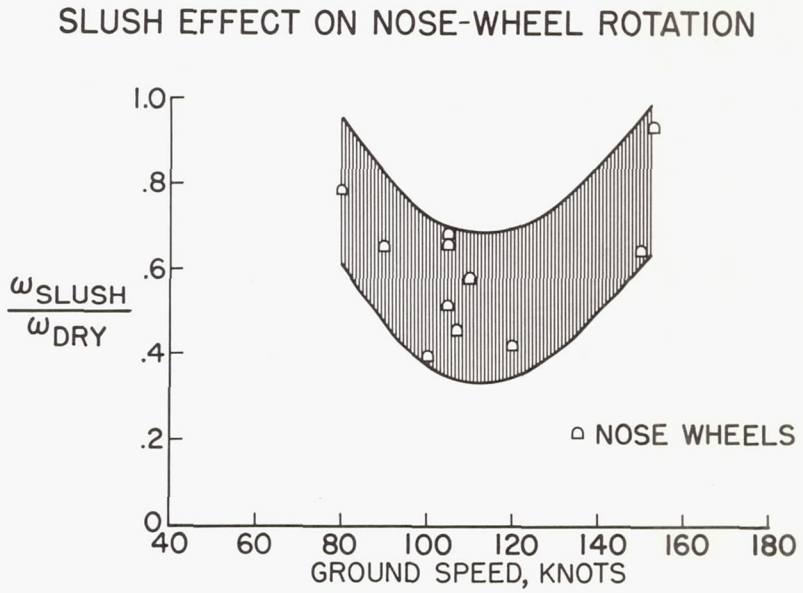

Figure 5

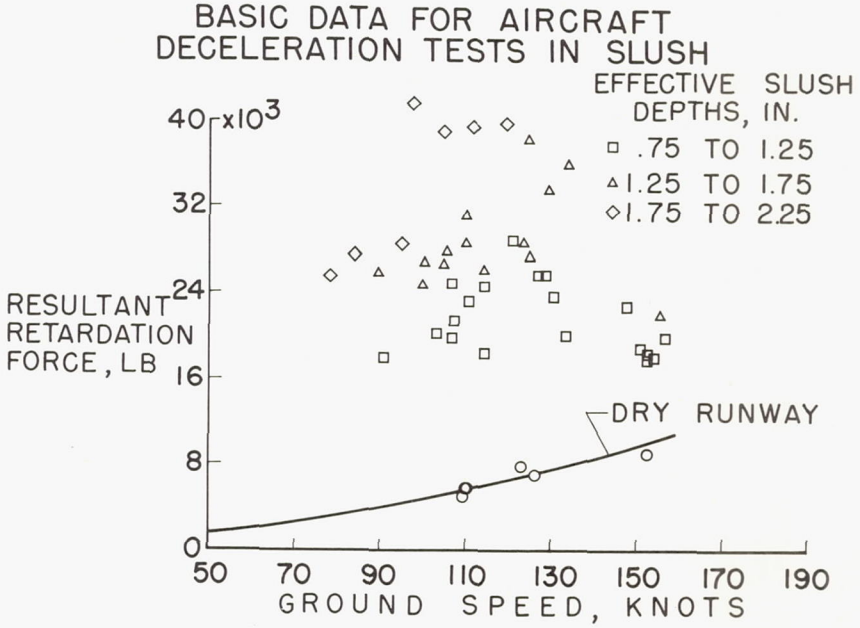

Figure 6

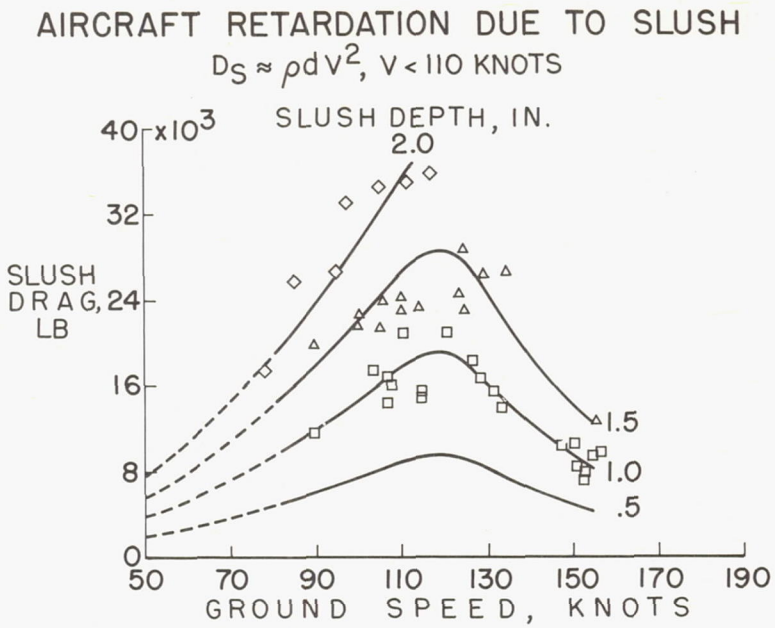

Figure 7

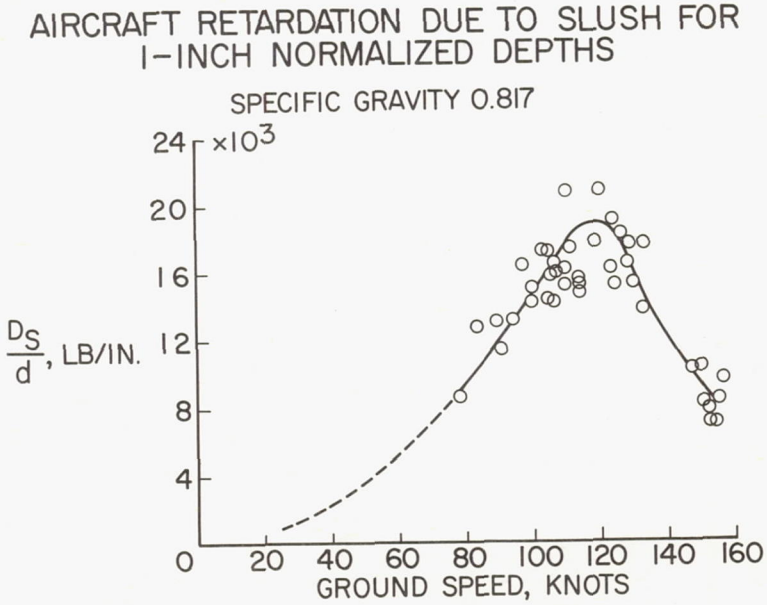

Figure 8

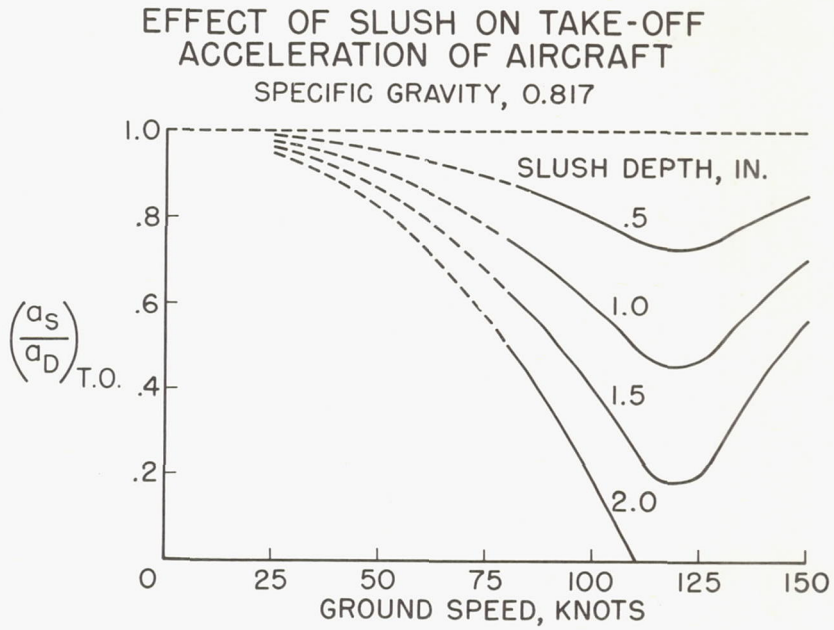

Figure 9

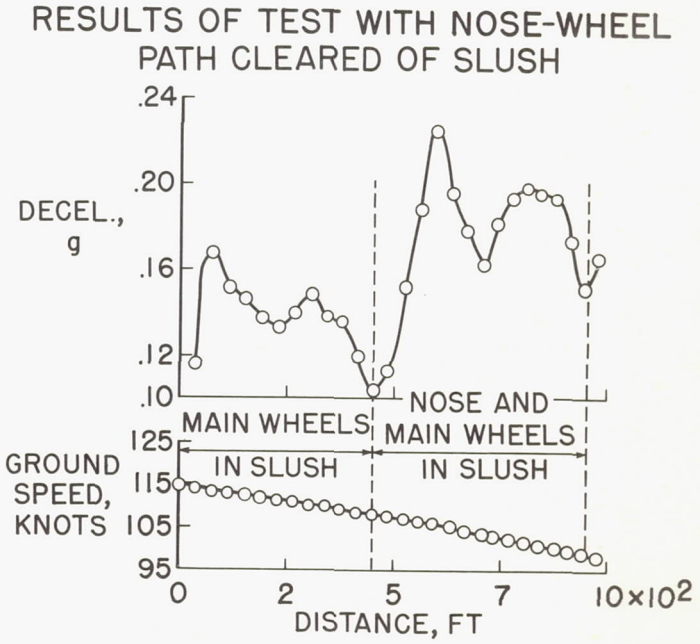

Figure 10

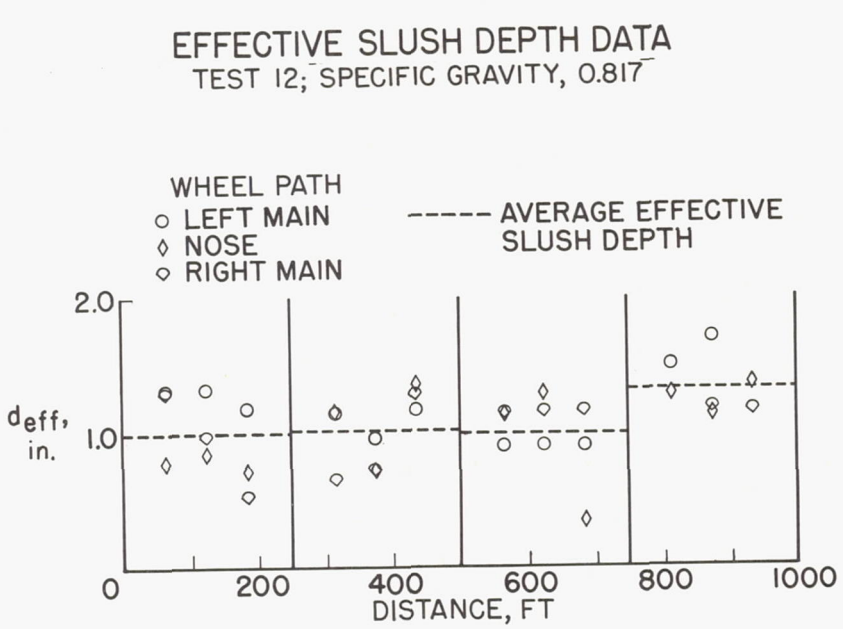

Figure 11

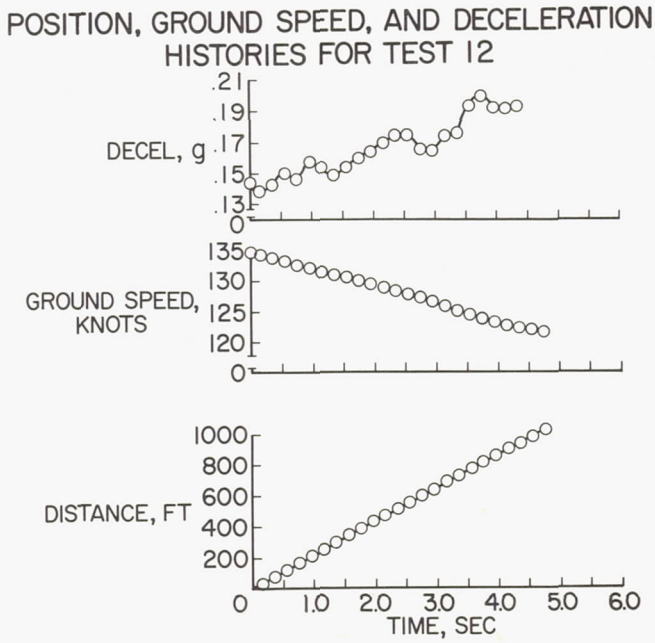

Figure 12

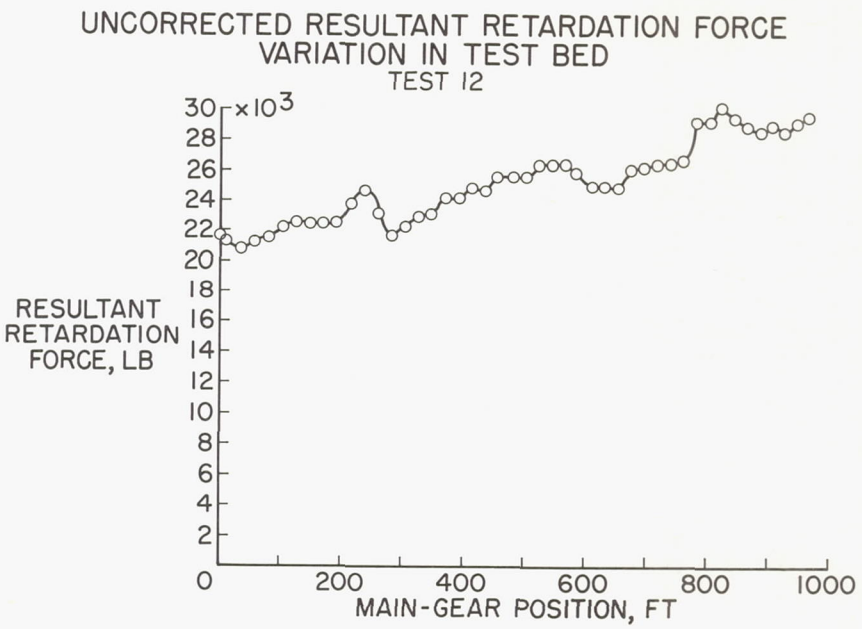

Figure 13

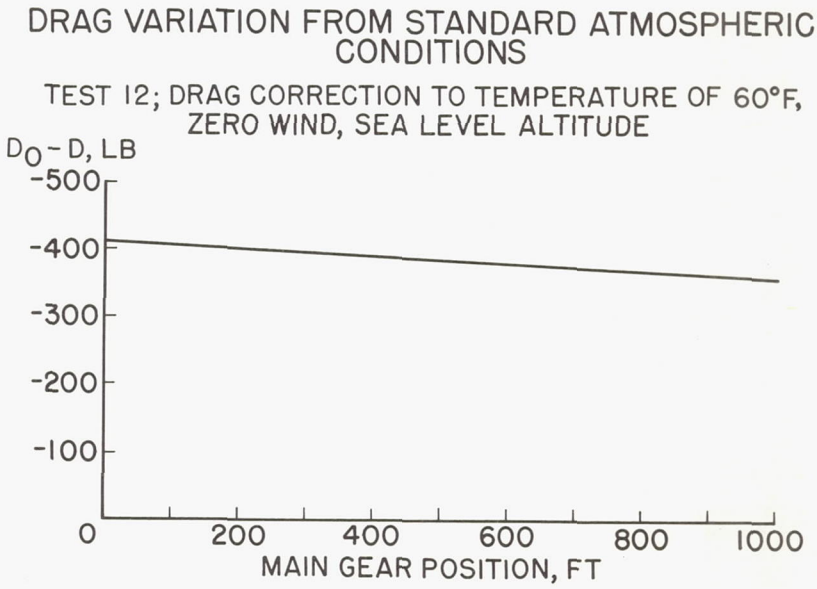

Figure 14

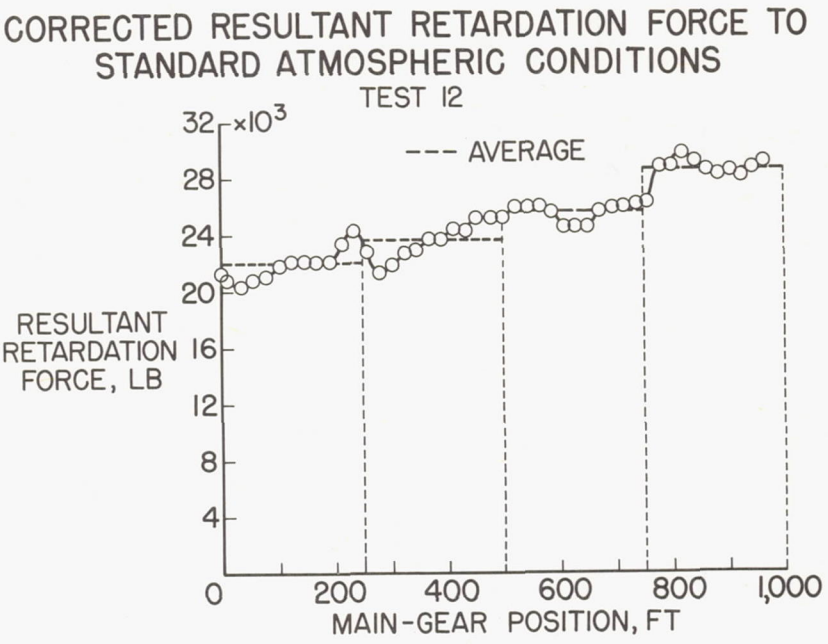
CORRECTED RESULTANT RETARDATION FORCE TO STANDARD ATMOSPHERIC CONDITIONS
TEST 12
32 ×10³
28
24
20
16
12
8
4
0
--- AVERAGE
RESULTANT RETARDATION FORCE, LB
200
400
600
800
1,000
MAIN-GEAR POSITION, FT

Figure 15

4. SLUSH SPRAY PATTERNS AND SLUSH DAMAGE

By Wayne D. Howell and Daniel E. Sommers

FAA

In conducting slush tests with the test airplane, attention was given to the pattern in which the slush sprayed from the wheels in an attempt to establish the following: (a) A relationship between slush spray pattern and impingement drag and (b) a relationship between slush spray pattern and impingement damage to the airplane.

SPRAY PATTERN AND RELATIONSHIP TO IMPINGEMENT DRAG

As was pointed out in the preceding paper by Eugene P. Klueg, slush drag forces obtained from this full-scale-airplane study are considerably higher than those obtained by NASA from a test of a single wheel (ref. 1). During one test when the nose wheels were running free of slush in the first 500 feet of the slush bed, it was determined that approximately 38 percent of the total slush drag on the airplane was contributed by the nose wheels. The slush drag coefficient $C_{D,S}$ calculated for the nose wheels during this run was 2.6. If $C_{D,S} = 0.75$, as obtained by NASA, and if the percentage of slush drag due to tire drag only is subtracted, it becomes apparent that approximately 27 percent of the total airplane slush drag is due to spray impingement from the nose wheels. (See table I.) This fact points out that impingement drag due to the slush spray contributes appreciably to the overall slush drag or retardation force on the airplane. Reference 2 indicates that if all slush displaced by the tires were intercepted by the airplane and carried forward at the velocity of the airplane, the drag would be three times as much as that acting on the tires alone.

With these facts in mind, an analysis was made of the slush spray patterns on the test airplane by closely studying the photographs obtained of the various runs, in hopes of determining a relationship between slush spray patterns and measured retardation forces. An attempt was also made to determine a relationship, if any, between slush angle or spray pattern with velocity of the aircraft and depth or density of the slush.

The film analysis was performed by utilizing a time- and motion-study projector which allowed a detailed frame-by-frame study of the movies taken of the various runs. Since photographic records were

not tied in to the test program timewise, spray patterns were established where the velocity and depth of slush could be determined from the records to a reasonable degree of accuracy. For example, the place where the aircraft either entered or exited from a slush bed was generally chosen as the spot where spray patterns were established for this study.

First, the effect of the airplane velocity on the slush spray pattern is considered. Figure 1 shows the spray pattern obtained at a velocity of 40 knots in a slush depth of 1.5 inches. The spray pattern from the nose wheels is wide but yet none of the slush is entering the intakes of the inboard engines. Also, some of the nose-wheel spray pattern is traveling over the wing, impinging on the leading edge and Krueger flap and under the wing in the area of the main flaps. Note the bow wave located directly in front of the main wheels and nose wheels. No noticeable amount of spray from the main wheels is striking the under portion of the wing or main flaps. Due to the low velocity of the airplane and a consequent low energy imparted to the slush, the slush spray drops rapidly in relation to the airplane with none reaching the horizontal stabilizers.

Figure 2 shows the spray pattern obtained as the velocity is increased to 100 knots and in a slush depth of 1.3 inches. Notice a definite narrowing of the spray pattern with considerable more nose-wheel spray passing over the wing or impinging on the wing leading edge, front flap, and under the wing in the area of the main flaps. Bow waves are very predominant on both the nose wheels and the main wheels. The spray pattern coming from the inboard main wheels mixes with that portion of spray which flows directly off of the nose wheel straight back along the under side of the fuselage. Note that the spray pattern from the main wheels is rising higher under the wing - some of it possibly impinging on the wing and main flaps. It appears that no slush is reaching the horizontal stabilizer.

Increasing the velocity even higher to 116 knots in the same depth of slush (1.3 inches) shows another change in pattern. (See fig. 3.) The spray pattern becomes narrower with respect to the aircraft. Less slush spray from the nose wheel is passing over the wing and as can be seen in the front and top views, it is not spreading as wide laterally. It appears that spray impingement from the nose wheels has become less than was shown in figure 2. Spray from the main wheels is not impinging on the under side of the wing or main flaps but is approaching the under side of the horizontal stabilizers. One very interesting fact to note in figure 3 is the lack of bow wave in front of the forward main wheels and nose wheels. In conjunction with this, it is also interesting to note that 116 knots is very close to the speed at which planing is

assumed to occur and, as described in the preceding paper by Eugene P. Klueg, it is close to the velocity where the slush drag begins to decrease as the velocity increases.

These points are brought out more emphatically by studying figure 4 where the airplane velocity is 155 knots and the slush depth is still 1.3 inches. The spray patterns have become so narrow with respect to the airplane that the spray coming from the nose wheel cannot be seen in the top view, only along the side of the fuselage beginning behind the wings. Spray from the main wheels is missing the wing and horizontal stabilizers entirely. A lot of spray from the nose wheels is hitting the under side of the fuselage from the vicinity of the leading edge of the wing back to the tail. As is shown in most of the previous figures, the spray pattern from the inboard wheels of the main gear is hitting the bottom rearward section of the fuselage and is mixing with that from the nose wheels. Again, note the lack of bow wave in front of the nose wheels and main wheels indicating planing. At this speed it is shown that very little slush drag was due to impingement.

A constant velocity of approximately 115 knots was selected for the study of the effect of the slush depth on the spray pattern. In this analysis, figures 3, 5, and 6 were selected to show the effect of the following depths of slush: 0.9 inch, 1.3 inches, and 1.7 inches. The first significant difference noted is the appearance of bow waves located in front of the main and nose wheels in figure 5 and a lack of such in figures 3 and 6. Also, a slight difference is even noted between the wheel pattern in figure 3 as compared to that in figure 6. In figure 3 (1.3 inches of slush), the side view shows the slush spray leaving the front main and nose wheels at the midpoint of the tire or directly beneath the axle; whereas, in figure 6, the slush spray is leaving the rearward portion of the nose and main wheels. As was previously indicated, 116 knots is near the speed at which planing is assumed to start. Therefore, it appears that an increase in slush depth increases the tendency for planing or for the wheels to ride up over the slush. Also, note that less spray is passing over the wings at the higher depths which also coincides with the loss in bow wave.

Figure 7 is included to show a typical spray pattern obtained at a relatively low airplane velocity in a very high depth of slush. Note the very predominant bow waves, especially their thicknesses when compared with those in the other figures. Generally, the patterns indicate high tire drag and impingement drag.

As a matter of interest, the width of removed slush troughs was determined for a few random test runs by scaling photographs taken of the slush bed after the test runs. Table II shows the results obtained. It is interesting to note that, for all practical purposes, the width

of removed slush troughs remained constant as either the velocity or the depth of slush varied. One possible explanation could be that the increased hydrodynamic pressure induced in the slush at higher velocities is cancelling the effect of reduced tire frontal area due to planing. Consequently, the same width of slush was removed as was removed at the lower velocities when the tire was in contact with the runway surface.

AIRCRAFT SLUSH DAMAGE

As a result of the spray patterns that have been previously described, some damage was noted on the airframe. This damage consisted of dimpling of the skin on trailing-edge flaps, on the lower inboard wing leading-edge fairing, on the wheel-well doors attached to the main gear, and on the skin directly behind the Krueger flap. Furthermore, antennas, antenna mounts, and an anticollision light located on the bottom of the fuselage were slightly damaged by slush spray generated by the nose wheel. During the lower speed deceleration runs (range of 85 to 120 knots), considerable slush was picked up in recessed areas such as the wheel wells, the open area in the wing directly behind the Krueger flap, the recessed area between the wing and leading edge of the main flaps, the air-conditioning-system chamber, and on the main-wheel assembly. Although slush accumulation did not present a problem during these tests, there is a possibility of this being detrimental to proper operation of these devices, especially if the slush were to freeze after a take-off and climb to altitude. Of considerable concern was the accumulative damage imparted to the air-conditioning equipment housed in the lower fuselage, which was open by means of cooling air ducts to slush spray generated by the nose wheel. The damage of shredding the insulation from the electrical wires and the flexible conduits of the air-conditioning system, along with the large accumulation of slush in this area, were considered a potential operational hazard.

The locations of the principal areas of slush accumulation or damage are shown in figure 8. Figures 9 and 10 show the accumulation of slush and the shredding of the electrical wires and the flexible conduits in the air-conditioning system. Figure 11 shows how the cooling air duct was blocked off after the fourth slush run to prevent accumulative damage to the air-conditioning system.

Figure 12 shows the cargo door handle unlatched. This unlatching occurred during a number of runs through the slush. It should be pointed out that just the latch came open and not the door itself. Figure 13 indicates that the brake heat shields on the rear wheels of both main-wheel bogies were distorted during the first run in the slush

(velocity of 120 knots; slush depth of 1 inch) because of impingement of the slush spray generated from the front wheels of each main bogie. Notice how the brake heat shields are distorted along the front edge in the direction of rotation. It is important to note that damage to the brake heat shield was not discovered until the airplane was being towed. The heat shields were removed after the first run and remained off until the slush tests were completed. In figure 14 the door attached to the main landing gear is shown. Note that the edges are bent and the skin on the inside surface of the door is dimpled in many places.

The accumulation of slush in the inboard recessed area behind the Krueger flap is shown in figure 15. Figure 16 shows the accumulation of slush in the main-wheel well area. Figure 17 shows the accumulation of slush in the inboard recessed area between the main flap and the wing. The accumulation of slush on the main-wheel bogie structure is shown in figure 18.

There was more accumulation of slush in some of the recessed areas, such as the Krueger flap, than shown in the previous photographs since a lot of slush fell out before the pictures could be taken. Generally speaking, it is believed that the increase in airplane weight due to slush accumulation would not be detrimental to the operation of the airplane.

CONCLUSIONS

1. A substantial amount of slush impingement and/or accumulation occurs under the fuselage, on the inboard flap surfaces, and on the inboard wing surfaces, as well as within the wheel wells, on the recessed areas for the flaps, in the direct-air inlet ducts, and on the rear wheels of the main-wheel bogies. Any components of light construction, exposed or protruding in these areas, are highly susceptible to damage.

2. Slush accumulation poses an operational hazard from the standpoint of being detrimental to the proper operation of critical component parts of the airplane if the slush were to freeze after take-off and climb to altitude.

3. Slush spray patterns become narrower with a consequent reduction of slush impingement at higher velocities of the airplane, especially beyond speeds at which planing occurs.

REFERENCES

1. Horne, Walter B., Joyner, Upshur T., and Leland, Trafford J. W.: Studies of the Retardation Force Developed on an Aircraft Tire Rolling in Slush or Water. NASA TN D-552, 1960.

2. Collar, A. R.: On the Drag Due to Slush. British A.R.C.22,491, Jan. 9, 1961.

TABLE I

NOSE-WHEEL SLUSH SPRAY IMPINGEMENT

$C_{D,s}$	Percent of total aircraft slush drag
[a]2.60	38
[b].75	-11
Difference	27

[a]FAA test (tire drag and impingement).
[b]NASA TN D-552 (tire drag only).

TABLE II

WIDTH OF REMOVED SLUSH TROUGHS

Velocity, knots	Ave. slush depth, in.	Width of slush trough, in., for:		
		Left main gear	Nose gear	Right main gear
76.5	2.0	50	30	50
102	1.3	50	30	50
108	1.3	50	30	50
115	.9	55	35	50
115	.9	60	40	60
128	1.1	50	38	50
131	.9	55	35	55
135	1.1	55	40	55
147	1.1	55	30	55
153	1.1	50	35	50
———	—	[a]34.5	[a]24.7	[a]34.5

[a]Actual gear width.

Page Intentionally Left Blank

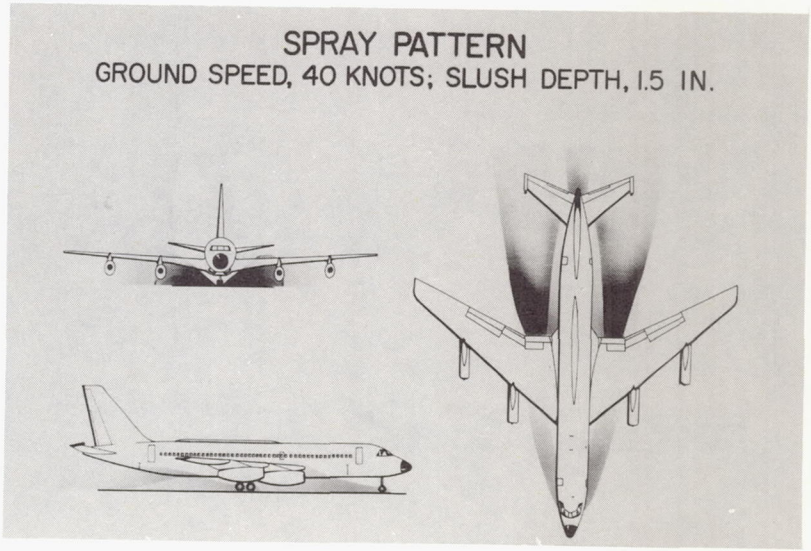

Figure 1

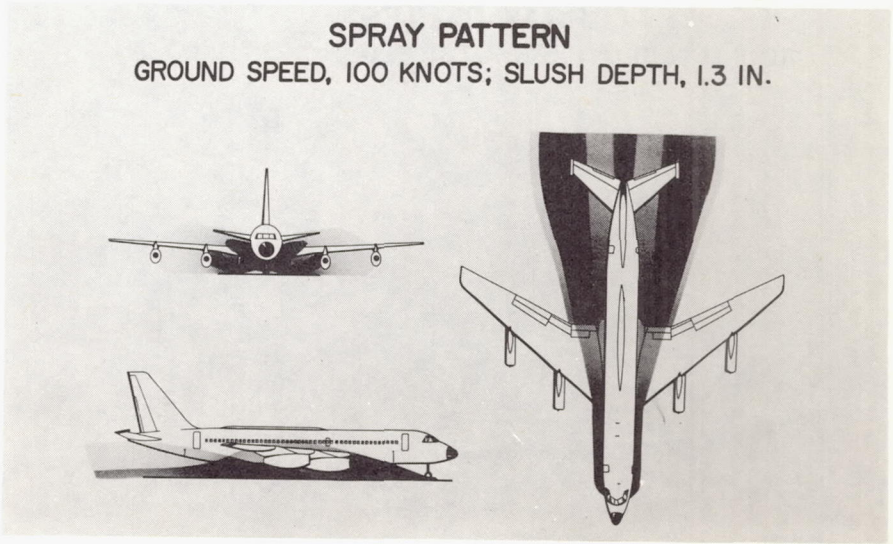

Figure 2

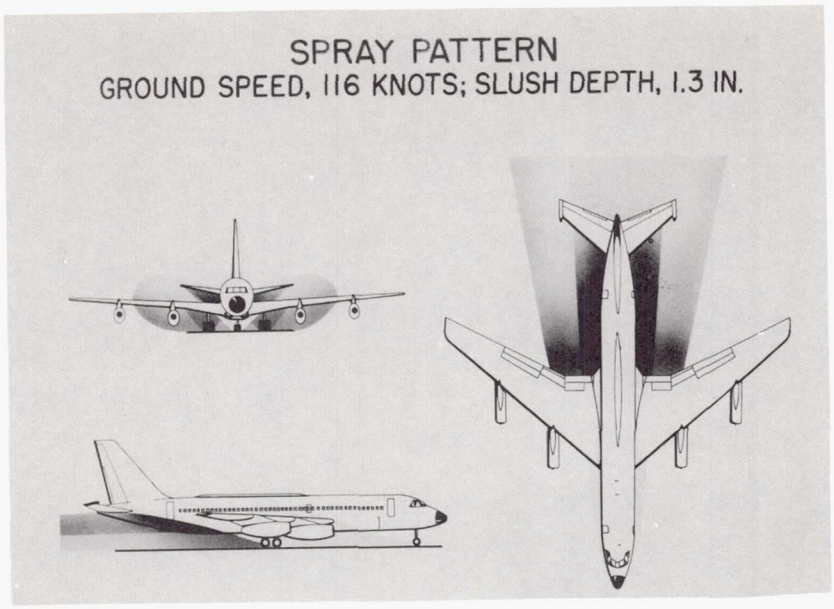

Figure 3

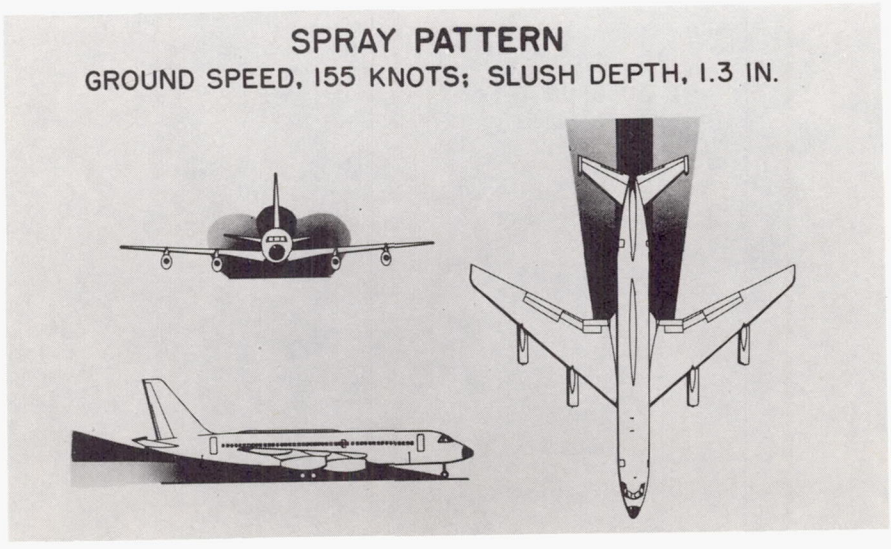

Figure 4

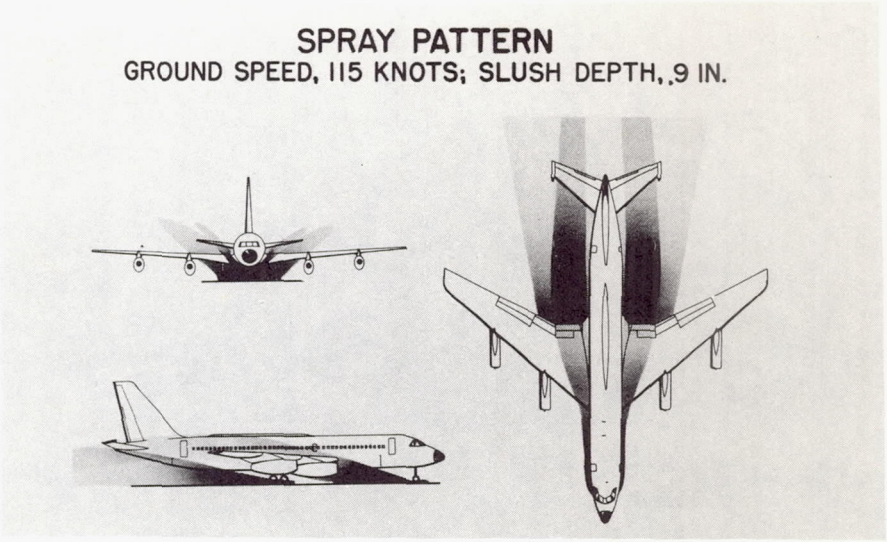

Figure 5

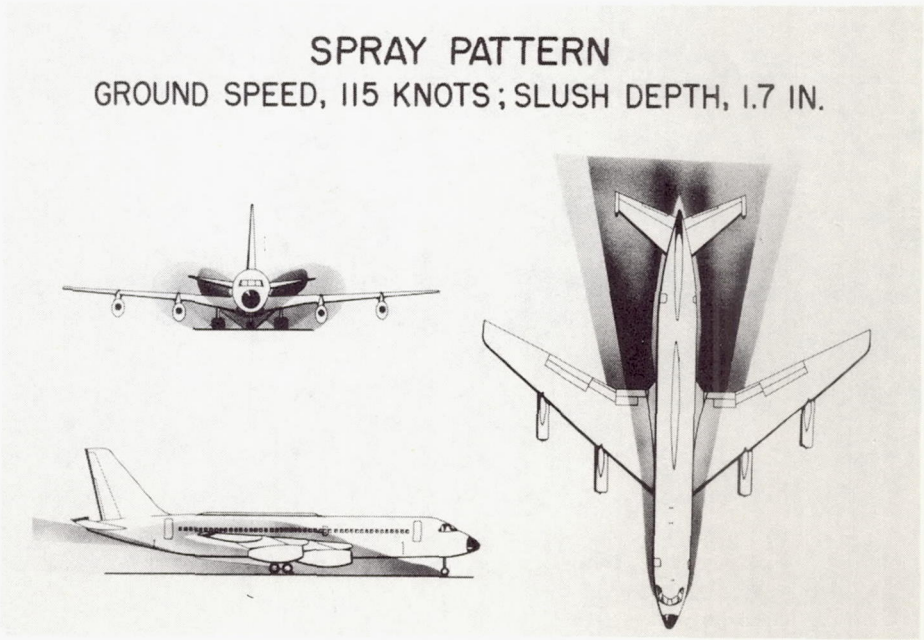

Figure 6

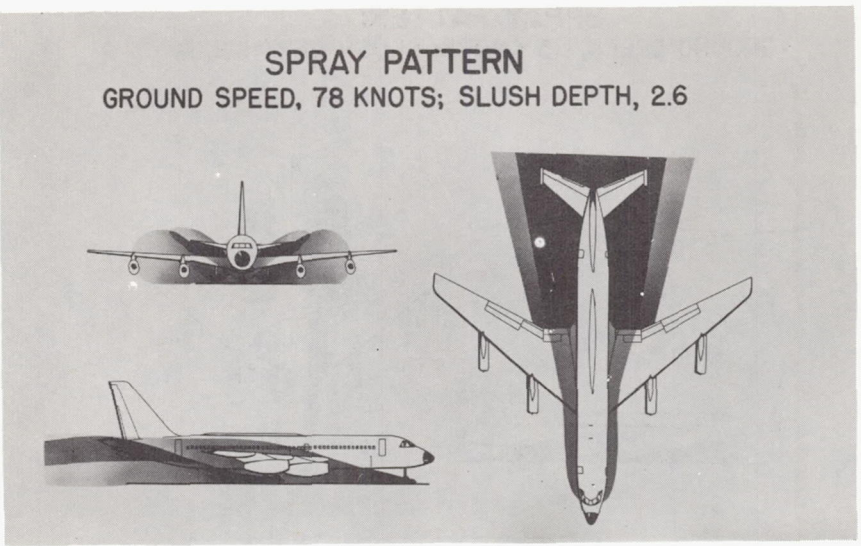

Figure 7

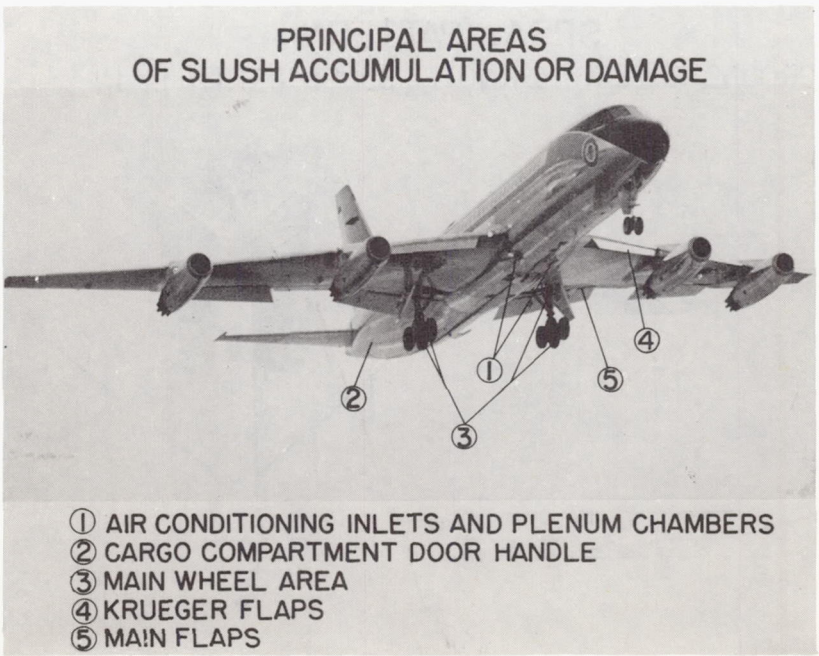

Figure 8

AIR CONDITIONING SYSTEM
INSULATION MATERIAL PEELED FROM WIRES
AND TORN OFF AIR DUCTS

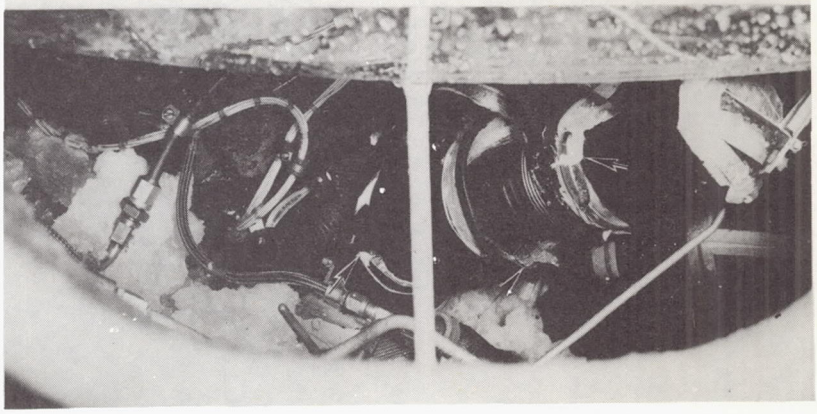

Figure 9 L-61-6963

AIR CONDITIONING PLENUM CHAMBER
ACCUMULATION OF SLUSH

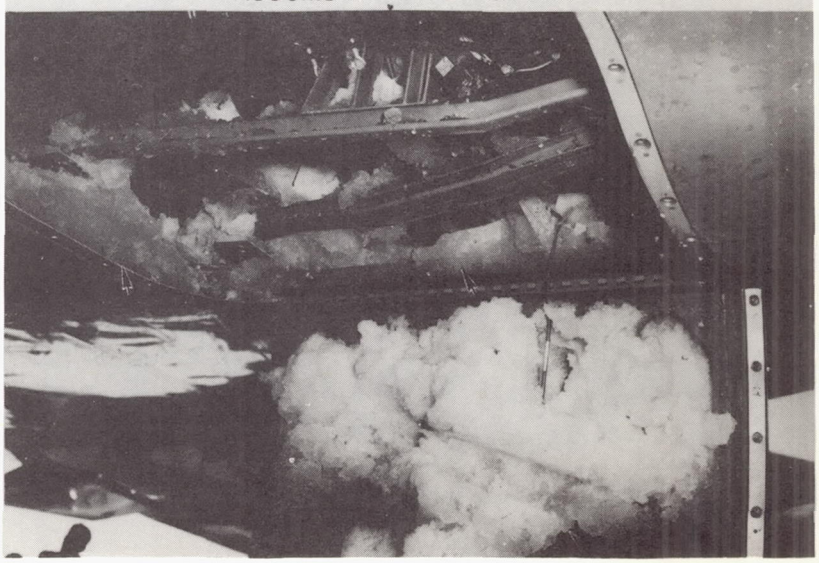

Figure 10 L-61-6964

INLET TO AIR-CONDITIONING SYSTEM
COVER TO PREVENT SLUSH ENTRY

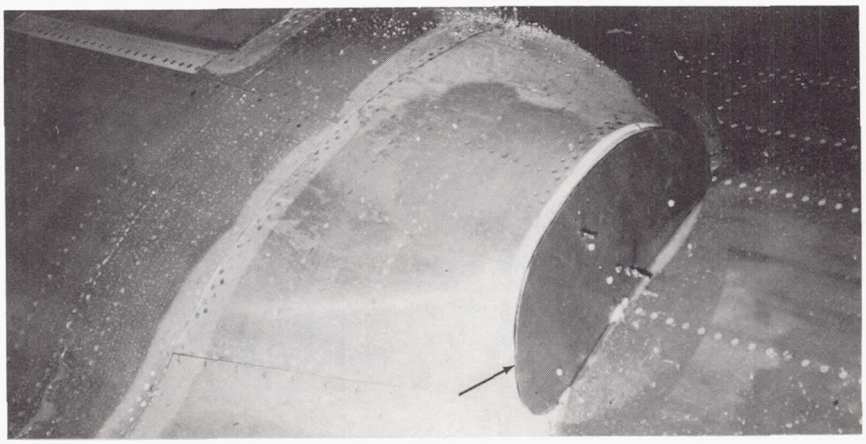

Figure 11 L-61-8416

CARGO DOOR HANDLE
UNLATCHED

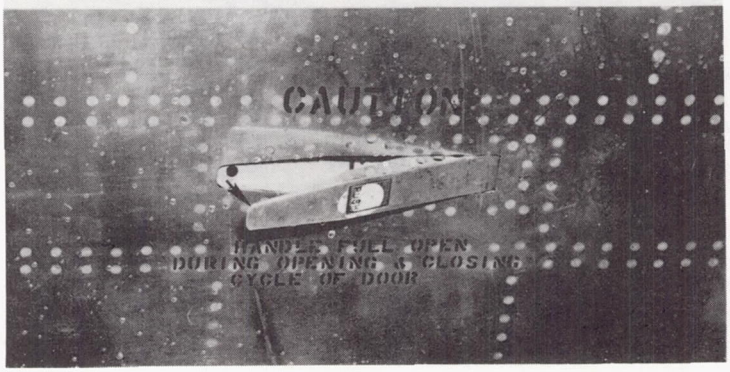

Figure 12 L-61-6968

REAR WHEEL BRAKE ON LEFT MAIN TRUCK
DAMAGED HEAT SHIELD

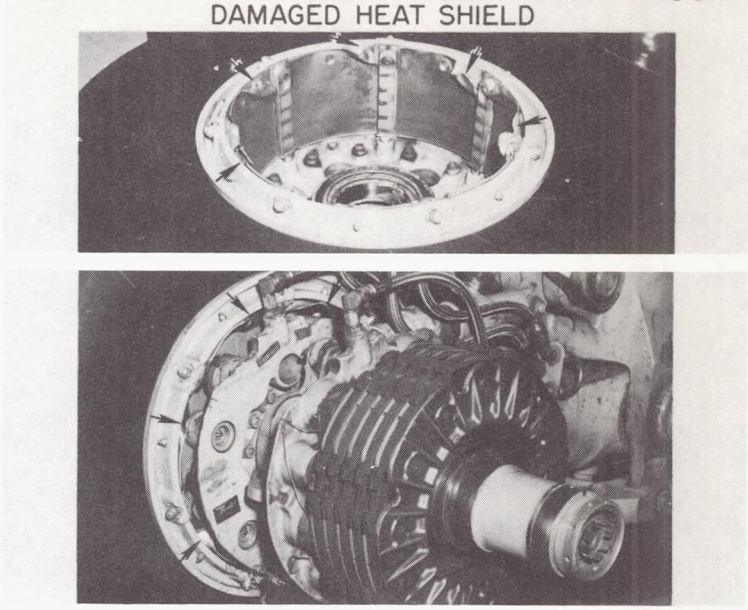

Figure 13 L-61-6965

DOOR ATTACHED TO MAIN WHEEL GEAR
BENT EDGE

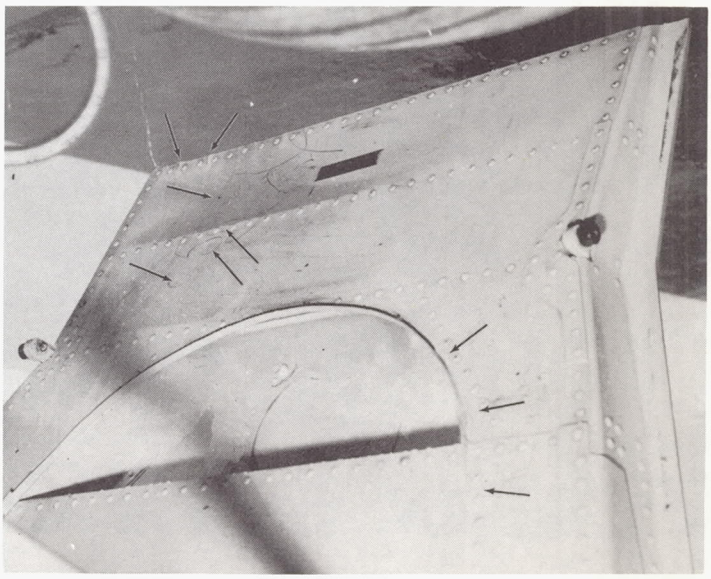

Figure 14 L-61-8417

Figure 15 L-61-6966

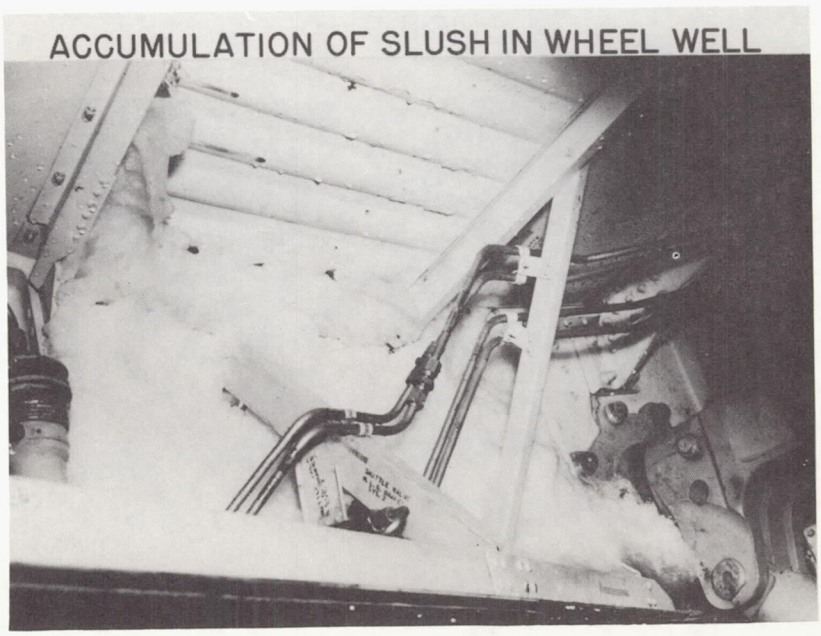

Figure 16 L-61-6967

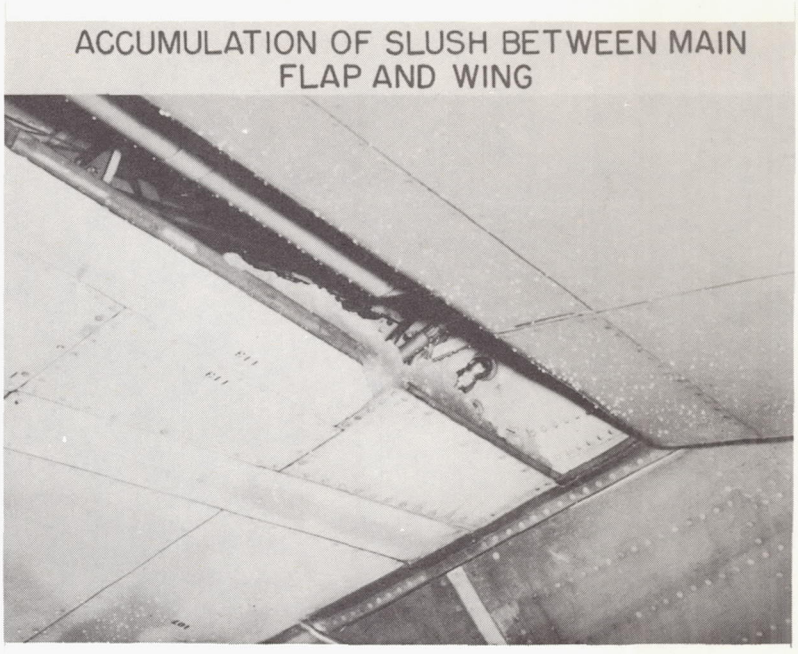

Figure 17

L-61-6957

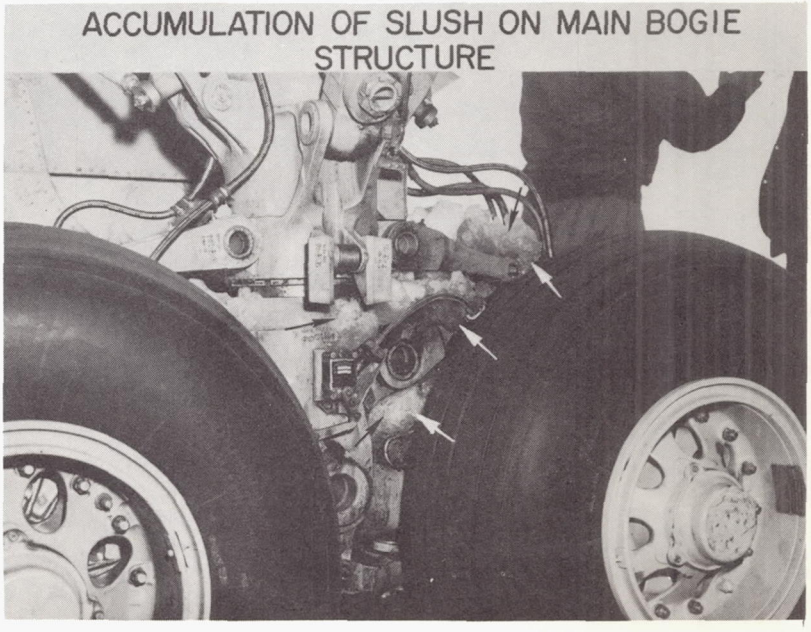

Figure 18

L-61-6958

Page Intentionally Left Blank

5. PREDICTION OF SLUSH DRAG ON AIRCRAFT PERFORMANCE

By Walter B. Horne and Trafford J. W. Leland

NASA

INTRODUCTION

The purpose of this paper is first to show the comparison between previous single-wheel slush tests reported in reference 1 and the test airplane results discussed in previous papers. Then there will be shown possible means of extending the slush prediction method of reference 1 to allow the representation of the reduction of slush drag at speeds above about 120 knots, which was discussed in paper no. 3 by Eugene P. Klueg and paper no. 4 by Wayne D. Howell and Daniel E. Sommers. Finally, the slush-drag data obtained by decelerating the test aircraft at engine idle thrust through the slush trough will be applied by calculating a take-off performance and comparing these results with an observed take-off of the test aircraft at full forward thrust through aircraft rotation and climbout of the slush bed.

The results obtained from the single-wheel tests at the Langley landing-loads track can be stated briefly:

1. Slush or water drag on the single wheel appeared to increase parabolically with increasing ground speed up to 104 knots, the maximum speed investigated.

2. Slush or water drag appeared to vary linearly with slush or water depth.

3. At the higher speeds of the test, near 100 knots, the unbraked wheel was observed to spin-down in the slush or water troughs on the runway, but no deviation from the parabolic drag relation was noticed within the accuracy of the test data (even though tire hydroplaning was incipient).

4. On tests performed with a single-tandem wheel arrangement (one wheel behind the other), the slush drag developed on the rear wheel was approximately 1/10 as great as the slush drag experienced on the front wheel (because of the path-clearing action of the front wheel).

The airplane slush-drag prediction method developed in reference 1 is based on these single-wheel results with the added assumptions that:

1. Spray drag due to slush or water displaced by the landing-gear wheels and impacting on the airplane is assumed to be negligible.

2. Slush or water impingement and displacement drag are assumed to be negligible for the rear wheels of tandem landing gears. On the basis of the observed path-clearing action of the front wheel, only the forward or leading wheels of the aircraft are assumed to experience drag due to slush or water.

3. Tire hydroplaning effects on slush drag are neglected.

At the time of the single-wheel tests, only one four-engine jet transport take-off in actual slush was available for comparison (for a slush depth stated to be 0.6 inch). For this case, the prediction of reference 1 was conservative and overestimated the actual take-off distance slightly.

SYMBOLS

A_G	gross tire contact area, sq in.
$C_{D,S}$	slush-drag coefficient
$C_{L,S}$	hydrodynamic lift coefficient
C_z	tire constant (0.03 for type III and type VII tires) (ref. 2)
D_B	drag force due to tire rolling at peripheral speed less than ground speed (for a braked wheel this force is same as braking force due to wheel brake application), lb
d_S	fluid depth, in
d_{st}	reference slush depth, 1 in.
D_R	tire rolling resistance drag, lb
D_S	drag due to fluid displacement, lb
F_V	vertical load on tire due to airplane or vehicle mass $(F_V = F_{V,G} + F_{V,S})$, lb
$F_{V,G}$	portion of F_V supported by the runway (footprint region A in fig. 7), lb

$F_{V,S}$	vertical hydrodynamic pressure force (footprint region B in fig. 7), lb
I	tire and wheel moment of inertia, slug-ft^2
p	tire inflation pressure, lb/sq in.
p_G	gross tire footprint pressure, lb/sq in.
p_r	rated tire pressure (1/4 tire bursting pressure), lb/sq in.
r	unloaded tire radius, in.
V	velocity, knots
V_G	ground speed, knots
V_P	tire hydroplaning velocity, knots
V_R	ground speed required for aircraft rotation, knots
w	maximum unloaded tire width, in.
x_c	vertical load center-of-pressure displacement, in.
α	wheel angular acceleration, radian/sec^2
δ	vertical tire deflection, in.
μ	tire-to-surface friction coefficient
ρ	fluid density, slugs/cu ft
ω	wheel angular velocity, radian/sec

DISCUSSION

First, the test airplane slush data will be compared with the prediction of reference 1. In figure 1, the ordinate is airplane drag due to slush normalized to an effective slush depth of 1 inch by multiplying the airplane drag due to slush D_S by the ratio of a reference or standard slush depth d_{st} to test slush depth d_S. Reference slush depth is defined as 1 inch of slush on the runway. This normalizing

procedure was necessary because no two runs were made through exactly the same depth of slush. This was discussed in paper no. 3 by Eugene P. Klueg. The abscissa in figure 1 is ground speed in knots. The circular data points represent the test airplane data and the solid line faired through the data points is the same curve given in paper no. 3 for 1 inch of slush. It should be mentioned that the results shown here will differ somewhat from the data given in paper no. 3. This is because the analysis of the present paper is based on ground velocity values obtained from the airborne indicated airspeed recorder corrected for ground effect and wind. Also all measurements of slush mass per unit area in the test bed were considered in this analysis whereas that of paper no. 3 considered slush mass per unit area values in the paths of the nose and main gear only. Despite the differing instruments and data reduction techniques used, it can be seen that good agreement was achieved. The dashed line represents the prediction of reference 1 for the conditions of the test. Major differences between the prediction and the test airplane data are apparent. For ground speeds from 80 to 110 knots, the test airplane develops approximately twice as much slush drag as the method predicts; above 110 knots the test airplane shows decreasing slush drag with increasing ground speed, while the prediction shows increasing drag with increasing ground speed.

In the low ground-speed region of figure 1, the test airplane slush drag is approximately twice the predicted value. This large difference at the lower speeds is believed to be due at least in part to two slush-drag effects experienced by the test airplane, which the prediction method ignores. First, slush-spray impingement drag on the aircraft (which Professor Collar of England calls in reference 3 the "Mudguard Effect") and second, slush interference drag on the rear bogie wheels. In papers 3 and 4, both of these slush-drag effects on the airplane are shown to be considerable at the lower speeds.

At speeds above about 110 knots, the airplane slush drag decreases sharply with further increases in speed and is believed to be associated with hydroplaning and decreased spray impingement. In paper no. 4 it is shown that at about 115 knots, spray impingement on the wings began to decrease with increase in speed. In paper no. 3, it is indicated that near a speed of 110 knots, all the leading wheels and occasionally some of the rear wheels of the test airplane's landing gear have spun down to values considerably below the equivalent dry runway angular velocity required for the ground speed. All this evidence points out that near and above 110 knots the airplane tires are hydroplaning and have lost contact with the runway. If it is assumed that runway slush behaves in this case as water and that the full dynamic pressure acts over the tire footprint area, an equation can be derived for tire planing velocity. (See appendix.) Some interesting numbers are obtained for the calculated hydroplaning velocities of the nose and main wheels of the

test aircraft. For the conditions of the test, the hydroplaning velocity of the main wheel is approximately 110 knots while that of the nose wheel is approximately 100 knots. These two effects the onset of tire hydroplaning and the decrease in spray impingement offer some explanation of the decreased slush drag at high speeds.

It is convenient to present the data in the form of slush-drag coefficients which could be used to correlate the results of this airplane investigation with other airplane results, and to estimate effects of variations in airplane parameters on slush drag.

Slush-drag coefficients for the test airplane, calculated from the drag results in figure 1 are shown in figure 2. These slush-drag coefficients are calculated by the method of reference 1 which is basically the V^2 law and by assuming slush drag on nose wheels and on only the front wheels of the bogie gear. Hence, the slush-drag coefficients include the various effects of wing-lift; spray-impingement drag on wings, flaps, and rear wheels; as well as the drag reducing effects of hydroplaning. The drag coefficient for the single-wheel track tests is shown for comparison.

Because the abrupt break in the slush-drag curve shown in figure 2 for the test airplane falls in the speed range where hydroplaning of the main tires is calculated to occur, it would seem that the hydroplaning speed might be a controlling factor in determining where the drag break occurs. On this basis in figure 3, the abscissa of figure 2 has been normalized with respect to the calculated hydroplaning speed of the main gear tires and the drag coefficient has been extended to zero speed on the basis of the V^2 trend. It is of interest to make use of this representation to examine some calculated trends in hydroplaning effects affected by gross weight of the test airplane. The hydroplaning speed was calculated for three gross weights by the method given in the appendix; the slush-drag coefficient versus velocity curves of figure 4 were obtained from the normalized velocity ratio of figure 3. Figure 4 shows a calculated effect of airplane gross weight on slush-drag coefficient at speeds above the hydroplaning speed. At a given speed, the lowest airplane gross weight indicates the lowest slush-drag coefficient. This analysis, based on the normalized curve, though not substantiated for any other airplane type, is suggested as a reasonable start toward developing a satisfactory means for correlating slush-drag effects.

Two test runs were made at take-off thrust or acceleration through the slush bed. The first run, through 3,000 feet of slush, is shown in figure 5.

Along the ordinate are the airplane attitude in degrees, ground speed in knots, and aircraft forward acceleration in g units all plotted

against runway distance in feet. Aircraft motion is from left to right. The sequence of events is as follows: to the left of the figure, the aircraft has been accelerating under full forward thrust and has attained approximately 100 knots ground speed on a dry runway. At 100 knots, the aircraft dry runway forward acceleration just before distance zero is approximately 0.23g. At distance zero, the aircraft enters the slush, which is approximately $1\frac{1}{8}$ inches deep on the runway. Immediately upon entering the slush, the aircraft acceleration is cut in half by slush drag, and the aircraft proceeds down the runway under reduced acceleration until it exits from the slush. At this point, the aircraft acceleration increases to the normal dry runway value, and rotation and take-off of the aircraft are accomplished. It should be mentioned that at V_R, aircraft rotation was started, but because the pilot did not want to leave the slush under a partial rotation, he stopped rotation and the aircraft left the slush bed in a three-point attitude on the runway. The short-dashed curve represents the predictions of reference 1, while the other dashed curve represents the calculated aircraft acceleration based on the previously discussed deceleration tests. It can be seen that the prediction of reference 1 underestimates by 50 percent the effect of slush in reducing the test aircraft acceleration, while the calculated aircraft acceleration in slush obtained from the deceleration tests fits the experimental acceleration data reasonably well.

Another take-off in slush is shown in figure 6. This figure shows the time history of airplane forward acceleration under take-off thrust during the test run in which the test aircraft entered the slush bed on the runway at a ground speed of about 130 knots, rotated, and then climbed out of the slush bed. The aircraft acceleration is shown as the ordinate and time as the abscissa. The circular data points represent the experimental acceleration values obtained during the run. The solid line represents the calculated dry runway acceleration for the conditions of the test. The dashed line represents the calculated aircraft acceleration in slush based on the slush-drag data obtained from the aircraft deceleration runs in slush. At about 0.8 second the aircraft entered the slush which was approximately 1.4 inches deep on the runway. Notice the sharp reduction in aircraft acceleration on entering the slush. At 1.4 seconds the nose wheels rotated out of the slush bed. Notice the subsequent increase in acceleration due to the absence of nose-wheel slush drag. After 1.4 seconds, the aircraft continued to rotate with lift-off or climbout of the main wheels from the slush occurring at 3.5 seconds. Notice the good agreement between the calculated curve based on the slush drag obtained from the deceleration tests and the experimental take-off data over most of the time history.

CONCLUDING REMARKS

Two conclusions that may be drawn from this paper are that it is evident that the method of reference 1 for calculating slush drag on aircraft should be expanded to include effects of spray drag and tire hydroplaning, and that slush-drag measurements obtained from aircraft deceleration runs through slush are valid for computing aircraft take-off performance in slush.

APPENDIX

DERIVATION OF TIRE HYDROPLANING VELOCITY

The following derivation of tire hydroplaning is based on an earlier derivation from an unpublished NASA paper. The net torques and moments acting on an unbraked tire must, at any time, equal the angular acceleration of the wheel. (See fig. 7.) Including hydrodynamic effects, this can be expressed approximately as

$$\alpha = \frac{F_V(x_c) - \left[D_R + D_S + (F_V - F_{V,S})\mu\right](r - \delta)}{12I} \tag{1}$$

When the vertical component of the hydrodynamic pressure force $F_{V,S}$ equals the vertical ground force F_V, the tire-ground frictional moment reduces to zero, and since at this point, the tire is entirely supported by the fluid on the runway, tire hydroplaning must exist. To predict the velocity at which this phenomenon will occur, it is assumed in line with hydrodynamic theory that the hydrodynamic pressure force $F_{V,S}$ is proportional to tire-ground gross contact area A_G, fluid density ρ, and to the square of forward velocity. Ignoring other variables such as the effects of tire-tread design, fluid viscosity, and runway surface texture, and assuming the fluid depth on the runway to be greater than tire-tread depth, the following approximate expression for tire hydroplaning velocity V_P may be obtained:

$$F_V = F_{V,S} = \frac{1}{2} C_{L,S} \rho A_G V_P^2 \tag{2}$$

Rearranging terms, the following equation may be used to find V_P in knots:

$$V_P = 0.592 \left[\left(\frac{F_V}{A_G} \right) \left(\frac{288}{C_{L,S}\rho} \right) \right]^{1/2} \tag{3}$$

This equation has been used to calculate hydroplaning velocities for trailer and automobile tires and these calculations are compared with experimental values for the hydroplaning velocity (fig. 8). To find the hydroplaning velocities of aircraft tires, the methods of reference 2 may be used to obtain a better definition of the term F_V/A_G, which is actually the gross footprint pressure p_G exerted by the tire

on the ground. Reference 2 gives the following expressions for p_G in terms of tire characteristics:

$$\frac{F_V}{A_G} = p_G = \left[0.6 + \frac{81}{1600C_z}\left(\frac{\delta}{w}\right)\right](p + 0.08p_r) \qquad \left(\frac{\delta}{w} \leqq \frac{40}{9} C_z\right) \tag{4}$$

$$\frac{F_V}{A_G} = p_G = \left[1.05 - C_z\left(\frac{\delta}{w}\right)^{-1}\right](p + 0.08p_r) \qquad \left(\frac{\delta}{w} \geqq \frac{40}{9} C_z\right) \tag{5}$$

Thus tire planing velocities may be approximately expressed for modern aircraft tires by the equations:

$$V_p = 0.592\left\{\frac{288\left[0.6 + \frac{81}{1600C_z}\left(\frac{\delta}{w}\right)\right](p + 0.08p_r)}{C_{L,S}\rho}\right\}^{1/2} \qquad \left(\frac{\delta}{w} \leqq \frac{40}{9} C_z\right) \tag{6}$$

$$V_p = 0.592\left\{\frac{288\left[1.05 - C_z\left(\frac{\delta}{w}\right)^{-1}\right](p + 0.08p_r)}{C_{L,S}\rho}\right\}^{1/2} \qquad \left(\frac{\delta}{w} \geqq \frac{40}{9} C_z\right) \tag{7}$$

These equations were used to calculate hydroplaning velocities for the aircraft tires in figure 8. The data shown in this figure indicate that reasonable agreement between calculated and experimental tire hydroplaning velocities occurs for a wide variety of tire pressures and vertical loads when $C_{L,S} = 0.7$ is used in equations (3), (6), and (7).

Figure 9, taken from Langley landing-loads track test data, illustrates the importance of tire pressure as it affects hydroplaning velocity. Test conditions for the two cases illustrated were similar, using the same tire, vertical load, and degree of runway wetness. Calculated hydroplaning velocity for each tire pressure is indicated on the figure as approximately 97 knots for the 115 lb/sq in. case, and approximately 148 knots for the 350 lb/sq in. case. It can be seen from the figure that the tire at 115 lb/sq in. starts to spin-down immediately on entering the wetted test section, and continues to spin-down until the dry runway is encountered.

REFERENCES

1. Horne, Walter B., Joyner, Upshur T., and Leland, Trafford J. W.: Studies of the Retardation Force Developed on an Aircraft Tire Rolling in Slush or Water. NASA TN D-552, 1960.

2. Smiley, Robert F., and Horne, Walter B.: Mechanical Properties of Pneumatic Tires With Special Reference to Modern Aircraft Tires. NASA TR R-64, 1960.

3. Collar, A. R.: On the Drag Due to Slush. British A.R.C. 22,491, Jan. 9, 1961.

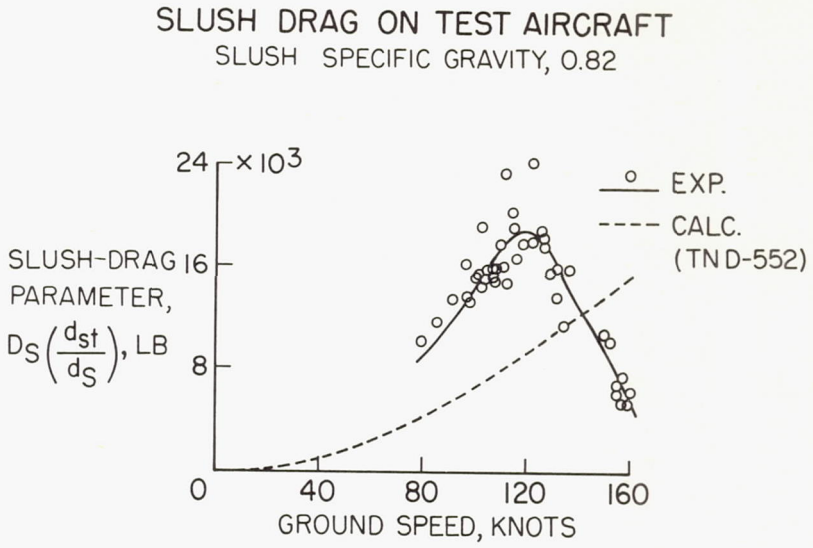

Figure 1

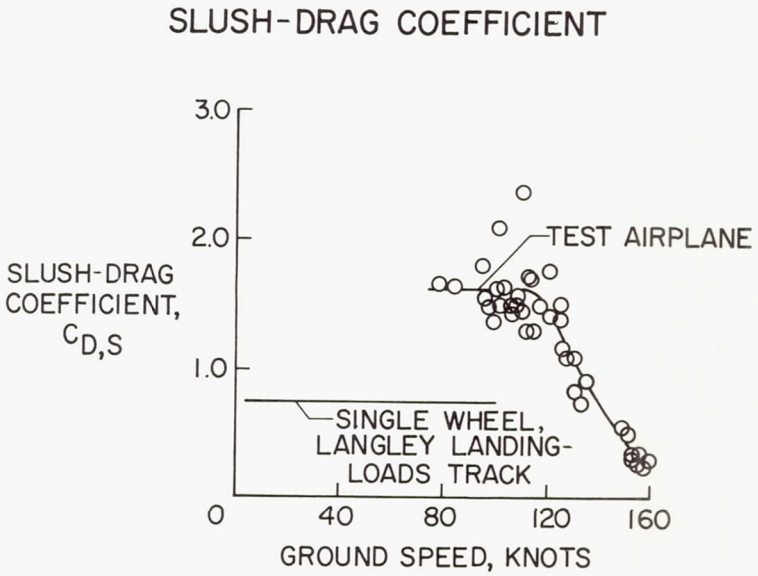

Figure 2

NORMALIZED AIRPLANE SLUSH-DRAG COEFFICIENT

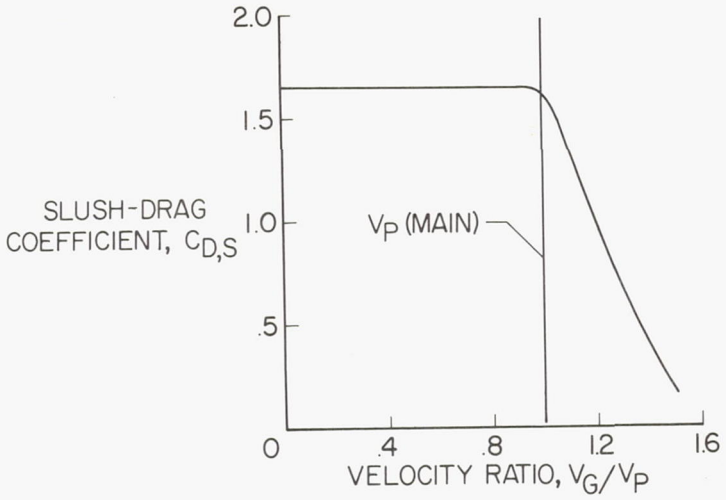

Figure 3

EFFECT OF VERTICAL LOAD
ON SLUSH-DRAG COEFFICIENT
MAIN WHEEL TIRE PRESSURE = 160 LB/SQ IN.

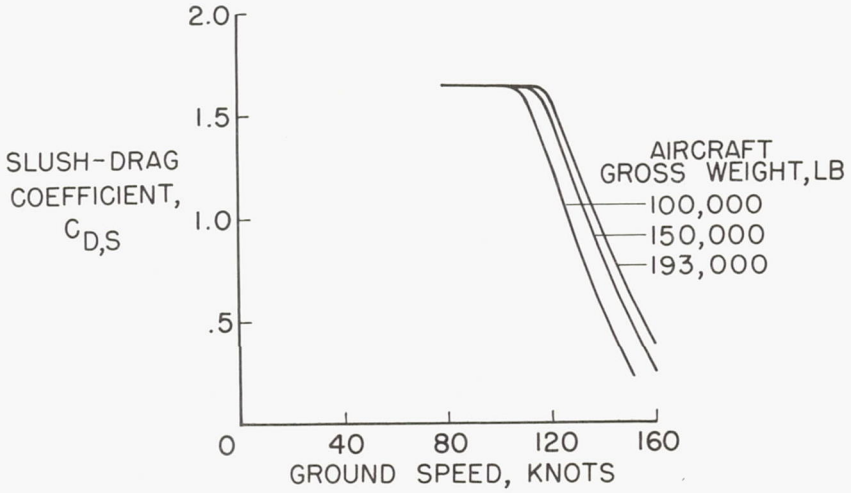

Figure 4

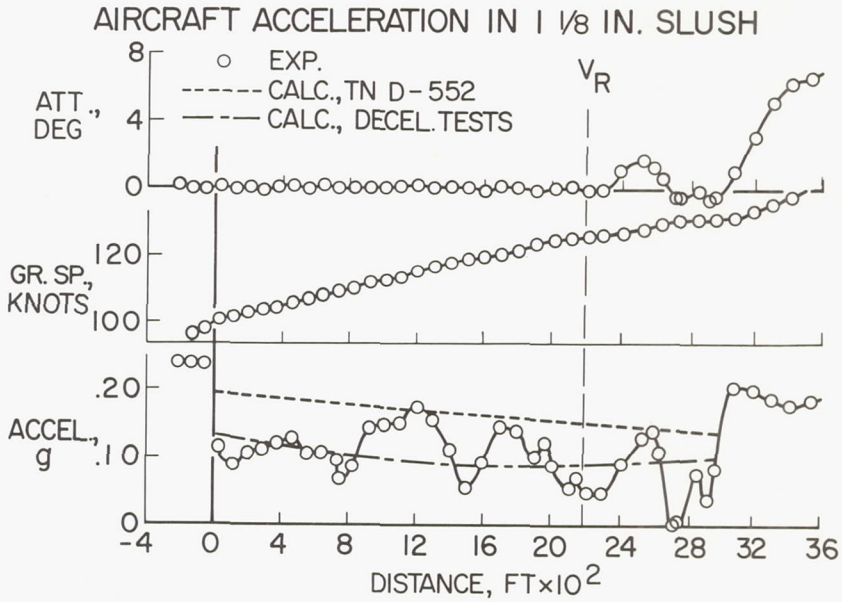

Figure 5

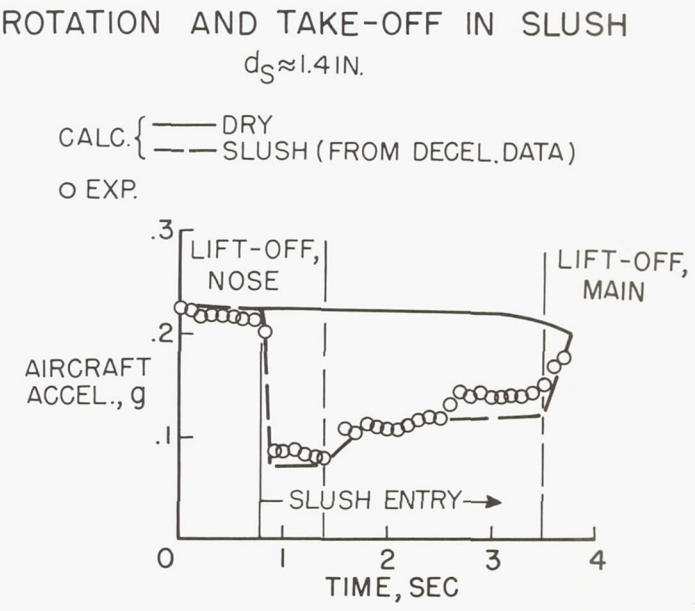

Figure 6

UNBRAKED ROLLING TIRE UNDERGOING SPIN-DOWN
ON FLUID COVERED RUNWAY

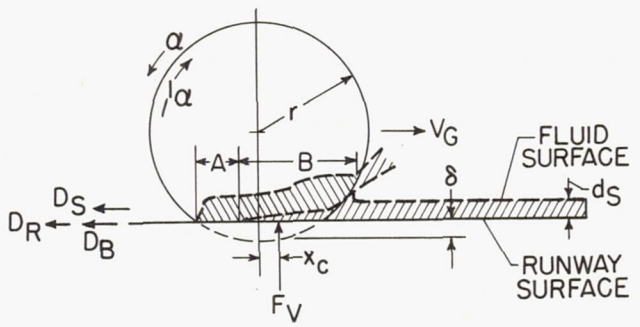

Figure 7

COMPARISON OF CALCULATED AND EXPERIMENTAL
TIRE HYDROPLANING VELOCITIES
WET RUNWAY

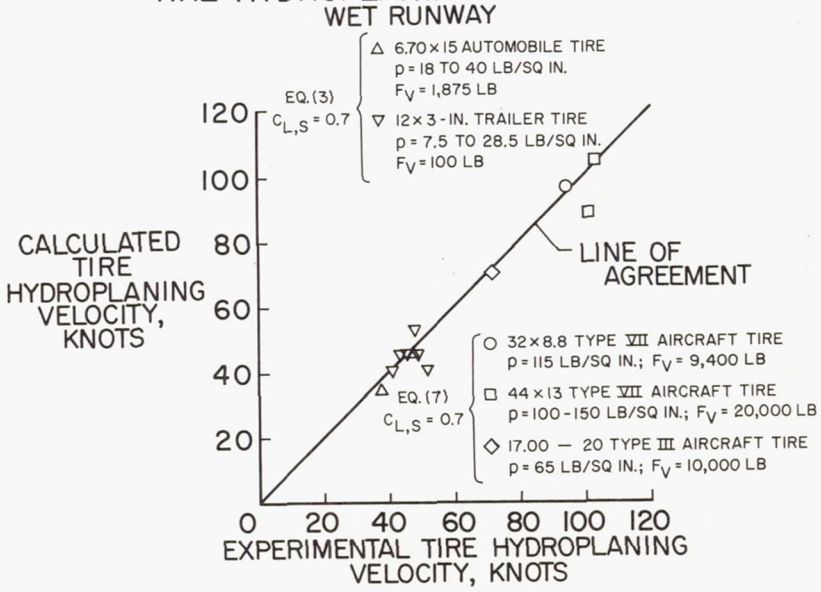

Figure 8

EFFECT OF TIRE PRESSURE ON TIRE HYDROPLANING

32×8.8 TYPE VII RIB TREAD TIRE; F_V=10,000 LB

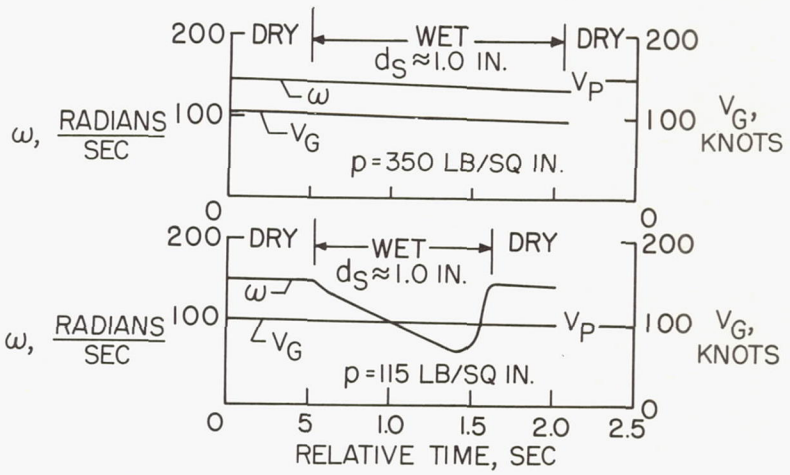

Figure 9

Page Intentionally Left Blank

6. OPERATIONAL METHODS FOR SLUSH MEASUREMENTS

By Richard H. Sawyer and B. C. Riddle, Jr.

NASA

INTRODUCTION

The results presented in a preceding paper by Eugene P. Klueg (paper no. 3) have shown that the depth and density of slush are significant factors in determining take-off performance. In order to account for these factors, some operational method must be developed and utilized for either measuring the depth and density of the slush or for predicting airplane performance by measuring the effects of the slush on some device with which the performance of the airplane has been correlated. The results obtained by either method would be applied through calculations to determine take-off performance for the existing conditions.

At present, no actual operational method for measuring the characteristics of or predicting the effect of slush is known to be in use. Snow committees, consisting of airline and airport representatives, do examine the runway under conditions of snow and slush to determine whether continued operations are deemed to be safe.

The purpose of this paper is to examine some of the possible operational methods for both slush measurement and for predicting the effect of slush. The methods will be examined with regard to practicability, the time required for measurements, and the expected accuracy.

SYMBOLS

A	area of slush sample, sq ft
a	deceleration, ft/sec^2
D_S	slush drag force, lb
d	depth of slush, ft
d_{eff}	effective depth of slush, ft unless otherwise indicated
f	function

g	acceleration due to gravity, ft/sec^2
m	mass of slush sample, slugs
V	ground speed, ft/sec unless otherwise indicated
v	volume of slush sample, cu ft
ρ	density of slush, slugs/cu ft
ρ_{mean}	mean or reference value of slush, slugs/cu ft

Subscripts:

a	airplane
c	automobile

METHODS

The methods considered in this paper are defined as follows:

(1) Spot manual - Manual measurement of the physical characteristics of the slush by taking samples at a sufficient number of spots on the runway.

(2) Spot vehicular - Determination at a sufficient number of spots along the runway of the retardation effect of the slush on a coasting automobile. The retardation effect is measured by means of an indicating accelerometer.

(3) Continuous vehicular - Determination of the slush drag force on a wheel pushed through the slush by a vehicle. The drag force would be continuously recorded on a strip chart.

All three methods will be examined in respect to measurement of the physical characteristics of the slush. The spot vehicular method will also be examined in respect to correlating the retardation effect of the slush on the automobile with retardation effect of the slush on the airplane.

EVALUATION OF METHODS

Spot Manual

As has been indicated in a previous paper by Charles M. Middlesworth et al. (paper no. 2), the physical characteristics of the depth and density of the slush can be expressed in terms of an effective depth. Since

$$D_S = f(\rho d)$$

and

$$\rho = \frac{m}{v}$$

where

$$v = Ad$$

then

$$D_S = f\left(\frac{m}{A}\right)$$

or

$$D_S = f\left(d_{eff}\rho_{mean}\right)$$

where

$$d_{eff} = \frac{m/A}{\rho_{mean}}$$

Thus, by measurement of the mass per unit area, an effective slush depth can be determined. Use of the effective depth reduces the number of measurements required to one at each spot along the runway.

However, it appears that the time required for a sufficient number of spot measurements to be taken to obtain a realistic average would be prohibitive. As stated in the paper by Charles M. Middlesworth et al. (paper no. 2), it was deemed necessary in the present investigation to make 36 spot measurements in 1,000 feet. On this basis, a 10,000-foot runway would require some 360 spot measurements. Even granting that the number of measurements in routine practice could be reduced, it still appears that the time that the runway would be closed for measurements would be of the order of 1 hour, which is considered prohibitive.

Spot Vehicular

The spot vehicular method would require use of an automobile equipped with an indicating accelerometer of the type generally used to assess automobile engine and braking performance. On the basis of the experience of the Scandinavians with a similar method used to assess braking conditions, it appears that this method might be marginal with respect to time required for measurement, inasmuch as on the order of 1/2 hour would be required to make enough spot measurements. With regard to accuracy, results obtained with a 1961 automobile equipped with a Tapley accelerometer during the present test program are shown in figure 1 as the ratio of the deceleration to the square of the velocity plotted against the effective depth. These results were obtained in each case during a coasting run through the slush bed a short time after the run by the test airplane.

The results shown in figure 1 indicate that the effective depth of the slush can apparently be measured by this technique. It appears that for effective depths of about 1 inch or less (the depths of most interest operationally), the depth can be measured to an accuracy of about 1/4 inch. Since the test runs for these results were made in an area of the slush bed onto which slush spray from the airplane had been thrown, it is probable that somewhat better accuracy would be obtained in better-controlled tests.

Continuous Vehicular

The continuous vehicular method would require the acquisition of an instrumented wheel designed to measure the slush drag force and would require a vehicle to propel the wheel. Extreme care would be necessary in the design of the drag-measuring device in order to prevent errors due to inertia effects resulting from acceleration of the propelling vehicle. In addition, a time-history recorder or integrating system would be required. From a time standpoint, this method would be the best of the methods considered. Experience with the Swedish Skiddometer indicates that a 6,000- to 7,000-foot runway can be surveyed in 2 to 3 minutes, with the total time from leaving the ramp to the time the record is analyzed and an answer prepared being of the order of 15 minutes.

In order to indicate the probable accuracy which might be obtained with such a device, results obtained with a single wheel (32 × 8.8, type VII aircraft tire) at the Langley landing-loads track are shown in figure 2. The ratio of the slush drag force to the square of the velocity is shown plotted against the effective depth.

The results shown in figure 2 indicate that the effective depth of the slush can apparently be measured with this technique. It appears that the effective depth can be measured to an accuracy of about 1/4 inch.

SIGNIFICANCE OF THE ACCURACY OF MEASUREMENT

To investigate the significance of errors in the determination of the effective depth of the slush, the effect of measurement error on the distance required to attain the rotational speed was calculated for the test airplane at the test weight of 150,000 pounds. These results are shown by a bar graph in figure 3 for measurement errors of 1/16 and 1/4 inch for a nominal slush depth of 1/2 and 1 inch and were calculated from the test results. The length of the clear portion of each bar represents the distance for no slush, the adjacent cross-hatched portion represents the added distance for the nominal depth of slush, and the final cross-hatched portion represents the added distance for underestimating the depth of slush by the error in measurement noted. It can be seen that 1/2 inch of slush adds approximately 650 feet to the basic 3,000 feet required and that underestimating the depth by 1/4 inch adds approximately 500 feet more. The 1 inch of slush adds approximately 1,800 feet to the basic distance required and the measurement error of 1/4 inch adds approximately 1,000 feet more for this case. The 1/4-inch measurement errors correspond to errors of about 3 and 6 seconds to reach rotational speed for the 1/2-inch and 1-inch cases, respectively.

It appears from these results that the 1/4-inch accuracy of measurement determined for the vehicular methods would not be satisfactory from an operational standpoint, without the penalty of adding a factor of safety of about 1.7 to the computed slush effect.

Improvement of the accuracy of measurement by some method to the order of 1/16 inch would apparently reduce the error in distance to a small enough value to be ignored. It should be pointed out, however, that the above calculations were based on virgin slush conditions. Passage of aircraft subsequent to depth measurement could deepen the slush on part of the runway, so that a factor of safety should be allowed in order to provide for this possible contingency.

CORRELATION OF A VEHICLE WITH THE AIRPLANE

For correlation of a vehicle with the test airplane, the faired slush deceleration measured with the automobile equipped with the Tapley accelerometer (the results previously presented in fig. 1) was

compared with the slush deceleration measured on the airplane (shown in fig. 4) for effective depth values of 1.56, 1.25, and 0.94 inches. This comparison is shown in figure 5 as the correlation parameter $\left(\frac{a_a}{a_c}\right)\left(\frac{V_c}{V_a}\right)^2$ plotted against the effective depth. The comparison is shown at airplane speeds of 100 and 110 knots. The results for other airplane speeds up to 125 knots are similar.

The results shown in figure 5 indicate that since the correlation parameter is practically constant with respect to effective depth, a definite correlation exists between the deceleration effect of the slush on the automobile and on the airplane. This indicates that the deceleration effect of the slush on the airplane at speeds of the order of 100 to 125 knots can be predicted by measurements of the deceleration effect of the slush on an automobile operated at speeds as low as 35 knots.

For this method, as for the depth-measuring method using the accelerometer-equipped car, the measurement time is marginal. Since the results for this method are based on the same automobile deceleration data used in the analysis of the depth-measuring method, the accuracy of prediction of the distance to rotational speed is the same and thus again indicates that with such accuracy, a factor of safety of about 1.7 for the calculated effect of slush would be required.

CONCLUDING REMARKS

None of the methods examined for measuring the effective depth of the slush appeared to be completely satisfactory. The manual methods were prohibitive in the time required to make a sufficient number of measurements. The use of an accelerometer-equipped automobile appeared marginal with respect to measurement time. Both the accelerometer-equipped car and a drag-measuring wheel gave results which indicated that a factor of safety of about 1.7 for the calculated incremental distance due to slush would be required because of the measurement accuracy. It appeared that if the accuracy of measurement for the drag-measuring wheel could be improved this would be a satisfactory method.

Correlation of the deceleration effect of the slush on an automobile with the deceleration effect on the airplane was shown to be an alternative method for predicting the effect of slush on take-off. This method was marginal with respect to the time required for measurement, and also would require use of a factor of safety of the order of 1.7 to account for measurement accuracy.

AUTOMOBILE DECELERATION IN SLUSH

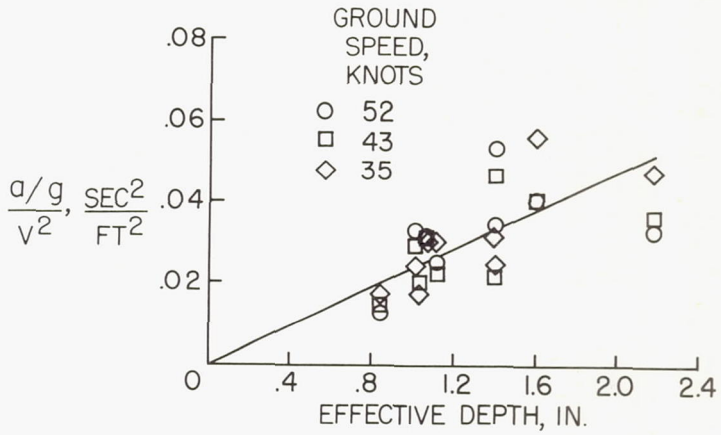

Figure 1

SLUSH DRAG ON SINGLE WHEEL

LANGLEY LANDING-LOADS TRACK;
GROUND SPEED, 65 TO 105 KNOTS

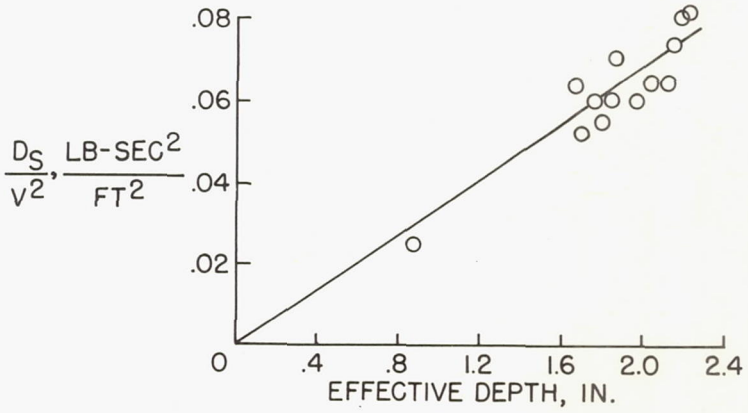

Figure 2

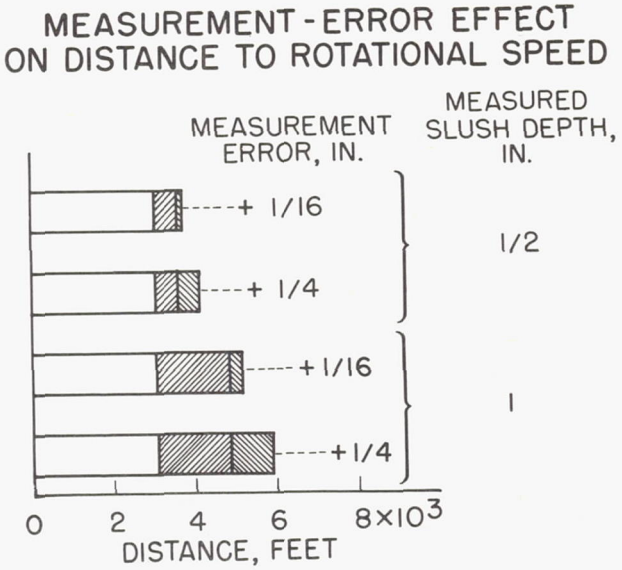

Figure 3

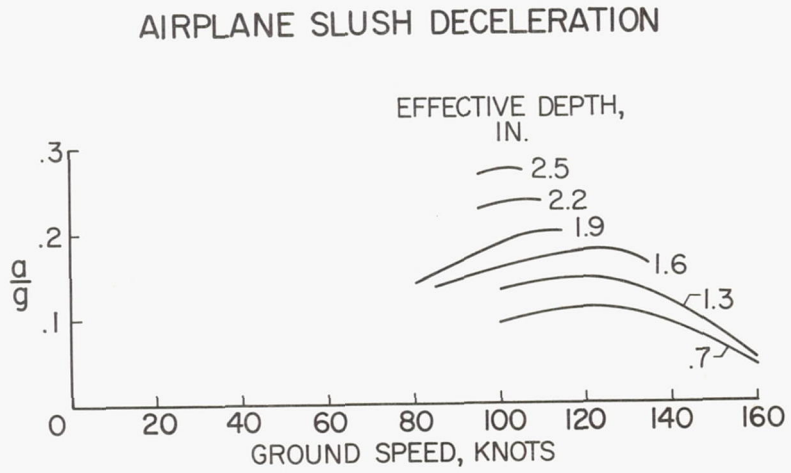

Figure 4

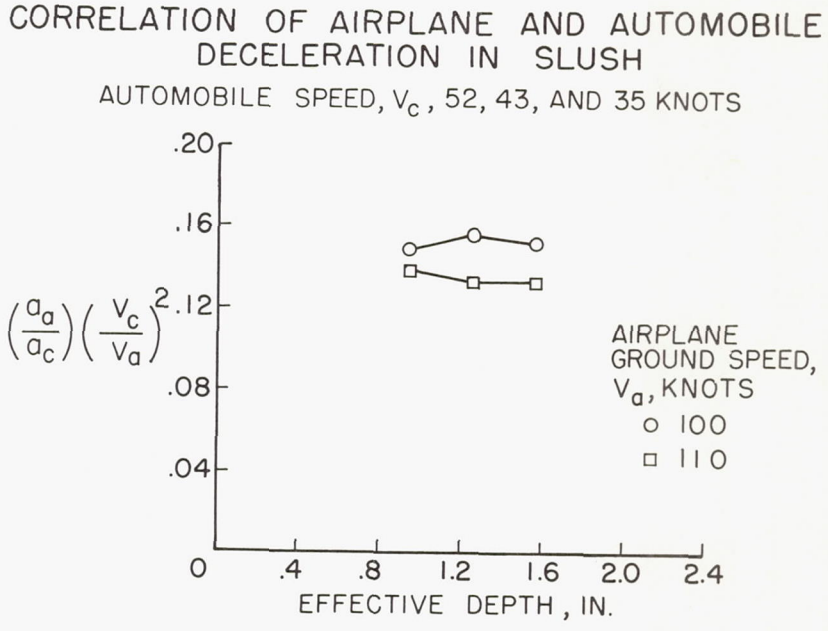
CORRELATION OF AIRPLANE AND AUTOMOBILE DECELERATION IN SLUSH
AUTOMOBILE SPEED, V_c, 52, 43, AND 35 KNOTS
$\left(\frac{a_a}{a_c}\right)\left(\frac{V_c}{V_a}\right)^2$
.20
.16
.12
.08
.04
0
.4
.8
1.2
1.6
2.0
2.4
EFFECTIVE DEPTH, IN.
AIRPLANE GROUND SPEED, V_a, KNOTS
o 100
□ 110

Figure 5

Page Intentionally Left Blank

7. OPERATIONS IN SLUSH AS SEEN BY THE PILOT

By C. E. Richards

FAA

Some of the information to be disseminated in this paper will be elementary to many of those who have operated in and out of slush for many years. It was not elementary to me, however, and may take on new meaning for all of us in the light of the present operation of turbine-powered, swept-wing aircraft.

Prior to discussing actual aircraft rotation and take-off, I should like to review slush damage, which on the aircraft tested did not appear to be excessive from the standpoint of basic airframe damage. It must be kept in mind, however, that many of the jet transports currently in use have air intake ducts, plenum-chamber openings, et cetera, which can and will ingest slush, water, snow, and ice. If the areas in question are large enough and are located within the areas of slush impingement from nosewheel or main gear spray patterns, they can collect slush and materially increase the gross weight of the aircraft. In addition, any equipment exposed in these areas can be damaged by slush impingement. After several exposures to only 1,000 feet of slush, this possibility was recognized to be a problem, and the plenum chamber inlet ducts were sealed off on the test aircraft for the remainder of the program.

In retrospect, I have tried to envision just what slush accumulations could be expected on an aircraft in 7,000 or 8,000 feet of exposure; what airframe gross weight increase and what center-of-gravity shift could be expected. I add runway length to compensate for weight growth, which adds exposure to more slush and more weight growth. I try to schedule stabilizer position on the basis of predicted center-of-gravity shift, and somewhere along the line I get lost. This is, of course, slightly exaggerated, but not out of reason. If, and when, we get this aircraft into the air, we still have a slush problem. The problem remaining stems from slush collected in wheel wells, behind exotic high lift devices, et cetera, which may freeze in flight due to the exposure to the flow of cooling air. Perhaps wheel wells are a poor example, as the landing gear is retracted early in the take-off flight path, but flaps and leading-edge devices may not be retracted for some time. Apply 3,000 pounds per square inch of pressure to the actuators and something is likely to give. I hope it's the ice! Many military pilots operating in northern areas can attest to the difficulty of extending landing gears that are held up by frozen doors and mechanisms. We did not operate a cold airplane in a cold atmosphere, but I feel that we might have encountered more difficulties in this test program if we had.

Let us get back to the take-offs. Motion pictures were taken of two take-off runs made in slush. The first take-off was planned as an acceleration in 1 inch of slush from 100 knots up to rotation speed V_R of 124 knots in the first 1,500 feet of a 3,000-foot strip followed by rotation and lift-off in the remaining 1,500 feet. As mentioned in earlier papers, the measured slush drag was considerably higher than theory predicted and the depth turned out to be 1/8 inch deeper than planned. Consequently, at the midpoint of the strip, we were 3 or 4 knots below V_R and didn't attain rotation speed until approximately 800 feet from the end of the strip.

Theoretically, slush drag produces rather large nose-down pitching moments on the aircraft, and a sudden reduction of these moments during actual rotation might lead to over-rotation and striking the tail. In view of this possibility, as I rotated and saw the end of the slush pit at about the same time, my enthusiasm for the take-off waned somewhat and I decided to exit the pit in a normal ground attitude.

The second take-off was in a 1,500-foot strip which was entered at V_R speed, and rotation was begun approximately 130 feet into the bed with lift-off occurring 420 feet later. Other film sequences show the weather-cocking which occurs on a slick runway with a reasonably small crosswind component.

The purpose of the take-off runs was not to demonstrate that airplanes can take off in slush. This has been amply demonstrated by air carriers for many years. The purposes of the acceleration and rotation were: (1) to demonstrate that drag data collected in deceleration runs earlier in this test program were valid for the full-power acceleration condition and (2) to demonstrate in an appreciable slush depth that drag on the wheels and slush impingement on the aft fuselage did not create a pitchdown moment so large as to prevent rotation or make the operation hazardous.

Figure 1 compares the actual airplane acceleration and the calculations based on the deceleration data collected. The results show close agreement. The solid line was calculated for slush $1\frac{1}{8}$ inches deep and the circles represent data points from the first acceleration and aborted lift-off run which was made in slush averaging $1\frac{1}{8}$ inches in depth.

Figure 2 shows the actual rotation in 1.4 inches of slush. The top trace is for attitude, the middle is for ground speed, and the bottom is for acceleration. On the lower trace after the drop in acceleration as the slush was entered, the acceleration increased slightly as the nose gear

lifted out, was somewhat gradual as wing lift began to pick the weight up off the main landing gear and extensive hydroplaning occurred, and again increased to airborne acceleration when the main gear left the ground. The gradual acceleration buildup which represents a gradual drag reduction appeared to have dissipated the nose-down pitching moment so that no unusual pitch-up was felt on lift-off. During the rotation and lift-off, I found the aircraft response to be slightly slow. This is difficult to define, as it followed control inputs well, but not as smartly as it did on a dry runway.

As can be seen the acceleration value of 0.22g on the dry runway prior to entering the 1.4-inch-slush test strip at rotation speed decreased in the test-strip area to approximately 0.09. I ask myself how much runway would have been required if the target rotation speed had been 140 knots rather than 124 knots. Further, if we had experienced an engine failure just prior to V_R, could we have ever reached our original 124-knot rotation speed on a 10,000-foot runway with 25 percent less power available? Data presented in a previous paper indicate that we could not.

It has been shown that a great deal of slush drag is created by the aircraft penetrating the slush thrown into the air by the nosewheel. This being the case, possibly a take-off technique in which the nosewheel is held out of the slush would improve the situation, but this too adds complication. The nosewheel should not be lifted prior to attaining the minimum control speed on the ground, which may be as high as V_R in some instances. Also, if the nose is lifted too high, the basic airplane drag may be as great as the slush drag or greater. From this it appears that no easy solution for reducing nosewheel spray is available unless deflectors can be installed to keep spray down below the airframe.

I have been asked to discuss aircraft control, noise, and vibration. Let me first discuss noise and vibration, as these are rather obvious. On all test runs in slush there was an increase in noise level, and also in vibration, but the crew of the modern jet is located half a city block in front of the main landing gear, and with the cabin door closed the only things that are really felt or heard are those originating from the nosewheel. We in the test crew felt them because we made a transition from smooth, hard-surfaced runway into a prepared slush bed. If we had started the take-off in slush, the difference would have been much less perceptible. The noise and vibration created by slush impingement on the airframe and that from the landing gear traveling through uneven slush are increased over dry runway operation, but I feel sure that the passenger will experience this to a much greater degree than the crew.

Let us now look at the control problems. First let me say that my previous experience with operations in slush was rather meager, so that the control problems can't be too bad. As you have seen, the test area was only 50 feet wide and from 1,000 to 3,000 feet long, and yet we were able to remain well within its bounds on all runs. In addition, we could not use brakes or nosewheel steering and were requested not to use spoilers unless absolutely necessary, since this changed the basic airframe drag to a large degree. The only thing left was rudder, and use it we did. I think we all tend to lose sight of the fact that these aircraft still are equipped with rudders. We have nosewheel steering, spoilers which give us complementary turning moments rather than adverse yaw, and we treat the rudder as a useless appendage until we lose an engine. Actually, the rudder was quite useful at speeds down to about 70 knots. Unfortunately, I did not have an opportunity to evaluate controllability in slush, throughout a complete take-off from start to lift-off, or a complete landing from touchdown to stop.

We have seen from earlier papers that, at the gross weights existing during the tests, the wheels started to spin down somewhere in the vicinity of 80 knots, and it can be assumed that for this condition we lose ground control from the standpoint of steering and brakes. Fortunately, just about this time aerodynamic control is becoming effective, so we can continue the take-off in relative safety. As previously mentioned, rotation in $1\frac{1}{8}$ and $1\frac{3}{8}$ inches of slush did not present a problem.

Impressions from only two take-offs (one and one-half, actually) can hardly be considered conclusive, but no control problems developed during this short exposure. The slush patterns presented in paper number 4 by Howell and Sommers showed slush spray over the stabilizer, and I am not in a position to state that longer periods of exposure would not create any problems from the standpoint of slush buildup on control surfaces or in control-surface hinge lines.

In order to retain continuity in my discussion of aircraft operation in slush, I should like to discuss braking. I do not intend to go into braking coefficients, or other details. These will be discussed in other papers, but I would like to make a few general points. In tests on a dry runway we were able to stop the aircraft from a speed of 120 knots in slightly over 1,400 feet using no reverse thrust. In slush 1 inch deep the picture was somewhat different. We entered the slush pit at approximately 105 knots, used full braking with spoilers up for 2,000 feet, then rolled free in the last 1,000 feet of slush with spoilers still up, and left the 3,000-foot test strip at 75 knots. This type of performance reminds me of a cartoon that many of you have probably seen. It shows a horse and rider in midair, falling after having galloped off a cliff, the rider leaning back, reins pulled taut, hollering "Whoa! You

ornery critter, Whoa!" It does little to instill confidence in the braking potential available in slush.

You have seen from earlier data and the present figures that main wheels have slowed down and, in some instances, are almost stopped while the aircraft is accelerating, rotating, and taking off. If this is true, and we have no reason to doubt it, let us apply this knowledge to our take-off flight path. Let us assume that we have taken into consideration all the necessary variables to insure that we can, in fact, take-off, even if we lose an engine at or above V_1. (V_1 represents critical engine failure speed.) What happens if we lose an engine prior to attaining V_1? Naturally, we will stop, but how and when? Our wheels have already slowed down or stopped, so what good does it do to apply the brakes? Of course, I'm being facetious, and I'm sure that when the braking coefficients are discussed, some advantages to applying brakes will be shown, but in the cockpit the aircraft feels like it is skating on ice and no real deceleration is perceptible until the ground speed has fallen to below 70 knots, at which point I assume the aircraft has ceased to plane and the tires can again reach the hard concrete below.

In conclusion, let me review some of the points I have tried to make:

1. Slush impingement and ingestion can be serious problems, depending on aircraft geometry.

2. High-speed braking is almost nonexistent in slush and can increase "accelerate-stop" and landing distances to impracticable values.

3. Aircraft performance suffers to such a degree from slush drag that deep slush would make take-offs impossible.

Page Intentionally Left Blank

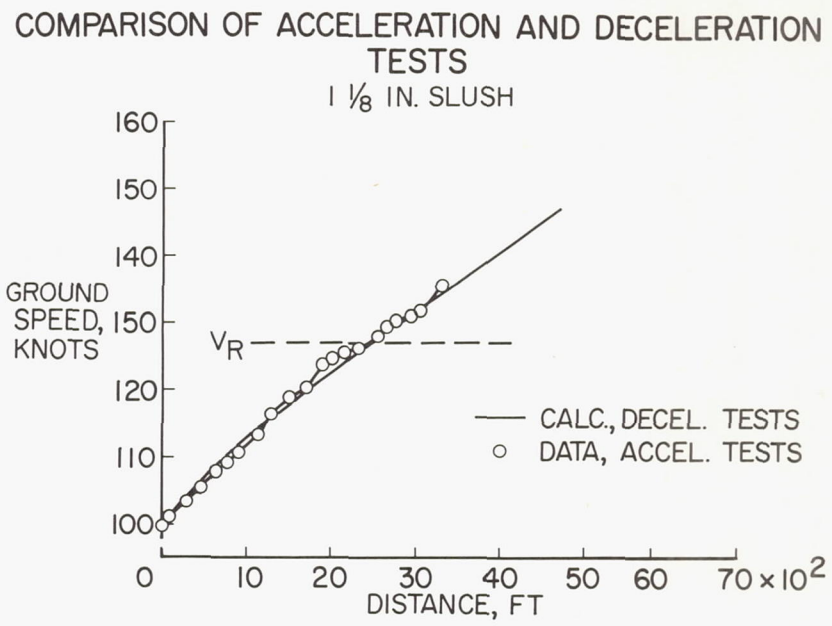

Figure 1

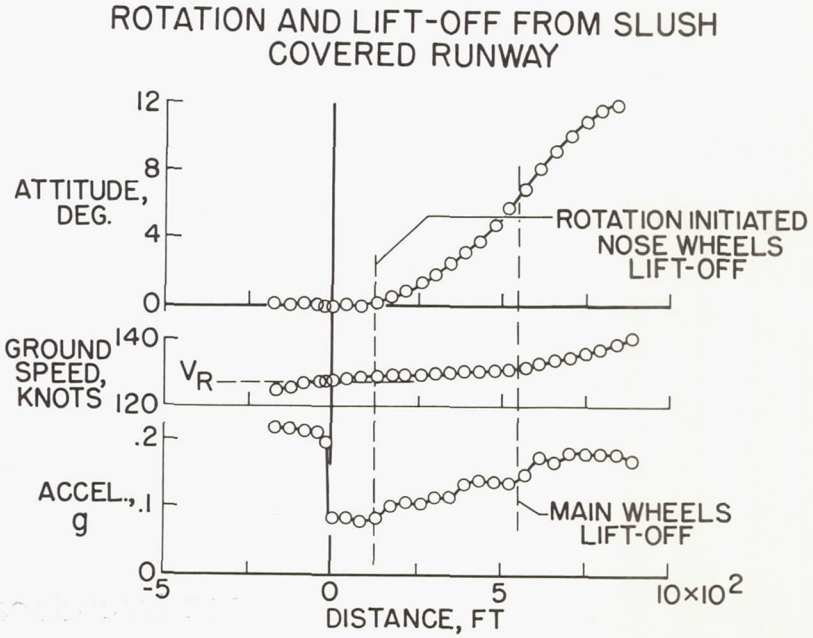

Figure 2

ge Intentionally Left Blank

8. SUMMARY

By Upshur T. Joyner
NASA

and Isaac H. Hoover
FAA

The slush investigation which has been described in the previous papers can be fairly described as a major effort on the part of the FAA to obtain enough full-scale information on slush retardation either to confirm the method of calculating slush effects on the take-off of airplanes based on single and tandem wheel tests (ref. 1), or to gather enough new information to serve as the basis for a revised method of calculation. As mentioned in previous papers, the method of calculation and the drag coefficient proposed in reference 1, where spray drag and rear bogie wheel drag were neglected, underestimates the effect of slush in the present full-scale tests by about 50 percent.

The principal points that emerged from the slush-drag measurements made in the present tests can be seen in figure 1 which shows variation of ground speed in knots with the slush-drag parameter $D_S\left(\frac{d_{st}}{d_S}\right)$, where D_S is observed slush drag, d_{st} is reference slush depth, and d_S is slush depth in inches. The observed slush drag at speeds below planing is a little over twice the drag predicted from the previous work. Two factors which were observed in the tests appear to contribute to this large drag. One is the large amount of spray which was thrown up by the nose wheels and then impacted on the wing, flaps, and other parts of the airplane. The second factor is the considerable amount of slush thrown up by the front pair of wheels on each main bogie which then impacted on the rear pair of wheels of the bogie. The total airplane slush drag seems to increase as the square of the speed, as indicated by the solid curve, until a speed near the calculated planing speed of the main tires is reached; the slush drag then decreases rapidly with further increases in speed until, at 160 knots, the slush drag is about 1/3 of the maximum value observed. This rapid decrease in slush drag is attributed to a rise of the tires out of the slush at high speeds and to the observed decreased impingement of slush on the airplane at these high speeds. At this time, no attempt has been made to calculate the rise of the tire in the slush. Further work is needed here. The differences between the slush-drag results obtained from the present investigation and those predicted from the previous work are large, due to the various conditions cited and possibly others not known; these differences should be resolved by further work.

Without intending in any way to minimize the differences which have been described, the extent to which these differences in slush drag translate into differences in take-off distance of one jet transport will be shown. In figure 2, airplane take-off distance is shown for a dry runway and for slush depths d_s of 1/2 inch and 1 inch, with the added distance due to slush calculated both by the method of reference 1 and by using slush drag as obtained from the present tests. The ratio of thrust T to weight W is 0.232. The variation of increased take-off distance with slush depth is highly nonlinear. In paper number 3 by Eugene P. Klueg, the airplane in 2 inches of slush reached a zero acceleration condition at a speed below the take-off speed. Take-off distance would go to infinity in this case. The difference in take-off distance calculated by the two methods mentioned for 1/2 inch of slush is 500 feet, and take-off distance is increased about 1,200 feet using test-airplane drag results; for 1 inch of slush, this difference goes up to 1,500 feet, and the take-off distance is 3,200 feet more than on a dry runway, again using test-airplane drag results. Thus, as important as it is to resolve the differences between the two predicted take-off distances, it is at least as important to be very sure that we never encounter an area of slush an inch deep during the later stages of a take-off run. On the basis of the time consumed and the manpower required in measuring slush over a maximum runway distance of 3,000 feet, and considering that an operational runway may be more like 10,000 feet long, it would seem that further development and use of a fast operational method for accurately measuring slush on a runway must be given a very high priority. Nothing in these tests would suggest any relaxation in the practice of limiting operations to 1/2 inch of slush or less for the current season. If in doubt about the depth, be conservative.

Since the objective of these tests was to establish a method of calculating slush drag which could be applied generally, the data have been reduced to coefficients where possible, by using the method of calculation proposed in reference 1. As a result, the effect of spray-impingement drag on the airplane and on the rear bogie wheels is included in the drag coefficient obtained. At such time as the spray drags can be separated from the total drag, some revision of the method of calculation may be necessary.

The following list includes areas for possible future study:

1. Development of operational methods for measuring slush: A car could be used to measure the amount of slush on a runway (paper no. 6 by Richard H. Sawyer and B. C. Riddle, Jr.), and could be quickly put into use. The car method obtains spot values only because it has to be brought back up to speed after each decelerating run through the slush. A pushed wheel on which drag force is recorded continuously would

provide a complete record of slush on the runway. This type of pushed-wheel measuring equipment would require some time for development.

2. Possible control of slush and water spray patterns: There is a need for a more general understanding of spray patterns and their effects so that estimations can be made for these effects for airplanes which have not been tested. Consideration should be given to undertaking a theoretical analysis of slush-spray patterns in order to determine whether mathematical relationships can be established which could be used to predict spray patterns and the resulting damage and slush impingement forces for different aircraft configurations. Possibly spray effects can be controlled and minimized by deflectors that do not produce drag. It may not be wishful thinking to hope that such deflectors might even convert some spray energy into thrust.

3. "Rooster tail" and spray interference on truck-type gears: A bogie gear in slush under closely controlled conditions should be investigated to understand more clearly the drag produced on the rear wheels. In such tests, both lateral and fore-and-aft wheel spacing should be varied, if feasible.

4. Hydroplaning, how to avoid or use to advantage: At present, it is not known how high the tire rises in the slush at speeds above the calculated hydroplaning speed, and predictions of slush drag while the tire is hydroplaning cannot be made. Tire hydroplaning is undesirable for braking and control, but would help reduce slush drag during take-off.

5. Program similar to current tests on other aircraft types: By testing airplanes of different types, it may be possible to isolate the effects of slush drag, rear bogie wheel drag, et cetera. For example, an F-27 has a high wing and the spray drag may thereby be small; also no rear bogie wheels are present and the method of reference 1 may therefore give a better prediction than in the present tests. Also, each airplane has vulnerable spots that may suffer damage or operational troubles, such as slush packed in flap openings or wheel wells and freezing on a cold airplane, thereby preventing operation.

Finally, even though this full-scale investigation has not settled the question of the determination of slush drag, it has demonstrated some effects of spray from the nose wheels on wings and fuselage, has shown rear bogie-wheel spray impingement, and a reduction in slush drag at speeds above the planing speed has been observed.

REFERENCE

1. Horne, Walter B., Joyner, Upshur T., and Leland, Trafford J. W.: Studies of the Retardation Force Developed on an Aircraft Tire Rolling in Slush or Water. NASA TN D-552, 1960.

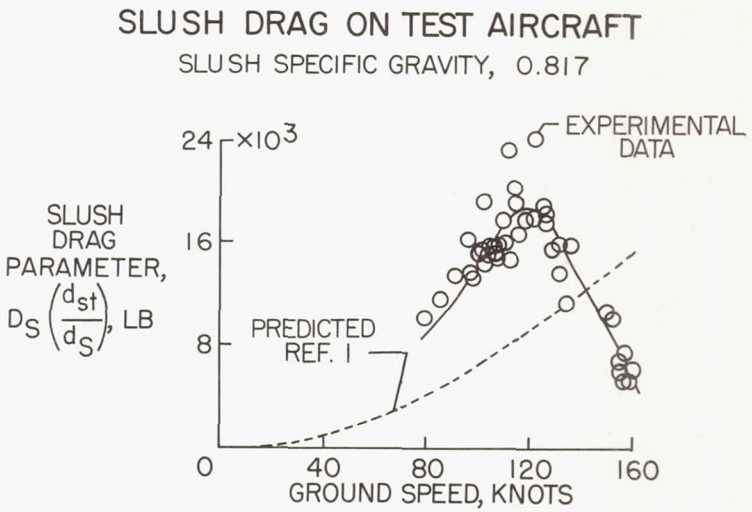

Figure 1

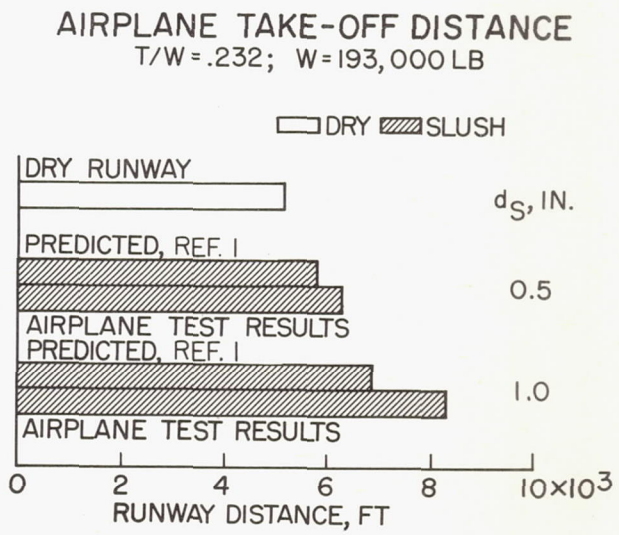

Figure 2

Page Intentionally Left Blank

9. INTRODUCTION TO THE BRAKING PROBLEM

By Upshur T. Joyner
NASA

and Nicholas S. Dobi
FAA

In introducing a session such as this, where the coefficient of friction between a vehicle and the ground is to be the subject under discussion, it would seem that the reason for interest is obvious; but some background should be given to explain the extent of this interest. The fact has long been accepted that the handling of a vehicle whose propulsion, braking, and steering is dependent on forces developed by ground contact is considerably more difficult when the ground surface is wet, icy, or covered with snow or other lubricants. This fact is learned first by walking on slick surfaces, and later by riding bicycles or motorcycles, or by driving a car on slick roads. Pilots know that airplanes are similarly affected on take-off or landing by reduced ground traction, or low coefficient of friction between the tire and the runway. When conditions on a runway are such that the tire-to-surface coefficient of friction is relatively low, braking effectiveness is reduced and the airplane is subject to overshooting on critical runways during landing or aborted take-off. Also, control of the path down the runway is reduced and the airplane may veer off the runway. This latter condition is aggravated by crosswinds. The extent to which these two conditions have been encountered in service by U.S. scheduled passenger carriers during the last 6 years is shown in table I. Several points can be noticed. First, when runways are slick, an incident or accident is more likely during landing than during take-off. Second, such incidents or accidents are about equally likely to be an overrun or a loss of control leading to veering off the runway, or ground looping. Third, these statistics indicate that the advent of jet transports does not seem to have greatly affected the picture. The total of 41 incidents or accidents shown here for almost 6 years may not seem too impressive, but if all such incidents or accidents were tabulated for all flying, including nonscheduled carriers, freight carriers, military, private and corporate planes, and so forth, the number would be much larger and correspondingly more impressive to all. It should be recognized that in many of the cases listed in table I, runway conditions were not the primary factor which caused the incident or accident. However, lack of traction very likely contributed to some extent in making the operation more critical. In fact, in a CAB tabulation of overshoot accidents in U.S. scheduled and irregular air carrier operations for transport-type aircraft for 6 years (1950 to 1955), there was only 1 overshoot on a dry runway, while 30 overshoots occurred on wet, snowy, or icy runways. Of these 30 overshoot accidents, 18 are listed as involving a high and fast approach,

while an additional 9 are listed as involving either a high or a fast approach. High and fast approaches surely occur under dry runway conditions, but are not recorded unless there is an incident. It appears that the really bad combination as far as overruns are concerned is a fast or high approach on a slick runway, as would be expected.

In order to illustrate the variations in stopping distance which can be caused by low coefficient of friction, figure 1 shows stopping distances from touchdown for a first-generation four-engine jet transport calculated by using tire-to-runway friction coefficients obtained from single-wheel braking tests. The dry-runway curve is calculated for a tire braking coefficient of friction of 0.6, the grooved-rib tire on wet concrete had an average coefficient over the speed range used of about 0.3, and the smooth tire on wet concrete had an average coefficient of about 0.15. The top plot of figure 1 is for thrust reversers operating, and shows that the stopping distance can vary from about 2,400 feet on dry concrete to about 3,600 feet on wet concrete with an effective tire tread, and up to about 5,100 feet with a smooth tire. If the thrust reversers are inoperative, the bottom plot of figure 1 shows that the dry-runway stopping distance is about 2,600 feet, an increase of only 200 feet over the curve for thrust reversers operating, but the other distances have increased to about 4,300 feet and 6,600 feet, respectively. It is easy to see from this figure why high or fast approaches can usually be successfully handled in landing on dry surfaces, while the high and fast approaches on wet surfaces more often show up in the type of statistics previously quoted.

The discussion so far suggests that a forewarning to the pilot of the exact braking conditions which he will encounter upon landing might make it possible for him to use this information, along with other considerations (for example, wind gustiness, crosswind component, etc.), in deciding on touchdown speed and point of contact. Knowing that the runway is slick, he may favor lower speed and early touchdown, or if this action is not considered safe, he may even elect to divert to another airport. This type of operational reporting of runway conditions is being done in Sweden by the Scandinavian Airlines System for runways which are covered by snow or ice that is not wet. For these conditions, the coefficient of friction does not vary too drastically with speed, and tire hydroplaning is not a problem. In this country, the Air Force has explored a method of measuring runway braking conditions by applying maximum braking on a station wagon traveling at 20 mph, noting the maximum deceleration, and statistically correlating this deceleration with observed airplane runout distance.

Because the known limitations on braking effectiveness on wet runways were recognized, and since it was desired to gain information which would aid in reducing the number of incidents and accidents on slick

runways, advantage was taken of the opportunity presented during the slush investigation at the National Aviation Facilities Experimental Center (NAFEC) to run the present series of braking tests with the following objectives:

1. Investigate methods for operational determination of runway braking conditions. Here, it was desired to bring together in one investigation of braking coefficient of friction, under identical runway surface conditions, a modern jet-propelled airplane and the various trailers and cars that might be used for operationally measuring coefficient of friction. At this point, the cooperation of the Swedish and British groups in making their equipment available for this investigation should be mentioned again. A trailer from the National Road Research Institute of Sweden and a trailer from the British Road Research Laboratory were brought over to this country for these tests, and friction measurements were made with these trailers and with a station wagon equipped with a decelerometer after the manner of the U.S. Air Force in order to see which, if any, might be suited for operational measurements of braking conditions and prediction of the braking performance of airplanes in landing on wet runways.

2. Establish a reproducible low-coefficient-of-friction test runway surface. In support of consideration being given to the measurement of airplane landing distance under wet runway conditions, and with the difficulty of maintaining a wet runway in some areas recognized, an attempt was made to establish a low-coefficient-of-friction runway which (a) could be reproduced at will, and (b) would remain in the same condition long enough for braking tests to be run. As a result of tests made at the Langley landing-loads track, where foam gave about the same coefficient as water, regular fire-extinguishing foam was deposited on the runway and braking tests were run with the airplane over this surface.

3. Correlate full-scale braking results and those results from the Langley landing-loads track. This attempt at correlation was made by taking the British trailer and the station wagon to the Langley Research Center and running braking tests at the landing-loads track with this same equipment that was used at NAFEC. Unfortunately the Swedish trailer was too wide to run on the Langley track. If a good correlation can be established, then not only will past work at the track be interpretable with more confidence directly in terms of airplane braking performance, but future development work at the track can be done with confidence that the trends observed can be directly interpreted in terms of a full-scale airplane.

Papers 10, 11, and 12 present the results of this braking investigation. Paper 10 describes how the tests were run, how the measurements were obtained, and presents the basic data. Paper 11 compares the data

from this investigation with data from another full-scale aircraft investigation, and with data from the Langley landing-loads track; and paper 12 discusses operational methods of determining runway surface braking conditions and compares airplane data with ground-vehicle data obtained at NAFEC. Finally, in paper 13 there is a summary of the investigation and a discussion of the implications and possible future tests.

TABLE I

INCIDENTS AND ACCIDENTS ON SLICK RUNWAYS
U. S. SCHEDULED PASSENGER OPERATIONS

INCIDENT	1956	1957	1958	1959	1960	1961	TOTAL
LANDING							
VEERED OFF RUNWAY	1	4	4	3	5+1[a]	2+1[a]	21
OVERRAN	3	—	2	3	3[a]	2+1[a]	14
TAKE-OFF							
VEERED OFF RUNWAY	—	—	—	—	1	1[a]	2
OVERRAN	—	—	2	—	1	1[a]	4
TOTAL	4	4	8	6	11	8	41

[a] JET AIRCRAFT

RUNOUT DISTANCE FOR 4-ENGINE JET TRANSPORT

W=160,000 LB; 50 PERCENT OF IDEAL BRAKING

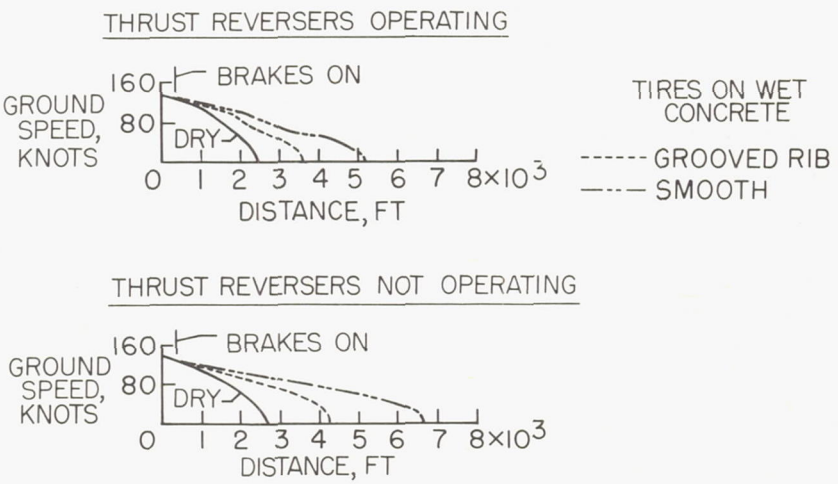

Figure 1

10. BRAKING TEST PROGRAM AND RESULTS

By Jack J. Shrager

FAA

INTRODUCTION

The variations in braking distance due to adverse weather conditions have been under investigation for many years by those in the field of automotive engineering. The results of some of these efforts were presented at a conference sponsored by the University of Virginia in the fall of 1958 (ref. 1). In addition some full-scale aircraft tests have been conducted in England under a contract of the Ministry of Aviation (refs. 2 to 7). One purpose of the FAA sponsored effort was the determination of the effects of simulated adverse weather conditions as they influence jet aircraft braking qualities. An additional purpose was to investigate the feasibility of determining operational runway conditions, as they influence braking, by use of specially instrumented vehicles. This effort was undertaken jointly by the Aviation Research and Development Service (ARDS) and the National Aeronautics and Space Administration at the National Aviation Facilities Experimental Center (NAFEC) in the fall of 1961. Specifically, the information sought was:

(a) The variation in the braking friction coefficient, with respect to velocity, for a modern jet aircraft under adverse weather conditions. The conditions to be simulated were damp (light rain), wet (heavy rain with puddling), and slush covered runway.

(b) The effect of these variations on runway accountability.

(c) The practicality of establishing runway braking friction coefficients, as they relate to a full-scale aircraft, with several vehicular traction measuring devices.

(d) The possible use of foam as a method of establishing a standard low-coefficient-of-friction surface.

METHOD

The test aircraft was braked through the prepared test bed under conditions which were intended to simulate a surface after a light rain, a heavy rain, a slush deposit, and a foam deposit, in addition to a normally dry surface. (See fig. 1.) The techniques employed to simulate these conditions were:

(a) Light rain (damp): the runway test strip was sprayed with water from fire trucks to moisten the surface without visible puddles. After the surface was sprayed, a motorized broom brushed the area to remove any standing water.

(b) Heavy rain (wet): the test strip was sprayed by fire trucks for approximately 1/2 hour to generate a highly reflective, moistened surface with standing water. The high crown of the runway precluded development of the exact runway condition desired, namely, a flooded runway surface with a large area of standing water.

(c) Slush covered surface: the slush covered runway was simulated in the manner described in paper number 2 by Middlesworth, Marcy, et al. of NAFEC. However, the test bed in all cases was a reuse of the bed remaining after a drag test. That portion which was cleared by the wheels in the previous test was filled by use of a motorized broom. The actual depth and density were not determined.

(d) Foam covered surface: this condition was developed by standard foam-generating fire fighting equipment. The organic foam layer was approximately 1 inch thick.

The aircraft, for all braking tests, was in the aborted take-off configuration. This configuration provides for flaps at normal take-off setting, engine at idle thrust, spoilers extended, maximum braking available (maximum energy) with the exception of the nose wheel braking, and an antiskid sensing system on each wheel. The antiskid system is designed to provide the maximum braking friction coefficient which nominally occurs at approximately 15 percent slip. A detailed description of such a system is contained in reference 8.

In the interest of safety, the maximum entrance velocities for the low-braking-friction-coefficient surfaces were less than V_R, which is the velocity at rotation. To obtain the entire velocity curve, it was necessary to overlap test entrance and exit speeds in the test area. Thus three runs were required for wet, two runs for foam, four for slush, and two for damp, to cover the entire velocity range.

The parameters of distance, velocity, and acceleration were established by the same method as that described in paper number 2 by Middlesworth et al.

THEORY

The results presented were obtained from the analysis of acceleration and velocity data plotted against distance, as shown in figures 2 to 6.

The following assumptions are made in the derivation of μ_B:

(1) Drag forces due to nose wheel are negligible.

(2) The antiskid system was set to provide a slip ratio which would give a maximum friction coefficient between the tires and the test surface.

(3) The change in aerodynamic lift due to geometric pitching was negligible.

(4) Pitching moment due to slush drag at the main gear was neglected.

(5) A test surface of uniform, 1/2-inch-deep slush with an average density of 50 lb/cu ft was assumed.

The braking friction coefficient, based on assumptions (1) to (5) and neglecting pitching moment about the main gear due to inertia, lift, drag, and thrust forces, is defined as:

$$\mu_B' \approx \frac{F_I - F_S - F_D + F_E}{0.9372\left(W_P + W_F\right) - F_L}$$

When corrections for pitching moments are made, the equation becomes:

$$\mu_B = \frac{F_I + F_E - F_D - F_S}{\left[0.9372\left(W_P + W_F\right)\right] - \left[(0.113)F_E + (0.944)F_L + (0.169)\left(F_I - F_D\right)\right]}$$

which is derived in appendix A. (See eq. (A9).) Symbols are also defined in this appendix. This equation was found to give approximately the same results as

$$\mu_B = \frac{\mu_B'}{1 - 0.2\mu_B'}$$

RESULTS

The curves of μ_B as a function of velocity for the test aircraft are shown in figure 7 based on the statistical analysis presented in appendix B. This family of curves represents all surface conditions. There is an observed decrease in μ_B with an increase in velocity for all surface conditions with the exception of the dry surface. The test results obtained for the first application of foam indicate that μ_B closely approximates the μ_B of a damp surface. However, reapplication of foam over the same test bed area reflects braking coefficients of friction lower than those obtained for the wet condition. Because of the high crown of the test bed, the results obtained for the wet surface do not necessarily reflect those which may exist for a flooded runway. The general trend is a decrease in μ_B with an increase in the depth of the surface moisture film. Figure 8 reflects the change in distance required to stop, with maximum energy braking only, with respect to velocity. As would be expected, the distance for any given entrance velocity increases with a decrease in μ_B. A more complete analysis of μ_B (eq. (A10), appendix A) will be contained in the final FAA report on the braking program. This report is currently in preparation.

The vehicular traction-measuring devices selected were those currently in use by other agencies, including the U.S. Air Force, for determining braking friction coefficients for runway accountability.

The English braking trailer (fig. 9) determined friction coefficient by measuring the peak induced pressure due to torque, which occurs at the instant the test wheel is locked. A description of this approach is contained in reference 9. This technique provides intermittent samples of the runway surface friction coefficient.

The variation of μ_B with velocity for each test condition except the dry surface for this vehicle is shown in figure 10 as obtained by the Road Research Institute personnel at NAFEC. Again, it is noted that the general trend is for μ_B to decrease with an increase in velocity and depth of surface-moisture film.

The results obtained with a conventional automotive vehicle with a peak reading accelerometer installed (fig. 11) are shown in figure 12. Again, the same general trend of μ_B is noted.

The Swedish Skiddometer (fig. 13) determines friction coefficient by measuring the developed torque between the driving wheels and a directly coupled smaller wheel. A detailed description of this device is contained in reference 10. The wheel-size ratio is selected to develop approximately 17 percent slip. The results obtained with this device are shown in figure 14. The maximum force limits for the particular torque-measuring link were reached on the other surface conditions and hence data for these conditions were not obtained. It should be noted, however, that other types of torsion-measuring links are available to obtain higher friction coefficients. The data shown are those furnished by the scientific personnel from the Institute of Road Research in Sweden. It should be noted that this device permits a complete runway-surface-profile analysis instead of an intermittent-sampling analysis. That is to say, a recording of runway friction coefficient for the entire length of the runway at some constant velocity is obtained. The comparison of the braking coefficient obtained with the test aircraft and that obtained with the various vehicular devices for each runway condition is shown in figures 15 to 18. Although the absolute value of μ_B is not the same, the general trends of the test results are very similar.

The ratio of the μ_B for the aircraft to μ_B of the particular vehicle for all conditions is shown in figure 19.

CONCLUSIONS

It is concluded from the results presented that:

1. The trend of a decrease in braking coefficient μ_B with an increase in velocity is similar to that previously reported for vehicles.

2. The general trend is for μ_B to decrease with an increase in depth of the surface moisture film.

3. The required distance to stop, using maximum energy braking only, increases with a decrease in μ_B.

4. Foam initially generates a low friction coefficient surface similar to that obtained for a damp condition. There is a tendency for

μ_B to approximate the wet condition upon subsequent applications of foam on the original surface.

5. Results obtained from tests of the aircraft are similar to those obtained with the special vehicular test devices.

APPENDIX A

ANALYSIS TO ESTABLISH EQUATION FOR BRAKING FRICTION COEFFICIENT

Vertical Force Expression

The vertical force on the main gear can be considered to be made up of two components, as follows:

(1) Direct load due to weight distribution in a static condition

(2) A vertical force component induced by the moment about the main gear due to inertia, lift, drag, and thrust forces.

The static vertical force distribution on the main gear can be obtained from

$$F = 0.9372\left(W_P + W_F\right) \tag{A1}$$

where the factor 0.9372 is the fraction of the total weight on the main gear and

W_P empty weight of aircraft, lb

W_F weight of fuel remaining at any instant, lb

F vertical force on main gear due to static load, lb

The dynamic vertical force components on the main gear due to pitching moments are illustrated in the following sketch:

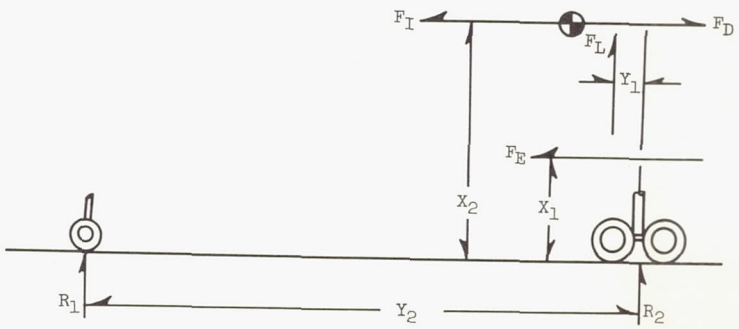

The sum of the moments may be expressed as

$$\sum M_{R_1} = 0 = R_2Y_2 + F_EX_1 + F_L(Y_2 - Y_1) + F_IX_2 - F_DX_2 \qquad (A2)$$

where

R_2 vertical force due to pitching moment

F_E effective thrust of engines corrected for density ratio

F_L effective aerodynamic lift corrected for density ratio

F_I inertia force $\frac{(W_P + W_F)}{g}a$

F_D aerodynamic drag corrected for density ratio

σ density ratio correction, $\left(\frac{\rho_{amb}}{\rho_0}\right)\left(\frac{t_0}{t_{amb}}\right)$

ρ_{amb} ambient density

ρ_0 standard density

t_{amb} ambient temperature

t_0 standard temperature

g local acceleration of gravity (assumed to be 32.174 ft/sec^2)

a aircraft acceleration obtained from NASA accelerometer data

Rewriting equation (A2) gives

$$R_2 = \frac{-F_EX_1 - F_L(Y_2 - Y_1) - F_1X_2 + F_DX_2}{Y_2} \qquad (A3)$$

For the test aircraft,

$$X_1 = 6.0 \text{ ft}$$

$$X_2 = 9.0 \text{ ft}$$

$$Y_1 = 3.0 \text{ ft}$$

$$Y_2 = 53.1 \text{ ft}$$

Substituting these values into equation (A3) yields

$$R_2 = \frac{6F_E - 50.1F_L - 9\left(F_I - F_D\right)}{53.1} \tag{A4}$$

Simplifying equation (A4) gives:

$$R_2 = -0.113F_E - 0.944F_L - 0.169\left(F_I - F_D\right) \tag{A5}$$

Since R_2 is the component of vertical force due to pitching moment, combining equations (A1) and (A5) gives total vertical force, or

$$F_V = \left[0.9372\left(W_P + W_F\right)\right] - \left[0.113F_E + 0.944F_L + 0.169\left(F_I - F_D\right)\right] \tag{A6}$$

Horizontal-Force Expression

The expression for the horizontal force may be derived by use of the parameters shown in the following sketch:

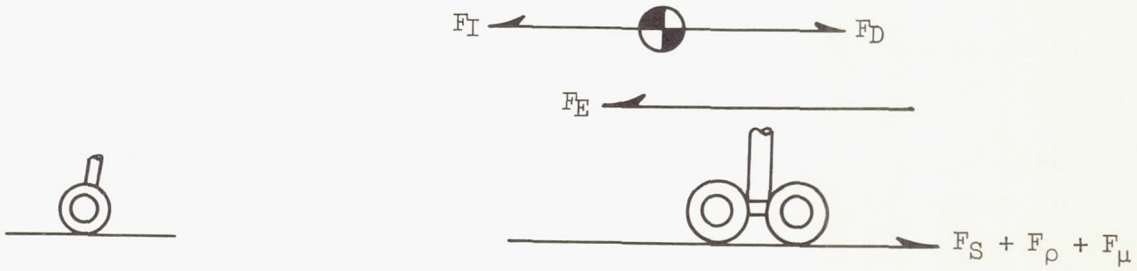

Thus,

$$\sum F_{\text{Horiz.}} = 0 = F_S + F_\mu + F_\rho + F_D - F_I - F_E \tag{A7}$$

where

F_S total drag force due to slush (obtained from data presented in FAA/ARDS Interim Report, Task 308-3T)

F_ρ retardation force due to friction produced when slipping occurred (coefficient of sliding friction obtained from locked wheel braking tests on test surface)

F_μ retardation force due to rolling friction of gear (coefficient varies with surface condition)

F_D aerodynamic drag of test aircraft (obtained from manufacturer's data and corrected for ambient conditions by multiplying by density ratio)

F_I force due to aircraft inertia, as defined previously

F_E force due to effective thrust, as defined previously

Braking Forces

The braking forces F_μ and F_ρ can be combined into a total braking term of the form

$$F_\mu + F_\rho = \mu_B F_V$$

Rewriting equation (A7) and substituting $\mu_B F_V$ for $F_\mu + F_\rho$ gives

$$\mu_B = \frac{F_I + F_E - F_D - F_S}{F_V} \tag{A8}$$

Substituting from equation (A6) yields

$$\mu_B = \frac{F_I + F_E - F_D - F_S}{\left[0.9372\left(W_P + W_F\right)\right] - \left[0.113F_E + 0.944F_L + 0.169\left(F_I - F_D\right)\right]} \tag{A9}$$

After correcting for dynamic slush force, the final expression for friction coefficient becomes

$$\mu_B = \frac{F_I + F_E - F_D - F_S}{\left[0.9372(W_P + W_F)\right] - \left[0.133F_E + 0.944F_L + 0.169(F_I - F_D)\right] - \left[0.1988\rho V^2\right]} \qquad (A10)$$

Derivation of complete braking coefficient equations is contained in FAA/ARDS Final Braking Report on Task 308-3T currently in preparation.

APPENDIX B

STATISTICAL ANALYSIS OF TEST DATA

Regression Analysis

The experimental data, though reflecting some scatter, showed either straight line or parabolic trends. It was therefore decided to attempt to resolve the scatter by a statistical regression analysis such as may be found in reference 11. When the data points appeared to approximate a straight line, the equations for estimating a linear regression were utilized. These equations can be developed as follows:

A straight line with the equation

$$Y = a + bx \tag{B1}$$

is to be fitted to n points with the coordinates

$$(X_1, Y_1),\ (X_2, Y_2),\ \ldots\ (X_n, Y_n)$$

It can be seen that the coordinates of any point X_i, Y_i will not necessarily satisfy equation (B1). If X_i is substituted into the general equation, a value of Y is obtained which differs from Y_i by a value δ_i, or

$$Y_i - (a + bX_i) - \delta_i \neq 0 \tag{B2}$$

Computing the discrepancy δ_i for each point of the set and forming the sum of the squares of these quantities yields:

$$E^2 = \sum_{i=1}^{n} \delta_i^2$$

$$= (Y_1 - a - bX_1)^2 + (Y_2 - a - bX_2)^2 + \ldots + (Y_n - a - bX_n)^2 \tag{B3}$$

where E^2 is the sum of the squares of the deviations.

The least-squares criterion now states that the parameters a and b should be chosen so as to make E^2 as small as possible. In order to minimize this function, the two first partial derivatives $\frac{\partial E^2}{\partial a}$ and $\frac{\partial E^2}{\partial b}$ are equated to zero to obtain the equations

$$\frac{\partial E^2}{\partial a} = 2(Y_1 - a - bX_1)(-1) + 2(Y_2 - a - bX_2)(-1) + \ldots + 2(Y_n - a - bX_n)(-1) = 0 \qquad (B4)$$

$$\frac{\partial E^2}{\partial a} = 2(Y_1 - a - bX_1)(-X_1) + 2(Y_2 - a - bX_2)(-X_2) + \ldots + 2(Y_n - a - bX_n)(-X_n) = 0 \qquad (B5)$$

Collecting terms on the unknown coefficients a and b yields:

$$na + b\sum_{i=1}^{n} x_i = \sum_{i=1}^{n} Y_i \qquad (B6)$$

and

$$a\sum_{i=1}^{n} x_i + b\sum_{i=1}^{n} x_i^2 = \sum_{i=1}^{n} X_i Y_i \qquad (B7)$$

Equations (B6) and (B7) may now be solved simultaneously for a and b. To simplify calculations, let

$$Y_1 = X_1$$

and

$$X_1 = X_2$$

Let

$$\bar{X}_1 = \frac{\sum X_1}{n}$$

and

$$\bar{X}_2 = \frac{\sum X_2}{n}$$

and

$$\sum x_1 x_2 = \sum X_1 X_2 - n\bar{X}_1\bar{X}_2$$

$$\sum x_2^2 = \sum X_2^2 - n\bar{X}_2^2$$

Now, solving for a and b gives

$$b = \frac{\sum x_1 x_2}{\sum x_2^2} \tag{B8}$$

and

$$a = \bar{X}_1 - b\bar{X}_2 \tag{B9}$$

The solutions for a and b are then entered into equation (B1) and the most suitable curve can be drawn.

In those cases where the plotted data appeared to approximate a parabolic curve, the least-squares method was used to determine the second-degree equation which best suited the data points. The analysis was begun by assuming a parabolic equation of the form:

$$Y = a + bX + cX^2 \tag{B10}$$

to fit the data points:

$$(X_1, Y_1),\ (X_2, Y_2),\ \ldots\ (X_n, Y_n)$$

Substituting these pairs of values into equation (B10) shows that a, b, and c, should satisfy the conditions:

$$a + X_1 b + X_1^2 c = Y_1$$

$$a + X_2 b + X_2^2 c = Y_2$$

$$a + X_n b + X_n^2 c = Y_n$$

In general, three unknowns cannot be made to satisfy more than three conditions; hence, the most that can be done is to determine values of a, b, and c which will best satisfy these equations. To set up the first of the three normal equations required by the method of least squares, each of the equations of condition is multiplied by the coefficient of a in that equation and the summation taken, which yields:

$$\sum_{i=1}^{n} a + bX_i + cX_i^2 = Y_i \qquad \text{(B11)}$$

The second and third equations are set up similarly, being multiplied successively by the coefficients of b and c and the summations taken of the respective groups of equations; that is, for the second equation,

$$\sum_{i=1}^{n} X_i\left(a + bX_i + cX_i^2\right) = Y_i \qquad \text{(B12)}$$

and for the third

$$\sum_{i=1}^{n} X_i^2\left(a + bX_i + cX_i^2\right) = Y_i \qquad \text{(B13)}$$

These three equations can now be solved simultaneously for a, b, and c, and the values substituted in equation (B10) to give the required solution.

Derivation of Velocity from Theodolite Data

Theodolite data from film are punched on cards and processed by a standard phototheodolite program to yield X,Y,Z coordinates. The X,Y,Z coordinates are then read into the runway slush program and used as follows:

1. To eliminate some of the noise in the X and Y tables of values and thus to provide for smoother differentiated curves, the X and Y tables are smoothed prior to differentiation using a 5-point least-squares smoothing formula. Thus,

$$(X_S)_M = \frac{\sum_{M-2}^{M+2} X_M}{\sum_{M-2}^{M+2} M^0}$$

$$= \frac{1}{5}\left(X_{M-2} + X_{M-1} + X_M + X_{M+1} + X_{M+2}\right)$$

$$(Y_S)_M = \frac{\sum_{M-2}^{M+2} Y_M}{\sum_{M-2}^{M+2} M^0}$$

where $(X_S)_M, (Y_S)_M$ equals smoothed values of X,Y and X_M, Y_M equals unsmoothed values of X,Y and M assumes all values from 3 to the value second from the end of the X,Y tables.

2. The smoothed values of X,Y are then differentiated to give velocities in the X and Y directions (V_X, V_Y) using an 11-point differentiation formula. Thus,

$$(V_X)_N = \frac{\sum_{N-5}^{N+5}{}' N(X_S)_N}{\sum_{N-5}^{N+5}{}' N^2}$$

$$= \frac{5\left((X_S)_{N+5} - (X_S)_{N-5}\right) + 4\left((X_S)_{N+4} - (X_S)_{N-4} + \ldots + (X_S)_{N+1} - (X_S)_{N-1}\right)}{5^2 + 4^2 + 3^2 + 2^2 + 1^2 + 1^2 + 2^2 + 3^2 + 4^2 + 5^2}$$

$$(V_Y)_N = \frac{\sum_{N-5}^{N+5}{}' N(Y_S)_N}{\sum_{N-5}^{N+5}{}' N^2}$$

where $(V_X)_N$ and $(V_Y)_N$ are differentiated values of $(X_S)_N$, $(Y_S)_N$ and N assumes all values from 8 to the value seventh from the end of the table.

3. Ground and air velocity are obtained from the formulas

$$(\text{Ground velocity})_N = \sqrt{(V_X)_N^{\,2} + (V_Y)_N^{\,2}}$$

$$(\text{Air velocity})_N = \sqrt{\left[(V_X)_N + V_{X,\text{wind}}\right]^2 + \left[(V_Y)_N + V_{Y,\text{wind}}\right]^2}$$

where $V_{X,\text{wind}}$ and $V_{Y,\text{wind}}$ are components of wind calculated from input data giving direction and magnitude of wind.

REFERENCES

1. Anon.: Proceedings First International Skid Prevention Conference. Parts I and II. Virginia Council of Highway Investigation and Research, Aug. 1959.

2. Anon.: Flight Tests to Determine the Coefficients of Friction Between an Aircraft Tyre and Various Wet Runway Surfaces. Part 1. S & T Memo 15/59, [British] Ministry of Aviation, Sept. 1959.

3. Anon.: Flight Tests to Determine the Coefficients of Friction Between an Aircraft Tyre and Various Wet Runway Surfaces. Part 2. S & T Memo 5/60, [British] Ministry of Aviation, Apr. 1960.

4. Anon.: Flight Tests to Determine the Coefficients of Friction Between an Aircraft Tyre and Various Wet Runway Surfaces. Part 3. S & T Memo 2/61, [British] Ministry of Aviation, Mar. 1961.

5. Tate, K. W.: Flight Tests to Determine the Coefficients of Friction Between an Aircraft Tyre and Various Wet Runway Surfaces. Part 4. Rep. No. P. 5, Vickers-Armstrongs (Aircraft) Limited Supermarine Works, Sept. 1961.

6. Tate, K. W., and Lalor, N.: Flight Tests to Determine the Coefficients of Friction Between an Aircraft Tyre and Various Wet Runway Surfaces. Part 5. Rep. No. P. 5, Vickers-Armstrongs (Aircraft) Limited Supermarine Works, Oct. 1961.

7. de Bourcier, P. G.: Flight Tests to Determine the Coefficients of Friction Between an Aircraft Tyre and Various Wet Runway Surfaces. Part 6. Rep. No. P. 7, Vickers-Armstrongs (Aircraft) Limited Supermarine Works, Sept. 1961.

8. Anon.: Maintenance Manual. Hytrol Anti-Skid Braking System 00-157D for Convair 880 Aircraft. Hydro-Aire Co., Div. of Crane Co. (Burbank, Calif.), Revised Nov. 1, 1960.

9. Giles, C. G., and Lauder, F. T. W.: The Skid-Resisting Properties of Wet Surfaces at High Speeds: Exploratory Measurements With a Small Braking Force Trailer. Jour. R.A.S., vol. 60, Feb. 1956, pp. 83-94.

10. Anon.: Scandinavian Procedures of Determining and Reporting the Braking Qualities of Icy or Snow Covered Runways. SAS Rep. GP/136, Scandinavian Airlines System, Aug. 19, 1960.

11. Wylie, C. R., Jr.: Advanced Engineering Mathematics. McGraw-Hill Book Co., Inc., 1951.

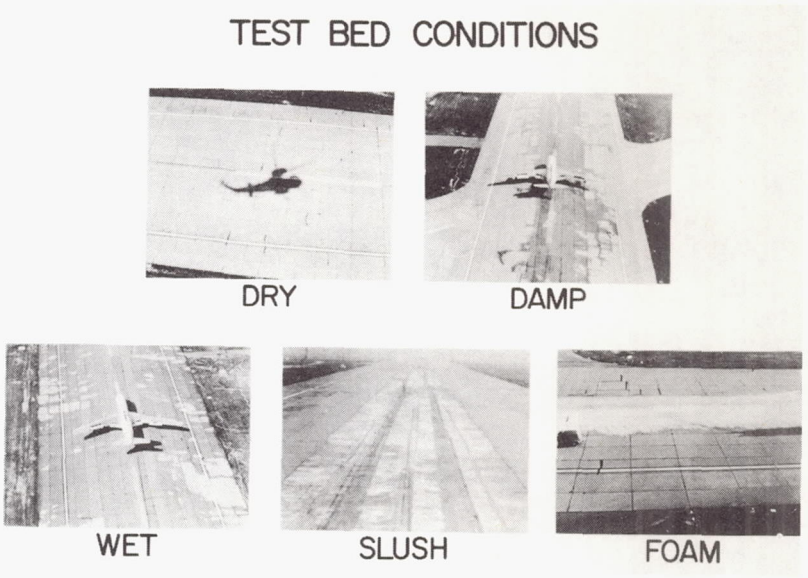

Figure 1

L-61-6961

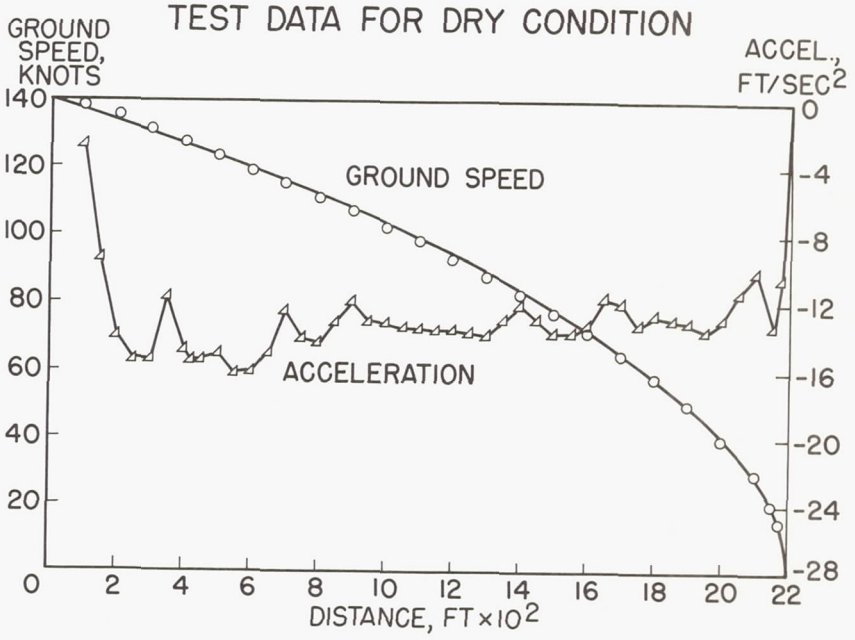

Figure 2

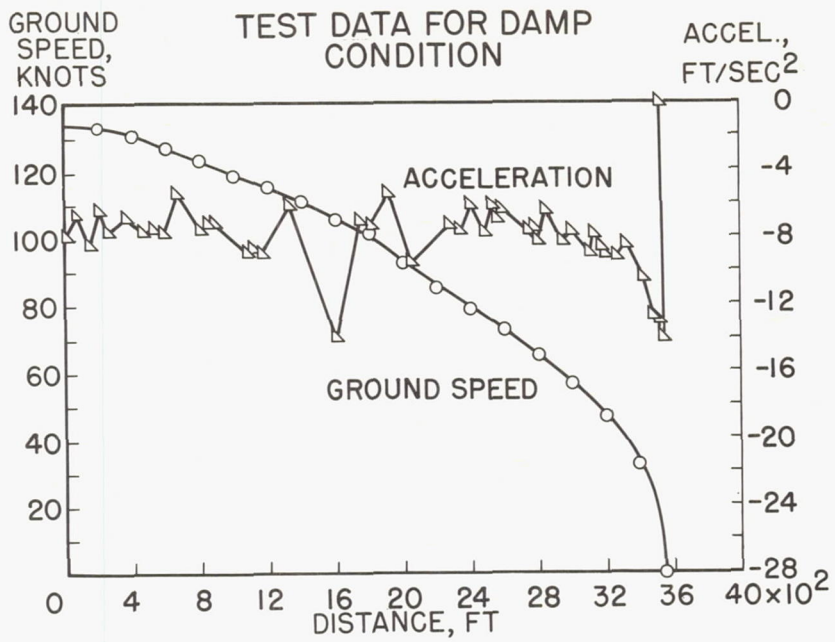

Figure 3

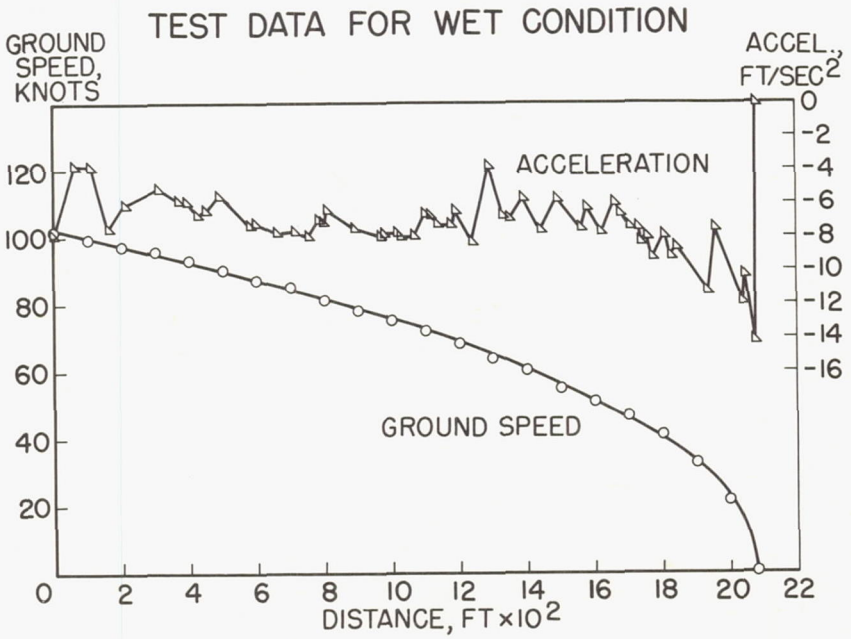

Figure 4

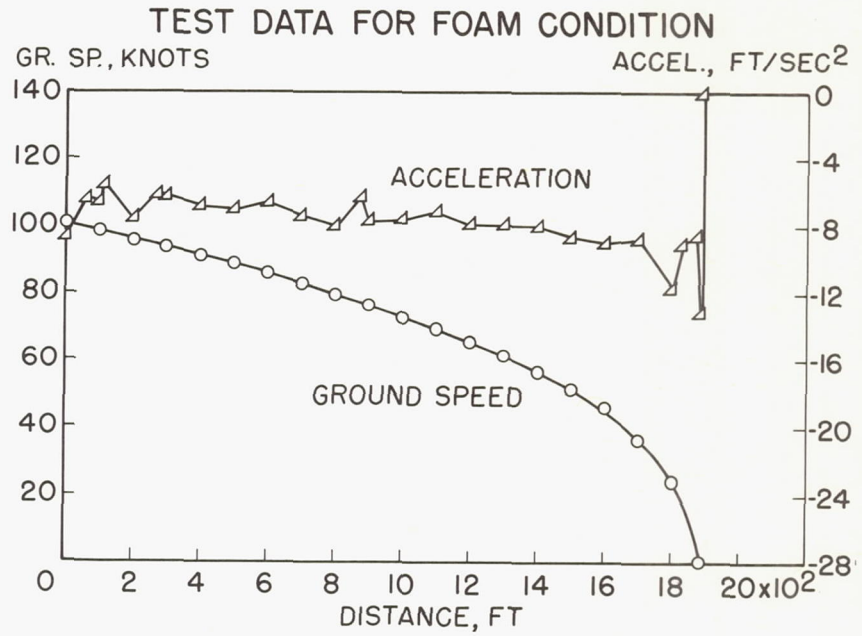

Figure 5

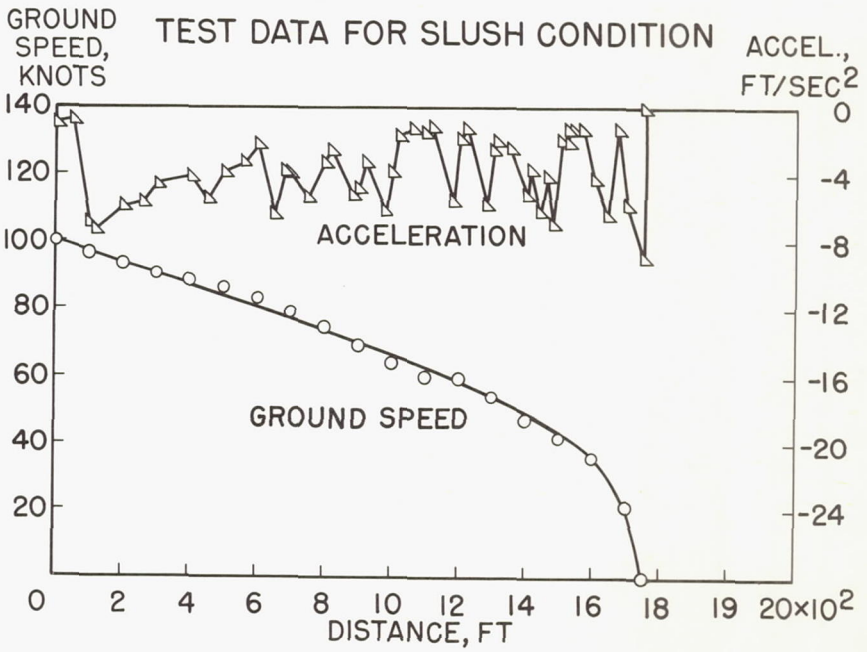

Figure 6

VARIATION OF μ_B WITH GROUND SPEED FOR AIRCRAFT

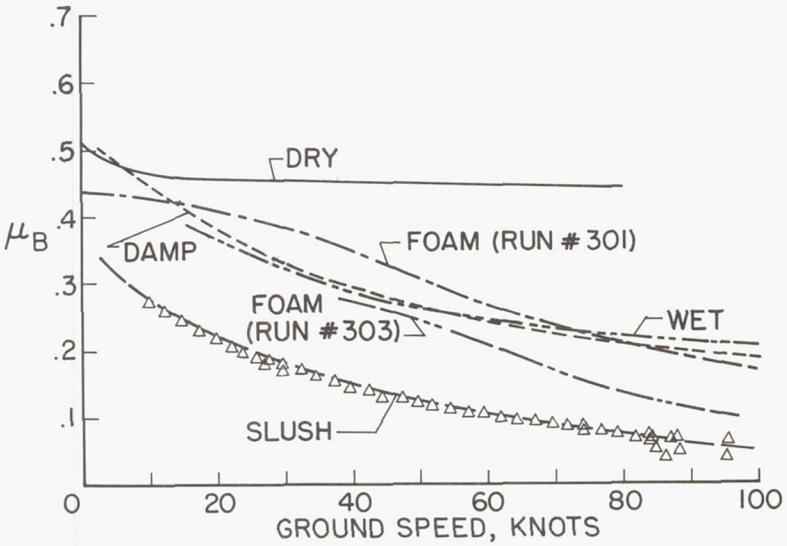

Figure 7

BRAKING DISTANCE COMPARISONS FOR VARIOUS RUNWAY CONDITIONS

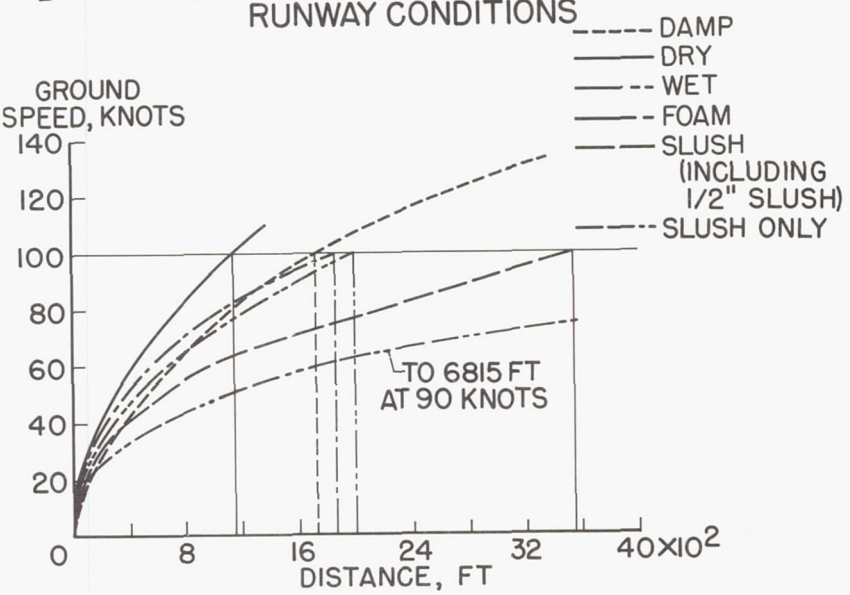

Figure 8

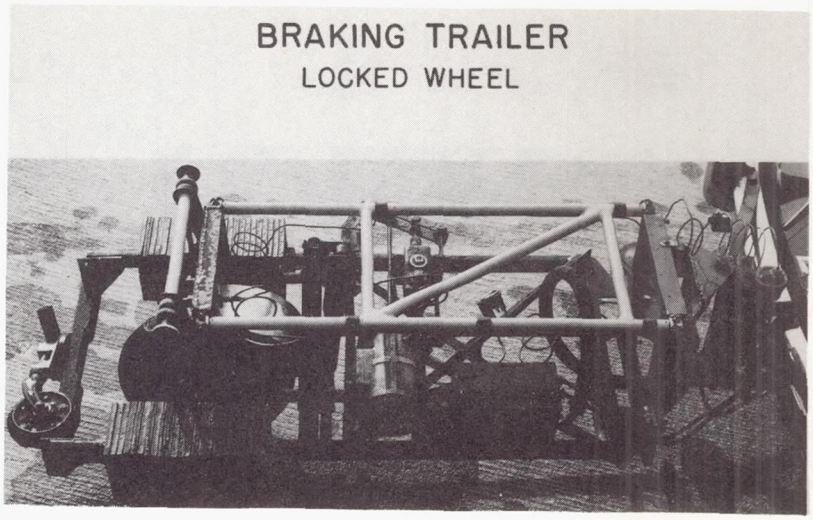

Figure 9 L-61-6962

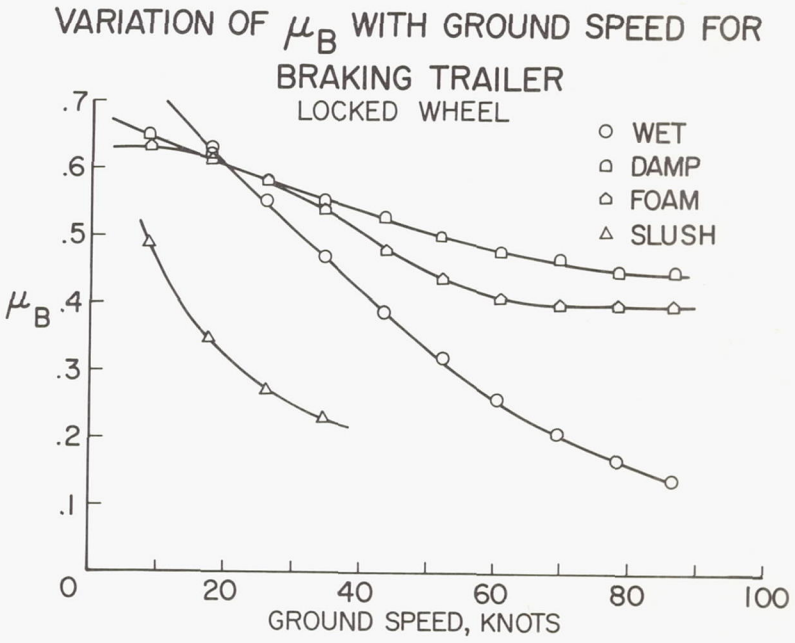

Figure 10

ACCELEROMETER

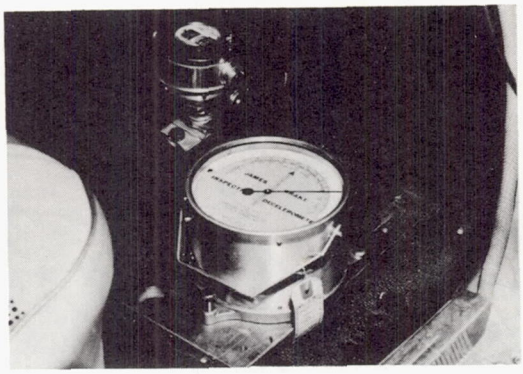

Figure 11 L-61-6959

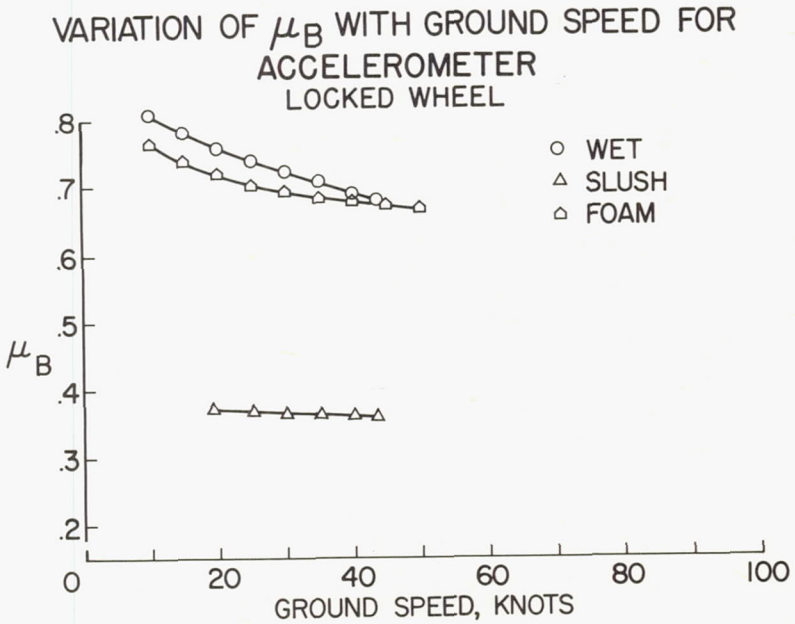

Figure 12

SKIDDOMETER

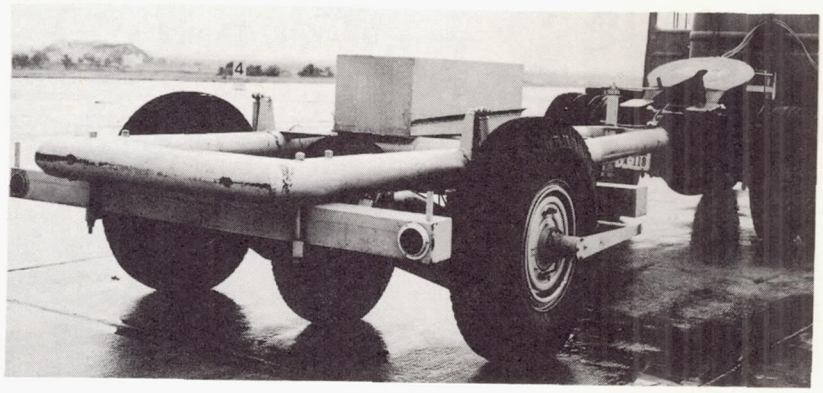

Figure 13

L-61-6960

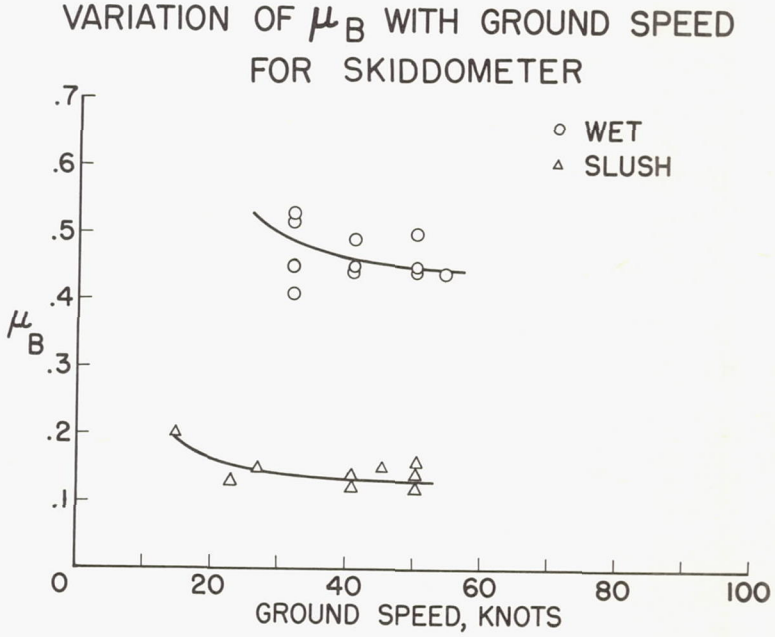

Figure 14

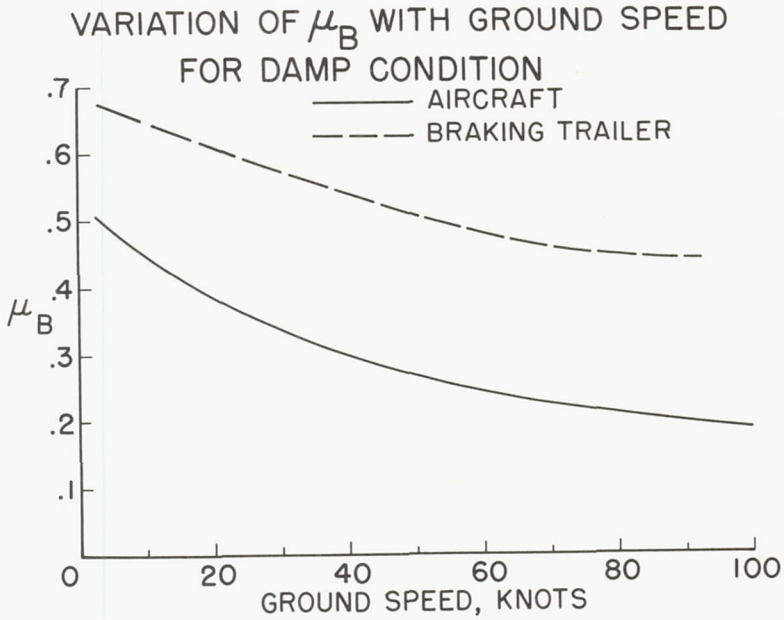

Figure 15

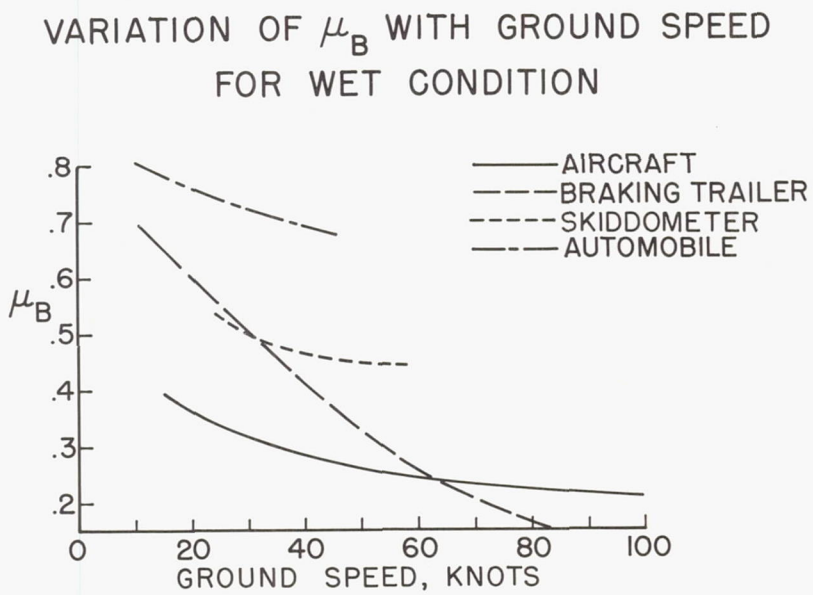

Figure 16

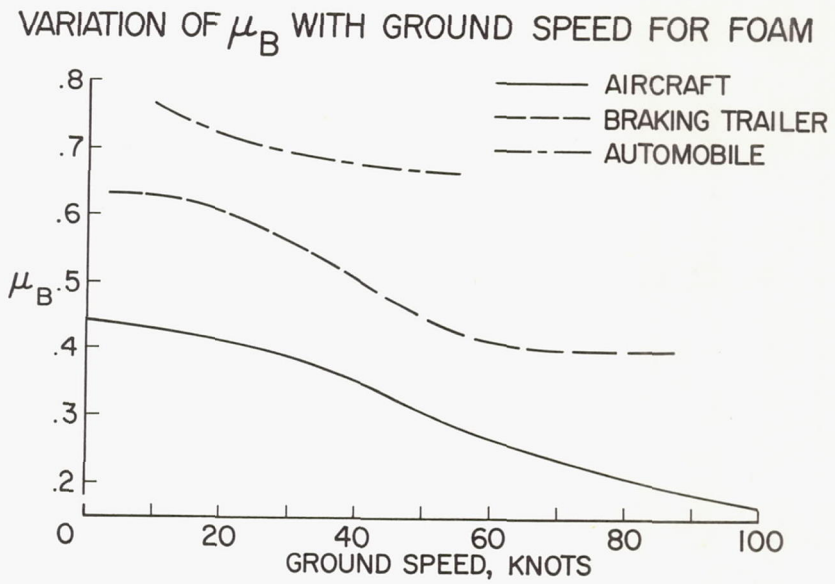

Figure 17

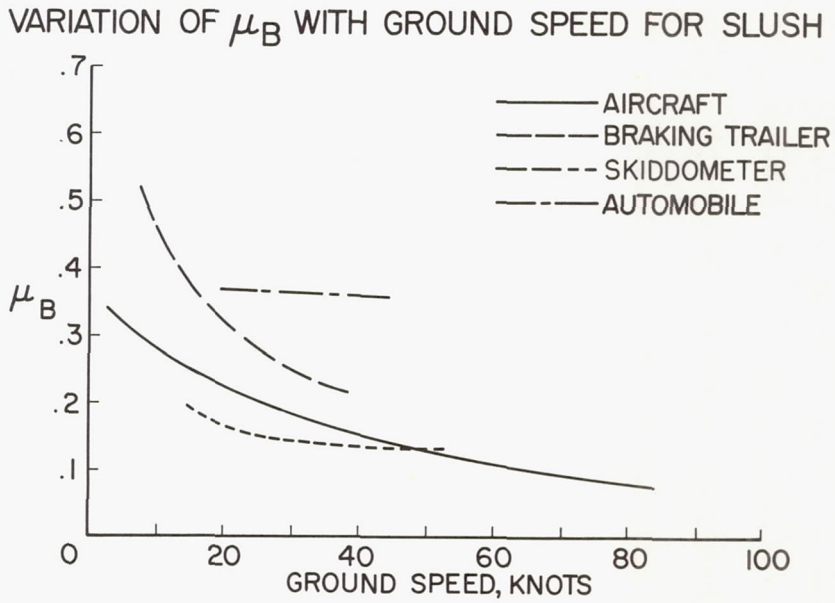

Figure 18

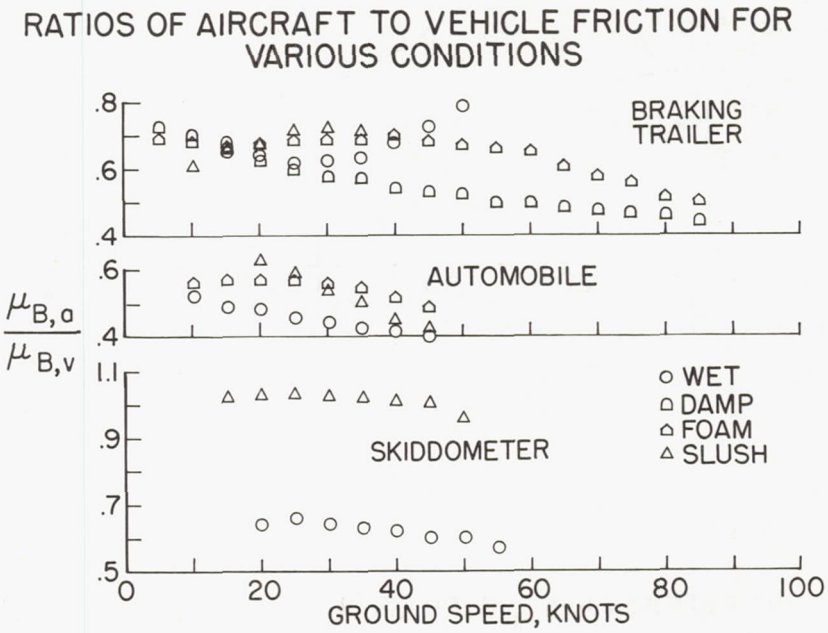
RATIOS OF AIRCRAFT TO VEHICLE FRICTION FOR VARIOUS CONDITIONS
BRAKING TRAILER
AUTOMOBILE
SKIDDOMETER
WET
DAMP
FOAM
SLUSH
$\frac{\mu_{B,a}}{\mu_{B,v}}$
.8
.6
.4
.6
.4
1.1
.9
.7
.5
0
20
40
60
80
100
GROUND SPEED, KNOTS

Figure 19

11. CORRELATIONS OF BRAKING ON SLIPPERY SURFACES

By Walter B. Horne and Trafford J. W. Leland

NASA

It is the purpose of this paper to show the comparisons between braking data for a full-scale jet transport aircraft and for single-wheel braking tests at Langley landing-loads track on concrete runways coated with water and slush. Also, it is shown that foam-covered concrete runways can develop tire-to-ground friction coefficients on full-scale aircraft similar to those obtained on wet concrete runways as was initially found in single-wheel braking tests at the Langley track. Brake effectiveness under dry and wet runway conditions is discussed.

Before any valid comparison can be made between the track braking data and the test-aircraft braking data, a comparison is required between the friction characteristics of the track and of the National Aviation Facilities Experimental Center (NAFEC) concrete runway. This comparison is shown in figure 1.

This figure shows braking coefficient of friction μ_B plotted as the ordinate and ground speed as the abscissa. The data shown were obtained on wet concrete surfaces by using the automobile-decelerometer method described by Shrager (paper no. 10). The shaded band indicates the envelope of data acquired on the track surface. The clear band indicates the envelope of data acquired on the test runway at NAFEC. The automobile braking coefficients obtained on the two concrete surfaces are seen to have about the same values in the velocity range covered. While the friction coefficient values shown are not at all indicative of what may be expected with more heavily loaded tires, the two sets of measurements do indicate that the two runways have approximately equivalent friction surfaces under the wet condition.

As a further preliminary to the comparisons to be made, consider briefly the effects of tire slip ratio on coefficient of friction μ. Figure 2 shows for a dry runway a typical friction coefficient variation with slip ratio as a braked wheel progresses from a free-roll condition at a slip ratio of 0 to a full-skid or a locked-wheel condition at a slip ratio of 1.0. As the wheel progresses from zero slip to full skid under increasing brake torque, μ reaches a maximum and then decreases to a lower value at full skid. It should be mentioned at this point that the peak friction coefficient μ_{MAX} from track and other available test data appears to be relatively independent of ground speed for dry concrete runways. The highest braking effectiveness, of course, occurs when the tire is maintained at the slip ratio

giving μ_{MAX}, indicated here at about 0.17. This is what antiskid braking systems in aircraft try to achieve, but, because of variability of runway surface friction and antiskid and wheel brake response rates, some undershooting and overshooting of the optimum slip-ratio point occurs during brake cycling. For this reason, the average friction coefficient between slip ratios of 0.1 and 0.5, μ_{AV} rather than μ_{MAX}, has been used in presenting track data because it is felt to be more nearly representative of the friction coefficient which might be obtained with an airplane equipped with an antiskid system. All the single-wheel track data are shown in terms of μ_{AV} just defined. The test-aircraft braking friction coefficients obtained are average friction coefficients obtained from all the eight braking wheels for slip ratios randomly varying around that for μ_{MAX}, and apparently over a larger range of slip ratio than 0.10 to 0.50. It is of interest to give a few numbers for the braking coefficients on a dry runway: (1) At the track, about 0.55 and insensitive to speed, (2) for the test aircraft, slight variation about a mean value of 0.45, and (3) for the other four-engine jet transport, variation from 0.42 for 40 knots down to about 0.1 for 130 knots. These differing experimental braking-friction results have been divided by the values of μ_{MAX} which would be expected to be available for the tire loading, tire pressure, and so forth being used, to obtain a braking effectiveness μ_B/μ_{MAX} as shown in figure 3. (Values of μ_{MAX} used in this paper were obtained by use of eqs. (31), (32), and (88) of ref. 1.)

This figure compares the dry-runway braking effectiveness of the track single wheel, the test airplane, and the other four-engine jet transport which was run on a concrete surface for which no correlation is known with the NAFEC runway or the track. It should be mentioned that the airplane data were obtained by use of automatic skid control, with no pilot brake modulation inputs. The track single wheel indicates a braking effectiveness of better than 90 percent for the ground-speed range investigated and is insensitive to speed changes. This high indicated effectiveness is a result of the definition of μ_{AV}; it does not mean that the track antiskid system used developed this effectiveness. The test airplane achieved a braking effectiveness of about 60 percent and showed a slight decreasing trend with increasing ground speed. The other jet transport achieved about the same braking effectiveness as did the test airplane up to a ground speed of about 80 knots. The reason for the fall-off in braking effectiveness at the higher ground speeds for this aircraft is not known at this time. It is clear that on a dry runway antiskid systems do vary in effectiveness, so that no direct comparison of average friction coefficient for different braking systems is valid as long as the antiskid system is controlling the braking.

Now consider wet concrete runways. In figure 4 are shown braking friction coefficients obtained on a wet runway in the same three investigations referred to in figure 3. In all these investigations an effective ribbed-tread tire was used, so it is not surprising that, at very low speed, the braking coefficients of friction obtained are almost the same as the values quoted previously for the dry surface. Referring again to the slip-ratio curve (fig. 2), it should be explained that on a wet runway, this type of variation of coefficient of friction with slip ratio is observed at low speed. As speed is increased, however, the peak of the curve is lowered, and eventually μ_{MAX} approaches μ_{SKID}. When this condition is reached, the limits of slip ratio through which an antiskid system controls the tire rotational speed are of little consequence, and all systems will give about the same value of average braking coefficient. Such a trend for the data from the three sources to converge at high speed is shown in figure 4, except for the unexplained fall-off of the dashed curve which was shown previously in figure 3 for the dry-runway data from this source.

Next consider effects of slush on braking. Figure 5 shows the braking coefficients obtained on a slush-covered runway at different ground speeds. The wheel-brake-only curve was obtained by subtracting the appropriate slush drag from the observed total drag. This is not the complete story, however, for the slush drag due to displacement of slush by the wheel must be added to the wheel-brake drag to obtain total wheel retardation. This has been calculated for the dashed curves for runway slush depths d_S of 0.5 inch, 1 inch, and 1.5 inches using airplane slush drag results.

It will be noticed that maximum (wheel brake plus slush drag) braking coefficients at the higher ground speeds are achieved at approximately 120 knots and increasing the ground speed beyond this value results in lowering the braking coefficient. This, of course, is due to the tire planing and spray effects described by Klueg (paper no. 3), Howell and Sommers (paper no. 4), and Horne and Leland (paper no. 5).

With regard to the operation of antiskid systems in slush, it will be remembered from the paper by Klueg (paper no. 3) that large front-wheel spin-downs of the order of 60 percent occurred during the airplane unbraked deceleration tests in slush at the test speeds from 80 to 160 knots. These spin-downs occurred at zero brake pressure and at corresponding zero brake torque. Under these conditions the antiskid system could not be expected to be effective.

Now compare the track single-wheel braking results in 1.5 inches of slush with test-airplane braking results under the same conditions. (See fig. 6.) The braking coefficients of the single wheel in slush

are noted to be very similar to, though higher than, those indicated for the test aircraft.

A summary of the test-aircraft braking results on dry, wet, and slush-covered concrete is given in figure 7. For the higher ground speeds (40 to 130 knots), the test aircraft developed braking coefficients on wet concrete which had only one-half the magnitude of the values obtained on dry concrete. On slush, the total aircraft braking coefficient shown by the dashed curve for 0.5 inch of slush on the runway is about one-half the magnitude of the coefficients obtained on wet concrete or about one-fourth of the braking coefficient values obtained on dry concrete. It should be restated at this point that all the aircraft tires used to obtain the data shown in this figure had relatively unworn rib treads. Track results obtained on smooth-tread tires and on ribbed-tread tires which were 80- to 90-percent worn indicate that these tires on wet concrete will give braking coefficients similar to those obtained on the test aircraft in slush depths under 0.5 inch for the higher ground speeds.

Braking tests made at the Langley track on organic- and detergent-foam-covered concrete runways indicated that the braking coefficients obtained were very close in magnitude to the coefficients developed on a wet concrete runway surface for the same ground speed. In these tests the organic-foam depth on the runway ranged from 3 to 5 inches while the detergent-foam depth ranged from 1 to 3 inches. The expansion ratio for these foams was approximately 12 to 1 or, stating it differently, these foams had only 1/12 the density of water. In figure 8, the track results are compared with the test-aircraft results for braking in organic foam approximately 1 inch deep on the runway.

Here again, braking coefficient is plotted against ground speed. The solid and dashed curves are the braking coefficients obtained on foam-covered and wet runways, respectively, by the test aircraft. The circles and squares represent the track braking coefficients on organic and detergent foams, respectively. The data shown in this figure indicate close agreement for the test aircraft and the track single wheel for the only comparable velocity of about 70 knots.

In conclusion, braking coefficient of friction results obtained at the Langley landing-loads track on wet, slush-covered, or foam-covered concrete agree well with results obtained from the test aircraft. Dry-runway braking-friction results obtained from the track with the brake effectiveness as defined do not agree closely with results obtained from the test aircraft, probably because of variations in antiskid effectiveness. The track is particularly useful for research in the low-coefficient-of-friction regime, where interest lies.

Foam-covered concrete surfaces develop full-scale aircraft braking coefficients of approximately the same magnitude as those developed on wet concrete surfaces, a result which substantiates the earlier findings of the NASA track during single-wheel braking on foam-covered concrete surfaces.

REFERENCE

1. Smiley, Robert F., and Horne, Walter B.: Mechanical Properties of Pneumatic Tires With Special Reference to Modern Aircraft Tires. NASA TR R-64, 1960. (Supersedes NACA TN 4110.)

Page Intentionally Left Blank

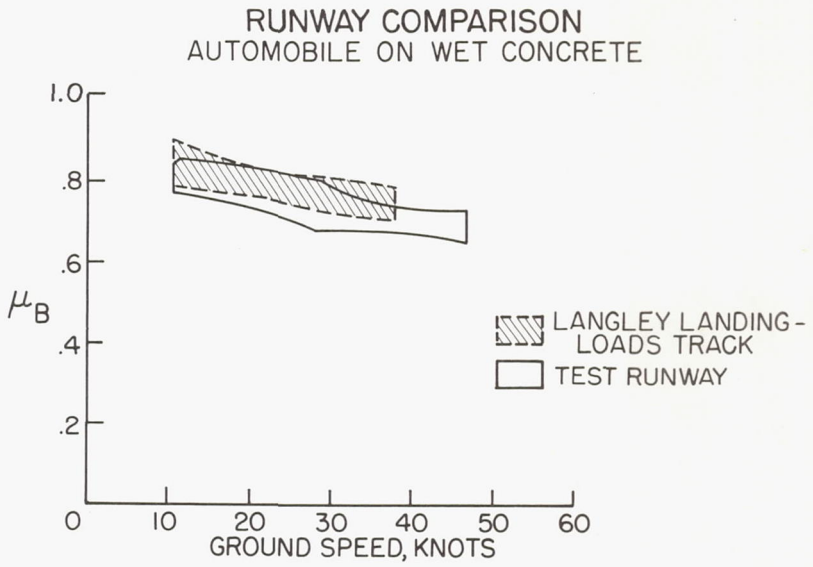

Figure 1

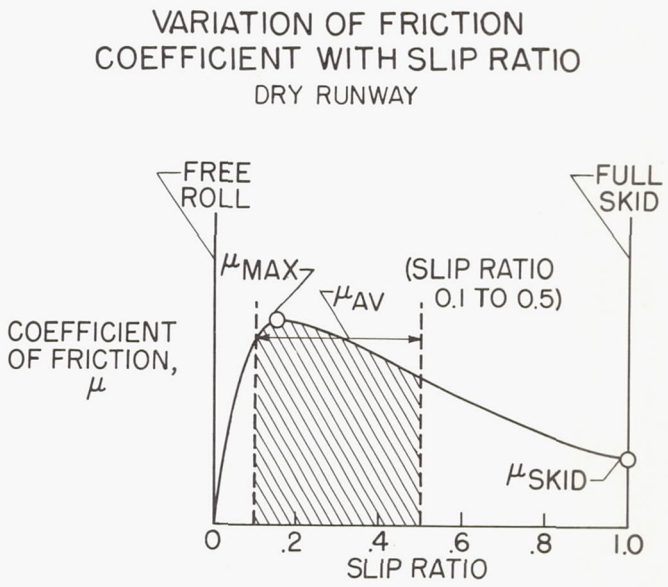

Figure 2

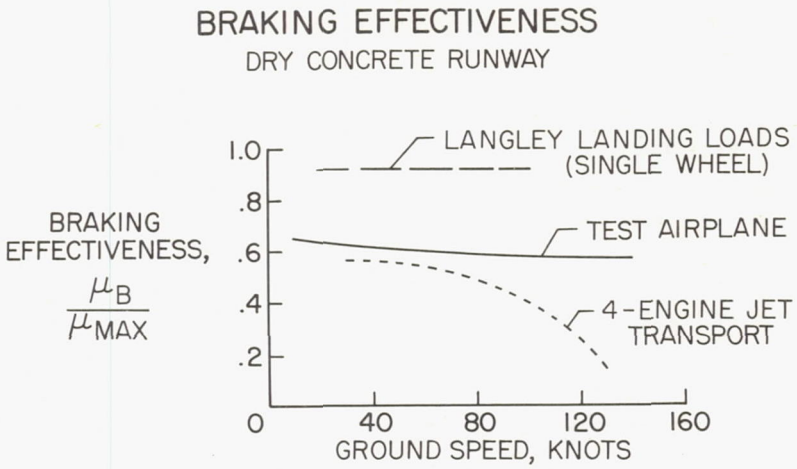

Figure 3

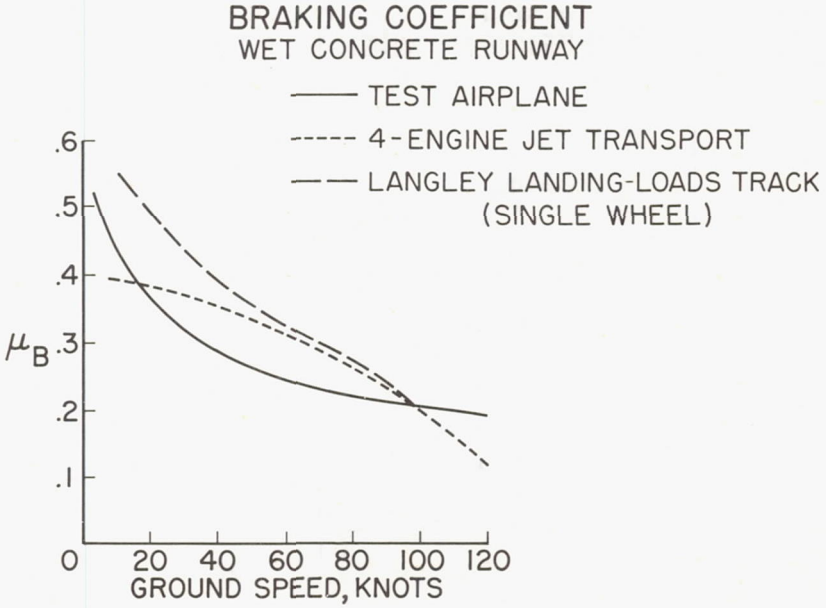

Figure 4

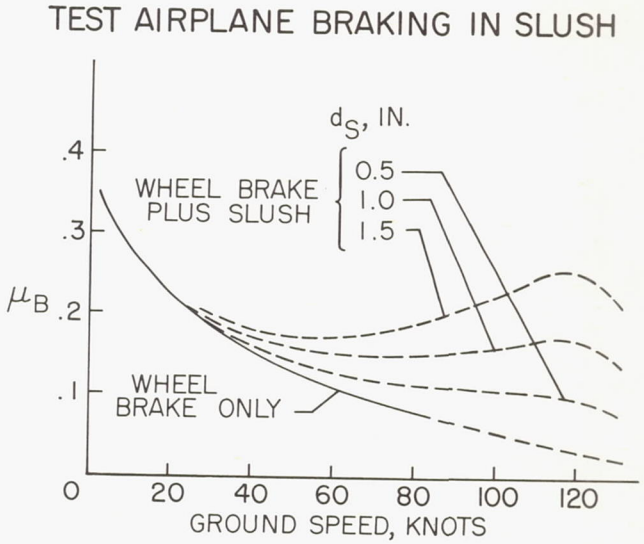

Figure 5

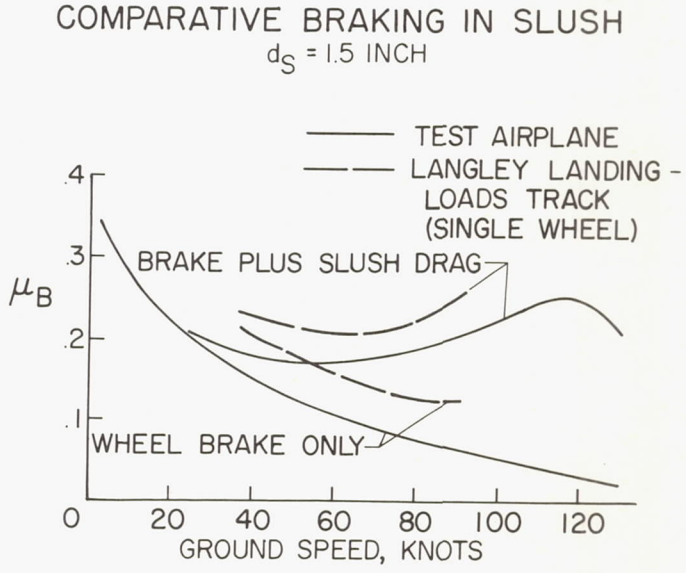

Figure 6

BRAKING ON CONCRETE RUNWAY FOR DIFFERENT SURFACE CONDITIONS

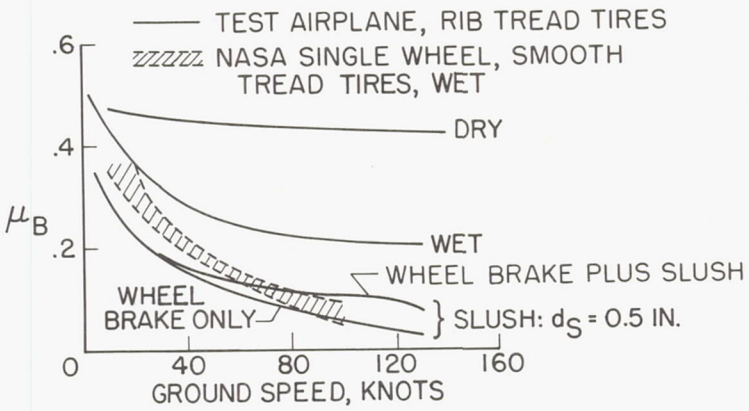

Figure 7

BRAKING ON WET AND FOAM-COVERED CONCRETE RUNWAYS

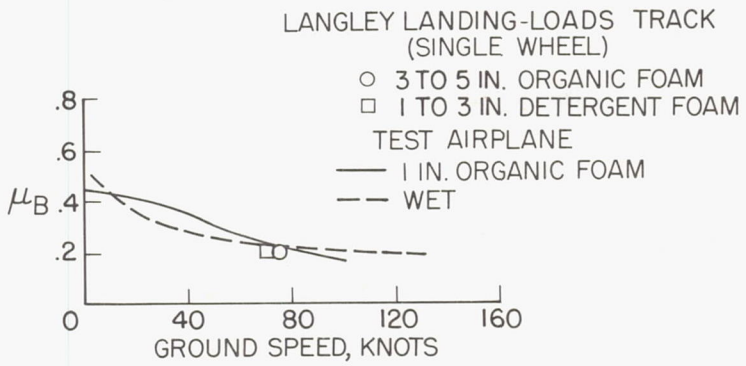

Figure 8

12. OPERATIONAL METHODS FOR DETERMINING BRAKING CONDITIONS

By Richard H. Sawyer

NASA

INTRODUCTION

As indicated in the paper by Upshur T. Joyner and Nicholas S. Dobi (paper no. 9), ground vehicles are being used to a limited extent for determining runway surface braking conditions for the advice of incoming traffic. The U.S. Air Force is using an accelerometer-equipped automobile at its airfields to determine the relative stopping distance under wet and icy conditions. The Scandinavians have used the same method extensively on icy and snow-covered surfaces and have developed the Skiddometer as an improved method for this purpose.

Previous NASA research regarding the capability of using a ground vehicle for the measurement of braking conditions (ref. 1) has indicated that for dry, uncontaminated surfaces and on surfaces covered with solid contaminants, such as packed snow and ice, the braking capabilities of an airplane can be defined by proper measurements with a ground vehicle. On such surfaces, there is generally little change of braking friction with speed. On fluid-contaminated surfaces, however, where hydrodynamic forces come into play, there is generally a loss of friction with increase in speed. These hydrodynamic forces are functions of such factors as speed and tire bearing pressure. Since such factors vary markedly between ground vehicles and airplanes, correlation of vehicle measurements with airplane braking is difficult for fluid-contaminated surfaces.

During the braking tests with the airplane, the opportunity arose to make measurements with the British trailer, the Swedish Skiddometer, and an accelerometer-equipped automobile on wet and slush-covered surfaces. The results of these tests allow a preliminary correlation to be made of the vehicle measurements with the airplane braking characteristics on these fluid-contaminated surfaces.

The results of the tests of the ground vehicles and the test airplane on the wet and slush-covered surfaces have been presented in a previous paper by Jack J. Shrager (paper no. 10). On the basis that, on these surfaces, the general loss in braking friction with speed is associated with the gradual lifting of the tire from the surface by the

hydrodynamic force, the ground speed V has been normalized with respect to the planing velocity V_P, the velocity at which the complete footprint would theoretically be supported on the fluid. The planing velocities for each vehicle and the airplane were determined as described in the paper by Walter B. Horne and Trafford J. W. Leland (paper no. 5) entitled "Prediction of Slush Drag on Aircraft Performance." The computed values of planing speed for the airplane and each vehicle are as follows:

Test airplane	110 knots
British trailer	50 knots
Swedish Skiddometer	68 knots
Automobile	58 knots

This approach in the comparison of the results was taken in order to eliminate, as much as possible, the effects of the factors which determine the hydrodynamic force.

ANALYSIS OF METHODS

A comparison of the braking results on wet concrete for the test airplane and each vehicle is shown in figure 1. It can be seen that the results for the various vehicles are still at different levels even though they have been normalized with respect to the planing velocity. This result is probably due to the differences in the friction coefficient measured, ranging from the full-skid value to the maximum value. In the case of the airplane, the result is probably influenced by the capability of the brake system and the efficiency of the antiskid system. Examination of the data shown in figure 1 and the similar data for the slush-covered runway (fig. 2) indicated that it might be feasible to determine, for each vehicle, a relationship between the airplane braking coefficient of friction and the vehicle friction coefficient which would be the same for both surfaces.

The results of this analysis for the British trailer are shown in figure 3. It is apparent that the ratio of the effective airplane braking coefficient to the vehicle coefficient, denoted by K, is nearly the same for both surface conditions and is largely independent of the speed ratio V/V_P for this vehicle. This result suggests that measurements with this vehicle at a selected velocity ratio V/V_P might serve to define the braking capability of the airplane at the corresponding speed for any type of natural fluid contamination on the surface. For this vehicle, the test speed could be low, since the planing speed (V/V_P of 1.0) is about 50 knots. Also, the small variations of K with V/V_P indicate that operational variations from the test speed

would not be critical. The use of this criterion would, of course, require a knowledge of the shape of the curve of braking coefficient against speed for the airplane in order to predict the overall stopping capability of the airplane.

The same analysis is shown for the automobile in figure 4. In this case, it can be seen that the values of the ratio K for the two surface conditions are different, in contrast to what was found for the British trailer. Also, for both surface conditions, the ratio K decreases with increasing velocity ratio V/V_p. Use of the automobile for this method would probably require the use of different values of the ratio K for the two surface conditions for sufficient accuracy and would require close tolerances on the vehicle test speed. It is possible, however, that a mean value of K would provide a satisfactory answer. The standard test speed could again be low inasmuch as the planing speed is about 58 knots.

Results of the analysis for the Swedish Skiddometer is shown in figure 5. In this case, it can be seen that large differences in the ratio K exist for the two surface conditions. For the wet surface, the ratio is fairly constant with V/V_p, but for the slush condition the ratio decreases with increase in V/V_p. Use of this vehicle for this method would definitely require use of different values of the ratio K for the two different surface conditions. Test-speed variations would be critical for the slush conditions.

EFFECT OF MEASUREMENT ACCURACY

Study of the expected accuracy of measurement of the airplane braking coefficient for the suggested method indicated that, with the use (in the cases of the British trailer and the automobile) of a mean value of the ratio K for the two surface conditions, the airplane braking coefficient could probably be established within a value of ± 0.05. The effect of underestimating the braking coefficient by this error on the stopping distance for both the wet and slush-covered surfaces is shown in figure 6. The results were calculated with the use of the test airplane weight of 150,000 pounds and an initial ground speed of 130 knots. Reverse thrust was assumed to be used from 130 knots down to 75 knots. The calculations were made with the use of the measured braking coefficients for the test airplane, the coefficients for the slush case including the drag effect for 1/2-inch depth of slush.

The upper pair of bars in figure 6 show the calculated stopping distances for the wet surface condition. The clear portion of the

bar represents the basic stopping distance, and the shaded area represents the effect on distance of underestimating the braking coefficient by 0.05. For the wheel-brakes-only case, the stopping distance would be increased about 600 feet, an increase of approximately 23 percent in the basic distance. For the wheel-brakes-and-reverse-thrust case, the distance would be increased about 250 feet, an increase of approximately 14 percent in the basic distance.

The lower pair of bars in figure 6 show the calculated stopping distances for the slush-covered surface condition. For this slipperier surface, the effect of the assumed error in measurement is more pronounced and results in increases of about 1,700 feet (38 percent of the basic stopping distance) and about 750 feet (29 percent of the basic stopping distance) for the wheel-brakes-only and wheel-brakes-and-reverse-thrust cases, respectively.

The results shown in figure 6 indicate that for wet and slush-covered surfaces, with the ability to predict the airplane braking coefficient with an accuracy of ±0.05, some reduction in allowable landing weight would probably be required to compensate for the possible error in stopping distance.

CONCLUDING REMARKS

In conclusion, a preliminary examination of a method of correlating friction-coefficient values measured with ground vehicles with airplane braking capability on fluid-contaminated surfaces has been made. At this stage, the method appears feasible; however, more work is required to validate the method for other fluid-contaminated surfaces and other airplanes.

REFERENCE

1. Sawyer, Richard H., Batterson, Sidney A., and Harrin, Eziaslav N.: Tire-to-Surface Friction Especially Under Wet Conditions. NASA MEMO 2-23-59L, 1959.

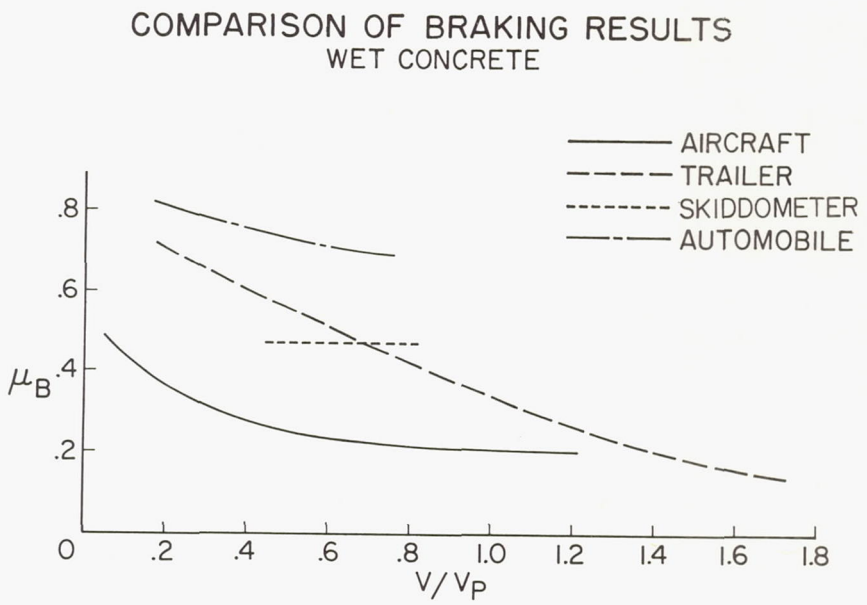

Figure 1

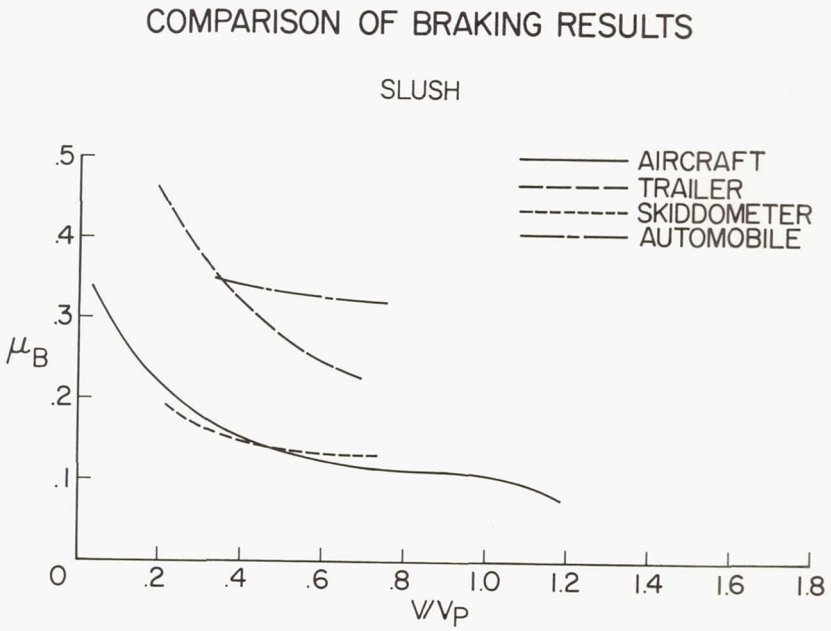

Figure 2

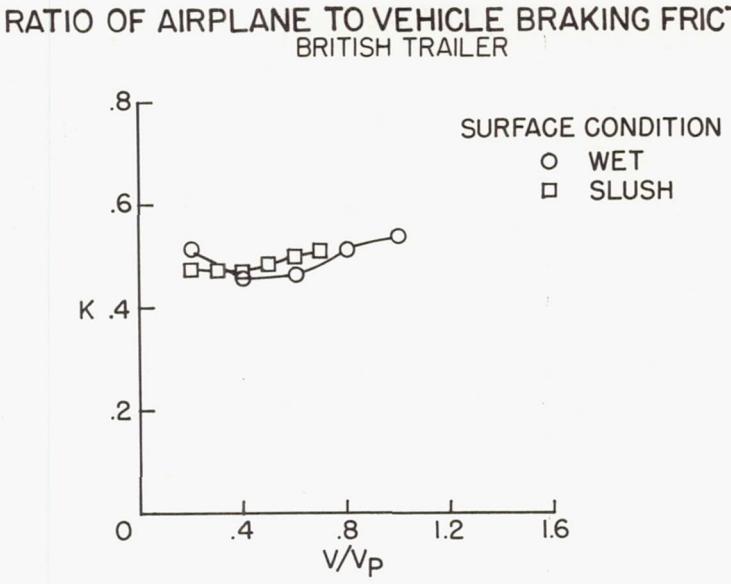

Figure 3

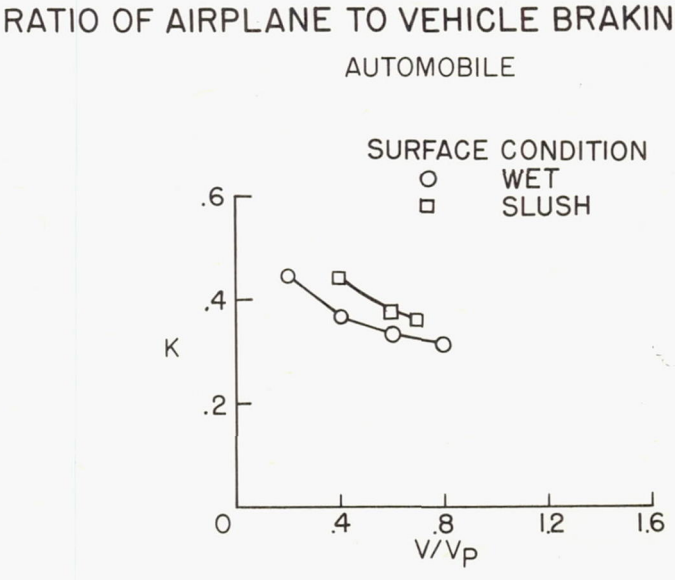

Figure 4

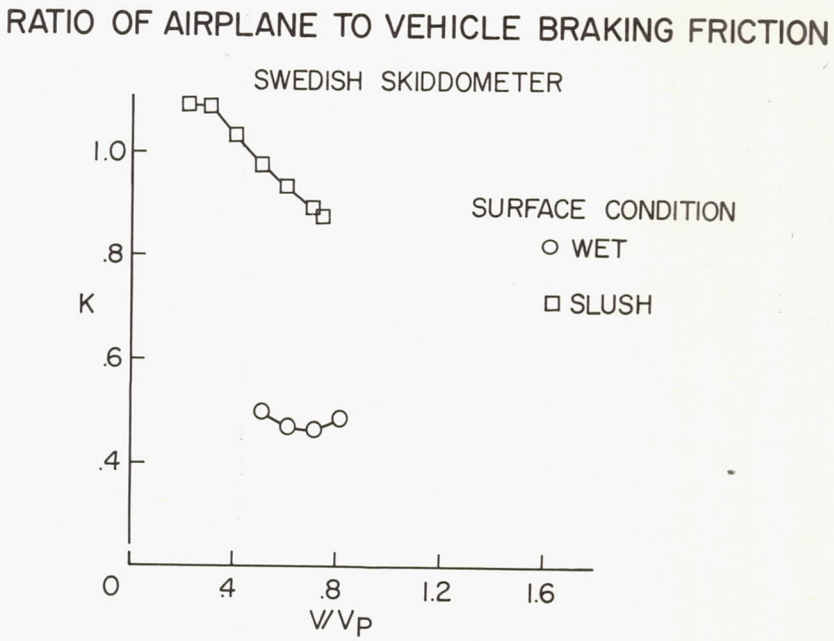

Figure 5

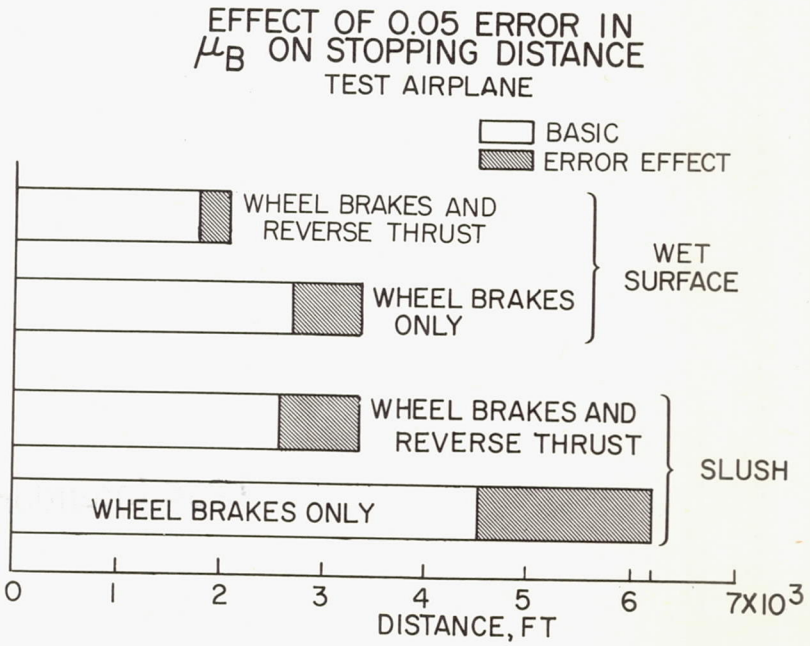

Figure 6

Page Intentionally Left Blank

13. SUMMARY

By Charles M. Middlesworth
FAA

and Upshur T. Joyner
NASA

In summarizing the recent work and the material presented on braking, first the fact that the problem of stopping vehicles on slippery surfaces is an old and well recognized one should be reemphasized. Major dependence has, in the past, been placed on effective braking and efforts have been made toward improving the coefficient of friction between the vehicle tire and the surface, or, in other words, toward reducing the effective slipperiness of the runway surface. This effort has been extensive and includes that provided by highway and road research groups and, in more recent years, by those concerned with aircraft.

Full-scale braking tests, including tests on grooved runways, have been conducted by the British. Investigations on the influence of tire tread, tire pressure, and other factors affecting braking action have been carried on by the National Aeronautics and Space Administration at the Langley landing-loads track. Furthermore, agencies in England, Sweden, and the United States have developed vehicles to provide a means of measuring runway surface condition and forecasting aircraft braking performance on slippery runway surfaces.

The previous papers are related to the matter of improved braking performance. Although the work involved does not lead directly to more effective braking, it does provide information that materially increases our knowledge of the relationship between vehicle measurements, measurements made at the Langley landing-loads track, and those obtained with the test airplane. The recent tests also provide data on the comparative slipperiness of various surface contaminants and the effect of airplane velocity on braking effectiveness.

Results of the recent airplane braking tests at the National Aviation Facilities Experimental Center are illustrated in figure 1. The coefficient of braking friction μ_B is assumed to be an indicator of aircraft braking effectiveness. This figure indicates, at least for the test airplane which was equipped with an antiskid system, that -

(1) Wet surfaces drastically reduced braking effectiveness at high ground speeds and the degree of reduction was related to the amount of water standing on the runway surface

(2) Braking effectiveness on slush was the lowest noted

(3) Braking effectiveness varied only slightly with increased velocity on a dry surface

(4) Braking effectiveness was nearly the same on foam as it was on the wet surfaces at all velocities

This last result confirms previous NASA test results on foam and encourages consideration of its use as a means of providing a standard slippery surface for aircraft performance tests when local conditions make it impractical to lay down a satisfactory water cover on the runway.

Interpreted in terms of stopping distance, the effect of the wet surfaces is shown in figure 2. In this figure, a practical application of the data was made for purposes of illustration by computing the distances required to stop the test airplane with brakes only. The aerodynamic drag resulting from the landing configuration is reflected in all the curves. The effects of drag from 1/2 inch of slush is also incorporated in the curve labeled "slush." The ratios of stopping distances shown with respect to that required for a dry runway are approximately 1.6 for the wet condition and 2.8 for the slush condition. The detrimental effect of a wet or slush-covered runway and the importance of surface drainage are thus illustrated to be appreciable.

An interesting and important aspect of aircraft braking systems (illustrated in paper no. 11 by Walter B. Horne and Trafford J. W. Leland) is shown in figure 3, in which the values of friction coefficient μ are plotted against slip ratios from 0 to 1.0. The antiskid system was described as operating the brakes across the peak of the upper curve under a dry runway condition and at low speeds on a wet runway. However, on a wet runway at high speeds the coefficient is much lower and approximately constant for all values of slip ratio. The antiskid system under these conditions cannot provide improved braking.

In considering the question whether vehicles can be used to predict effective braking performance of an airplane, reference is made to recent test data which indicate that the vehicle measurements of surface conditions were quantitatively different from each other and from the braking performance obtained with the airplane but that, in some cases, a fairly constant relationship existed between the measurements. This means that further development of a measuring vehicle would probably provide a method of accurately measuring runway surface condition.

The comparison of data obtained from single-wheel tests at the Langley landing-loads track with aircraft braking data (see fig. 4) indicated that use of the track produces results which are related to full-scale aircraft braking performance and can be used as a controlled test means for conducting further aircraft braking studies.

Finally, in consideration of the problem of stopping large aircraft on slippery runways of limited length, it should be recognized that improvements in braking systems and tire design alone will never fully satisfy requirements. Further research in this area and on runway surfaces to prevent the slippery surface condition is needed. However, careful consideration should also be given to studies of improved supplemental means of stopping, such as increased reverse thrust and the use of arrestment systems.

Page Intentionally Left Blank

VARIATION OF μ_B WITH GROUND SPEED FOR AIRCRAFT

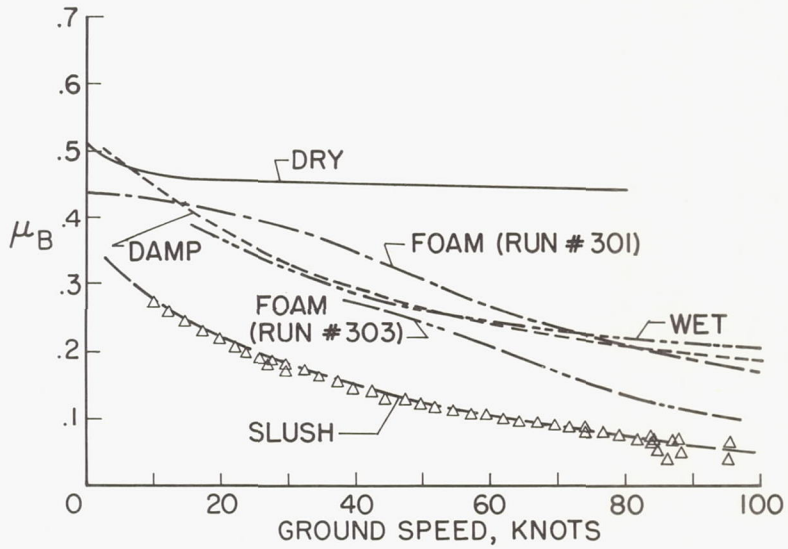

Figure 1

EFFECT OF SURFACE CONDITION
ON STOPPING DISTANCE

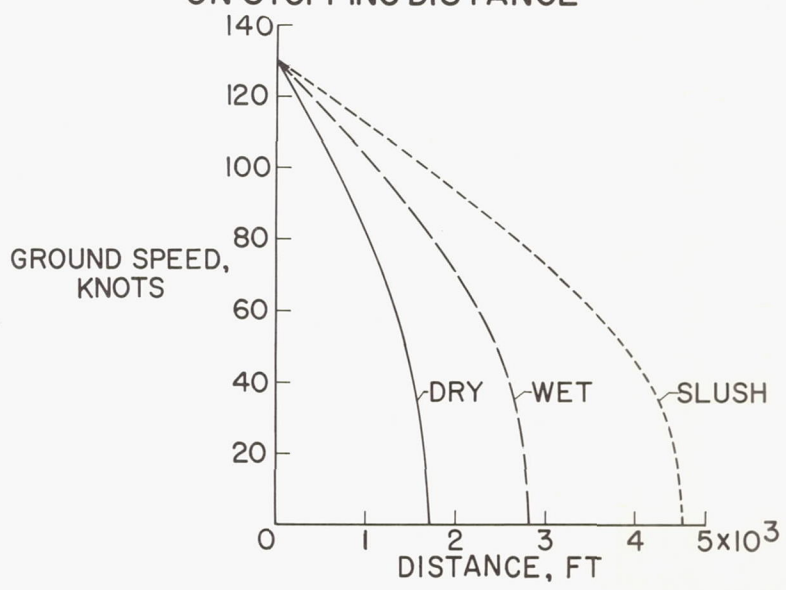

Figure 2

VARIATION OF FRICTION
COEFFICIENT WITH SLIP RATIO
DRY RUNWAY

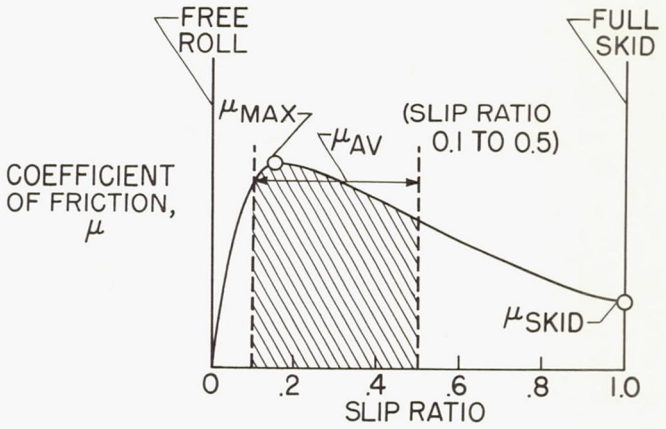

Figure 3

BRAKING COEFFICIENT
WET CONCRETE RUNWAY

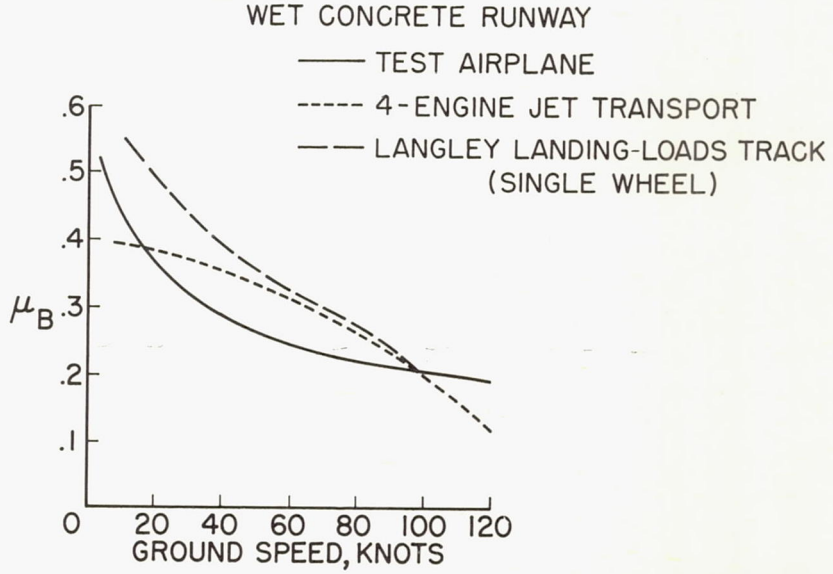

Figure 4